THE IN SITU SYNTHESIS OF SUPPORTED RUTHENIUM CARBONYLS

by

Joseph John Bergmeister

Dissertation submitted to the faculty of the
Virginia Polytechnic Institute and State University
in partial fulfillment of the requirements for the degree of

DOCTOR OF PHILOSOPHY

in

Chemistry

APPROVED:

B. E. Hanson, Chairman

J. G. Mason

M. E. Davis

J. S. Merola

J. P. Wightman

December, 1989
Blacksburg, Virginia

THE IN SITU SYNTHESIS OF SUPPORTED RUTHENIUM CARBONYLS

by

Joseph J. Bergmeister

Brian E. Hanson, Chairman

Chemistry

(ABSTRACT)

The compound $Ru^{+2}(CO)_3Cl_2(THF)$ spontaneously adsorbs onto MgO, Al_2O_3, SiO_2, and NaY zeolite from THF solution evolving less than 0.1 equivalent of CO to yield a light yellow supported complex. Based on reaction stoichiometry, CO evolution and in situ infrared spectroscopy, the adsorption was found to produce two different surface bound species depending on the support used. On SiO_2 and NaY zeolite, the surface species $Ru^{+2}(CO)_3Cl_2(SURFACE)$ is formed by a ligand substitution of THF for a surface hydroxyl group. When the adsorption is performed on MgO or Al_2O_3, the inorganic oxide acts as a chloride acceptor to form the surface species $Ru^{+2}(CO)_3(SURFACE)_3$.

A molecular analog of the adsorbed species $Ru(CO)_3Cl_2(SURFACE)$ was synthesized and characterized by infrared spectroscopy, ^1H NMR, and a X-ray crystal structure. The infrared spectra of the adsorbed species, $Ru(CO)_3Cl_2(SURFACE)$, and the model compound were in close agreement. Model compounds of $Ru(CO)_3(SURFACE)_3$ were also synthesized: however, these could not be structurally characterized.

The reactivity of the adsorbed species, $Ru(CO)_3Cl_2(SURFACE)$ and $Ru(CO)_3(SURFACE)_3$, towards the formation of supported bimetallics, polynuclear ruthenium carbonyl clusters, and ruthenium bipyridine coordination compounds was investigated. On SiO_2 and NaY zeolite, the chemistry of $Ru(CO)_3Cl_2(SURFACE)$ paralleled that of $Ru(CO)_3Cl_2(THF)$ in solution. On Al_2O_3 and MgO, the chemistry of $Ru(CO)_3(SURFACE)_3$ was indicative of an adsorbed ruthenium carbonyl containing no chloride ligands.

The bimetallic cluster $RuCo_3(CO)_{12}^-$ was synthesized on hydroxylated Al_2O_3 by the disproportionation of $RuCo_2(CO)_{11}$. The trimeric cluster $RuCo_2(CO)_{11}$ is spontaneously adsorbed onto Al_2O_3 from a pentane solution yielding the adsorbed species "$RuCo_2(CO)_{10}$", this was then transformed to the tetrameric cluster $RuCo_3(CO)_{12}^-$ by the addition of THF. The adsorbed cluster anion $RuCo_3(CO)_{12}^-$ could also be synthesized on Al_2O_3 by the deprotonation of the hydridic cluster $HRuCo_3(CO)_{12}$. Depending on the route, infrared evidence suggests formation of a solvated or unsolvated anion on the surface.

ACKNOWLEDGEMENTS

I would like to thank my advisor, Dr. Brian E. Hanson, for his help, guidance, and patience during the course of this work, as well as the rest of my advisory committee, Dr. Mark E. Davis, Dr. John Mason, Dr. Joseph S. Merola, and Dr. James Wightman for their role in my professional development. A special thanks is given to Dr Joseph S. Merola for his help and guidance with the single crystal X-ray diffractometer.

I would also like to thank Dr. George Wagner, Dr. Melissa Wagner, Dr. Dennis Taylor, , and Dr. Imre Toth for their help and advise in the laboratory. Grants from the National Science Foundation supporting this research are greatfully acknowledged.

TABLE OF CONTENTS

LIST OF FIGURES

LIST OF SCHEMES

LIST OF TABLES

CHAPTER 1
INTRODUCTION

1A INTENT OF THESIS

Organometallic compounds supported on inorganic oxides are best synthesized in one of two ways, either by direct adsorption or by in situ synthesis. Direct adsorption of an organometallic compound consists of first the synthesis and purification of the desired complex followed by its adsorption onto the support. An in situ synthesis incorporates the co-adsorption of one or more precursors onto the support, with subsequent synthetic steps to take place on the surface. The most common type of in situ synthesis is the formation of a polynuclear metal carbonyl cluster from an adsorbed monomeric species. This is well documented for the formation of supported Rh [1,2], Co [3], and Fe [4] carbonyl clusters. The most widely used synthetic method for preparing supported organometallics is the direct adsorption of specific compounds.

The goal of the work presented here was to develop synthetic techniques for the in situ synthesis of supported metal carbonyls. In particular it was hoped to synthesize a well defined supported ruthenium carbonyl system and use it as a precursor for the in situ synthesis of supported bimetallic clusters, ruthenium coordination compounds, and homonuclear clusters. In this study the complex $Ru(CO)_3Cl_2(THF)$ was chosen as the ruthenium precursor based on its known solution chemistry (scheme 1.1). The supports used in this study were MgO, Al_2O_3, SiO_2, and NaY zeolite, whose surfaces were fully hydroxylated. A hydroxylated surface was chosen in an attempt to displace coordinated THF and/or CO with the surface hydroxyl groups, a reaction also observed in solution with similar donor ligands. The surface species were characterized by CO evolution and FTIR spectroscopy. The probe reagents $Co(CO)_4^-$, bipyridine, and CO, were used to investigate the reactivity of the various surface species which were compared to known solution chemistry. Molecular analogs incorporating oxygen donor ligands were also synthesized in attempts to understand structural properties of the surface compounds. The

model compounds were characterized by ^1H NMR, FTIR, and x-ray crystallography.

Scheme 1.1 shows the chemistry of $Ru(CO)_3Cl_2(THF)$ in solution. The ruthenium carbonyl chloride can undergo ligand substitution reactions which involve displacement of THF and/or CO by mono or bi-dentate donor ligands [5]. Clusters can also be synthesized from $Ru(CO)_3Cl_2(THF)$ in the presence of a halide acceptor and a reducing agent, such as Zn [6]. Bimetallic clusters containing ruthenium and cobalt have also been synthesized; the size of these clusters can be controlled by using the appropriate solvent [7,8].

1B GENERAL

Metal carbonyls supported on inorganic oxides have been shown to be catalytically active for a wide range of reactions [9,10,11]. It has been demonstrated that, in some cases, heterogeneous catalysts derived from metal carbonyls can show higher selectivity and activity than those prepared by conventional means [12,13]. Also, it has been suggested that the nature of the support can affect catalytic activity for similarly bound species [14]. Ruthenium carbonyls, in particular, have been shown to catalyze the reduction of CO [15], the water gas shift reaction [16], and the hydrogenation of olefins [17]. For these reasons, a great deal of attention in the chemical literature has been given to the chemistry of supported metal carbonyls.

The adsorption of metal carbonyls onto refractory supports can be performed in one of several ways: adsorption from solution, dry mixing, or sublimation, the most common mode being adsorption form solution. This method yields the most accurate metal loadings of the desired metal complex. The most critical variable is the choice of solvent; it must be unreactive toward both the support and the supported organometallic complex, and it must be relatively volatile. Many of the neutral metal carbonyls readily sublime onto supports under a high vacuum to give very pure adsorbed metal complexes; however, the weight loading of the complex is difficult to control due to incomplete sublimation. Sublimation is most desirable where exposure of the adsorbed

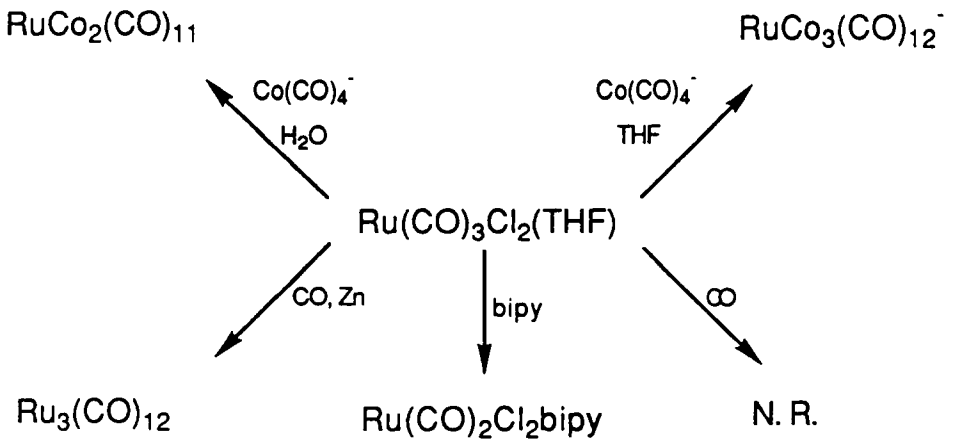

Scheme 1.1 The reactivity of $Ru(CO)_3Cl_2(THF)$ with various reagents in solution.

complex to solvents and other impurities must be kept to a minimum. Dry mixing is similar in nature to sublimation. In this method, the desired metal complex is mixed with the support, usually with a mortar and pestle: the mixture is then heated, sometimes under vacuum, to sublime the complex onto the support. The major disadvantage of this method is the decomposition of the metal complex during the activation period; the decomposed material cannot be separated from the desired supported product.

The adsorption of metal carbonyls onto inorganic oxides can take one of two pathways: physisorption (physical adsorption) or chemisorption (chemical adsorption). Chemisorption is characterized by the occurrence of a surface reaction in which the adsorbed carbonyl undergoes a chemical reaction with the surface to produce a surface bound complex, chemically different from the starting material. In physisorption, the adsorbed metal carbonyl interacts with the surface in such a way that it can be extracted from the support unchanged; these interactions can be either weak or strong. The precipitation of a metal complex onto a support would be considered a weak interaction. Once adsorbed, the complex can usually be extracted from the surface by a solvent wash. A strong physisorption interaction can be seen in the formation of Lewis acid-base adducts [18] which is illustrated by equation 1.1

$$M\text{-}C\text{-}O: \dashrightarrow Al^{+} \qquad 1.1$$

Acid-base interactions are consistent with a partial donation of electrons, or electron density, from the carbonyl oxygen (a base) to a surface cation (an acid). This interaction is usually confirmed by a shift of the carbonyl stretching frequency in the infrared spectrum to lower wave numbers for the interacting carbonyl group. Sometimes a shift to higher wave numbers for the non-interacting carbonyls is also seen [19]. Metal carbonyls adsorbed at Lewis acid-base sites can usually be extracted off the surface, but poisoning of the acid sites is often required so that readsorption of the metal carbonyl does not occur [20]. This is accomplished by a metathesis reaction with a nucleophilic

solvent, such as THF or MeOH.

In general, the adsorbed species is considered physisorbed if it can be extracted off the surface with out change in chemical composition, regardless of the degree of interaction between the adsorbed species and the support.

Many types of surface reactions can lead to a chemisorbed metal carbonyl. One of the most fundamental surface reactions between a metal carbonyl and an oxide support is a ligand substitution of a carbonyl ligand with a surface oxo or hydroxyl group. This has been shown to be the mechanism for the adsorption of $Mo(CO)_6$ onto gamma alumina, by Burwell et al. During the adsorption, three equivalents of CO are evolved to form the surface species $Mo(CO)_3(SURFACE)_3$ [21].

The literature contains many examples of the effect of surface pretreatment on the adsorption of metal carbonyls onto supports [22]. As mentioned above, when a metal carbonyl is brought into contact with a dehydroxylated surface, Lewis acid-base adducts are most likely to occur. However, when a metal carbonyl is adsorbed onto a hydroxylated surface, nucleophilic attack on the carbonyl carbon is more probable (eq. 1.2).

$$Ru_3(CO)_{12} + HO\text{-}Al \longrightarrow HRu_3(CO)_{11}^- + Al^+ + CO_2 \qquad 1.2$$

This mechanism is consistent with the evolution of CO_2 gas and the formation of a metal hydride complex. Since this reaction scheme produces a metal carbonyl anion, it can also be classified as a redox reaction. Basset et al. have proposed that the adsorption of $Fe_3(CO)_{12}$ onto hydroxylated alumina proceeds via nucleophilic attack on a bridging carbonyl to form $HFe_3(CO)_{11}^-$. During the adsorption, no CO_2 was observed; however, the authors suggest that evolved CO_2 was adsorbed as CO_3^{-2} on the alumina surface [23]. It was determined later by Hanson et al. that Basset's proposed mechanism was only one of several simultaneous surface reactions[24].

Supported polynuclear metal carbonyls can be readily synthesized in situ on

inorganic oxides from mononuclear precursors. When $H_2Os(CO)_4$ is adsorbed onto MgO and exposed to a 1:1 CO/H_2 (10 atm) atmosphere at temperatures above 275°C, the metal cluster $H_3Os_4(CO)_{12}^-$ is readily synthesized [25]. It has also been shown that $Co_2(CO)_8$ can also be transformed under mild conditions to $Co_4(CO)_{12}$ on silica gel [26]. Rhodium clusters with as many as six metal centers have been reported to occur on the surfaces of zeolites and silica as a result of the cabonylation or $Rh(CO)_2$(ads) [27]. An interesting aspect of in situ cluster synthesis is the possibility that large metal clusters may be synthesized in the α cages of zeolites. These are formed by adsorbing small, usually mononuclear precursors into the zeolite cages and then reacting them to form a carbonyl cluster which is too large to exit the cage. This type of synthesis has been observed for ruthenium [28], cobalt [29], and rhodium [30] on various zeolites. Since the clusters are too large to be removed through the zeolite channels, these are often referred to as molecular ships in bottles [31].

When determining the composition of a surface bound metal carbonyl, one must use a combination of several techniques. Although single crystal X-ray diffraction is the most powerful tool for determining structural information of pure compounds, it cannot be used for supported noncrystalline materials. For surface bound species, the most widely used technique has been infrared spectroscopy. There are several elaborate cells, described in the literature, which allow for the in situ adsorption of substrates onto pressed pellets of inorganic oxide to be monitored by infrared spectroscopy [32,33], allowing for the adsorption to be carried out under an inert atmosphere or vacuum, at various temperatures. Raman spectroscopy has also been used to complement infrared spectroscopy in the regions where the support has strong absorptions in the infrared [34]. However, many samples cannot be analyzed by raman spectroscopy, since they decompose upon exposure to the raman laser. A common method for the detection of metal to metal bonds has been monitoring the $\sigma \dashrightarrow \sigma^*$ transition in the metal bond with diffuse reflectance UV-Vis spectroscopy [35,36].

X-ray photoelectron spectroscopy, XPS [37], has also been used for the

characterization of supported organometallics, but it can only be used on samples which can withstand ultra high vacuum and high energy x-rays. A powerful surface technique applied to supported organometallic complexes is Extended X-ray Adsorption Fine Structure, EXAFS [38]. This technique allows for the determination of the nearest neighbors and their bond distances provided good models for the surface complexes are available. Although this is a very powerful technique, resembling a surface crystal structure, it is not available to every laboratory. It should be noted that even though several surface analytical techniques are available for the study of adsorbed metal carbonyls, they are usually used as a secondary tools next to infrared spectroscopy.

When using infrared spectroscopy, many researchers tend to over interpret spectral data. This is most obvious in the assignment of oxidation states. Many times, oxidation states are determined solely by the position of the infrared absorption. Such an interpretation is consistent with the fact that metals in high oxidation states π backbond less than metals in low oxidation states. Thus the triple bond character of the CO ligand attached to a metal in a high oxidation state will be greater than if the metal is in a low oxidation state. Therefore the infrared absorption associated with the CO ligand will be at higher wavenumbers for the CO on the metal in the higher oxidation state as compared to the metal in the lower oxidation state. This is usually an inadequate approach since many factors can influence the bonding properties of the surface species, such as the degree of hydroxylation, the presence of Lewis acid sites, and the presence of ligands other than CO in the coordination sphere of the metal.

Structural information about the nature of the surface species has been obtained through the use of model compounds [39,40]. This approach consists of synthesizing metal carbonyl complexes with donor ligands which are coordinatively similar to the believed surface species. Most often molecules containing oxygen, such as ethers, alcohols or oxides, are used as donor ligands, although amines and phosphines have also been used. Once a model compound has been synthesized and yields similar spectroscopic information to the adsorbed species, it can be suggested that the surface

species may have a similar structure.

1C THE ADSORPTION OF RUTHENIUM CARBONYLS ONTO REFRACTORY SUPPORTS

The adsorption of ruthenium carbonyls on inorganic oxides has received considerable attention in the chemical literature. The thrust of the work has focused on the adsorption and decomposition of $Ru_3(CO)_{12}$ on Al_2O_3 [41], MgO [14], SiO_2 [42], and zeolites [43], with some mention of ruthenium carbonyl cluster containing four and six metal centers [44]. Ruthenium carbonyls in higher oxidation states, namely +2, have been addressed in only a few papers [40,47].

Zechina and coworkers [41] have shown that the adsorption of $Ru_3(CO)_{12}$ on hydroxylated alumina produces a surface species where the trinuclear framework remains intact. Only after exposure to temperatures greater than 200°C and various gases does the cluster fragment into surface bound dicarbonyl species.

When $Ru_3(CO)_{12}$ was adsorbed onto hydroxylated alumina under an inert atmosphere, a chemisorption process took place to form the surface grafted complex $Ru_3(CO)_{12-x}(HOAl)_x + xCO$, where x was believed to be three and HOAl is a surface hydroxyl group. This assignment was supported by the observation of three equivalents of CO during the adsorption and through the use of model compounds. The adsorbed complex was modeled by $Ru_3(CO)_9L_3$, where L= $PEtPh_2$, both the model compound and the adsorbed species gave similar UV-Vis and infrared spectra. After exposure to high temperatures under vacuum, the adsorbed species fragmented to form mononuclear ruthenium dicarbonyl fragments.

Zechina et al. also postulated that, depending on the conditions used, the decomposition can leave the ruthenium in three different oxidation states. When the $Ru_3(CO)_{12}/Al_2O_3$ system was decomposed under H_2 at 200°C, all bands in the infrared corresponding to the grafted cluster disappeared, and two new bands appeared at 2054 and 1977 cm^{-1}. This new surface species was assigned the formula $Ru^o(CO)_2$(ads), where

the ruthenium bonds to two surface oxygens and is in the zero oxidation state. Similar dicarbonyl species were seen when the decomposition was carried out in vacuo at 100°C. When the decomposition was performed under O_2 at room temperature a second set of infrared absorptions were seen at 2072 and 2005 cm^{-1}. These infrared bands were assigned to a ruthenium dicarbonyl complex, with ruthenium in the +2 oxidation state. A third set of bands were seen at 2138 and 2075 cm^{-1}, when the adsorbed species was decomposed under O_2 at 150°C and recarbonylated with CO. These were assigned to ruthenium in a higher, unspecified oxidation state.

All three species observed by Zechina, exhibit two carbonyl infrared stretching frequencies, which is consistent with, but not unique to, a dicarbonyl moiety. The shift to higher wavenumbers which was seen in the infrared for the pair of absorptions as the oxidation state of the metal increases, is consistent with the fact that metals in higher oxidation states cannot participate in π back bonding to the same degree as metals in lower oxidation states. It should be noted that the shift is qualitative and not quantitative, i.e. oxidation states cannot be assigned based only on the shift in the infrared spectrum.

Bell and coworkers [45] have performed similar experiments for the adsorption of $Ru_3(CO)_{12}$ on both hydroxylated and dehydroxylated alumina. They report that when the adsorption of $Ru_3(CO)_{12}$ is performed on hydroxylated alumina either in vacuo at temperatures greater than 100°C or in air at 20°C, a dicarbonyl species $(Ru(CO)_2(ads))_n$ is formed on the surface, where the ruthenium bonds to two surface oxo or hydroxyl groups and n is unknown. In their study, they do not assign an oxidation state to the ruthenium, but they observe a similar infrared spectrum, two peaks at 2050 and 1968 cm^{-1}, to $Ru^o(CO)_2(ads)$ assigned by Zechina et al. Once the dicarbonyl species was formed it could then be carbonylated with CO to form a mixture of $(Ru(CO)_3(ads))_n$ and $(Ru(CO)_4(ads))_n$.

Bell et al. observed that the amount of ruthenium that was adsorbed onto the support was dependent on the pretreatment of the surface. High metal loadings were observed for those surfaces that were fully dehydroxylated or fully hydroxylated, while

low metal loadings occurred on partially dehydroxylated surfaces. If the surface was dehydroxylated, then the adsorption was believed to be governed by the formation of Lewis acid-base adducts, however, on hydroxylated surfaces nucleophilic attack by a surface hydroxyl group allowed for high loadings. On partially dehydroxylated surfaces neither mechanism dominates the adsorption process.

Darensbourg and et al [46] have also shown that ruthenium dicarbonyl fragments can by synthesized on partially dehydroxylated alumina (150°C under vacuum). When $Ru(CO)_5$, $H_4Ru_4(CO)_{12}$, or $Ru_6C(CO)_{17}$ are adsorbed onto partially dehydroxylated alumina, and then activated to 200°C under H_2, the characteristic two peak infrared spectrum is observed. Bands observed at 2043 and 1963 cm^{-1} were suggested to result from ruthenium in the zero oxidation state. Upon exposure to CO, a new surface species yielding three infrared bands arises. This is assigned the structure $(Ru(CO)_y(ads))_n$ where y = 3 or 4 and n is unknown. They have also shown that the adsorption of $Ru_3(CO)_{12}$ proceeds via a nucleophilic attack by a surface hydroxyl group, keeping the cluster framework intact, to form the cluster anion, $HRu_3(CO)_{11}^-$. The hydrido cluster $H_4Ru_4(CO)_{12}$ was shown to adsorb through a cluster deprotonation reaction producing $H_3Ru_4(CO)_{12}$-(ads).

Iwasawa and coworkers [42] were the first to apply EXAFS to adsorbed ruthenium carbonyls. In their study they reported that the adsorption of $Ru_3(CO)_{12}$ on Al_2O_3 dehydroxylated at 300°C evolves two equivalents of CO to form the grafted cluster $HRu_3(CO)_{10}(OAl)$. This was characterized by the following: an infrared spectrum similar to $HRu(CO)_{10}SC_2H_5$, CO evolution, and the intermolecular distance between the ruthenium atoms, which was 2.68 Å. The cluster framework could then be fragmented at 200°C to produce $Ru^{+2}(CO)_2(ads)$ (infrared 2080 and 2030 cm^{-1}). Iwasawa reports no Ru-Ru bonds in the range of 2 to 4 Å are observed for the ruthenium dicarbonyl. It is well known that $Ru_3(CO)_{12}$ reacts with hydroxylated Al_2O_3 to form the anion $HRu_3(CO)_{11}^-$; however, this is the first time a grafted cluster has been structurally characterized for an adsorbed ruthenium carbonyl cluster on Al_2O_3. This difference in

reactivity can be attributed to the surface pretreatment. In this study, the aluminum oxide was heated to 300°C under an inert atmosphere prior to use, thus producing a partially dehydroxylated surface. Similarly, the osmium analog, $Os_3(CO)_{12}$, readily reacts with hydroxylated or dehydroxylated alumina to form the grafter cluster $Os_3H(CO)_{10}(OSi)$.

In the literature, there is almost a unanimous consent that the adsorption of $Ru_3(CO)_{12}$ onto SiO_2, either hydroxylated or dehydroxylated, proceeds to form the grafted cluster $HRu_3(CO)_{11}(OSi)$. In Psaro's study [47] he found that when $Ru_3(CO)_{12}$ was sublimed onto silica, pretreated at 500°C under vacuum, physisorbed $Ru_3(CO)_{12}$ was obtained. Once adsorbed $Ru_3(CO)_{12}$ is stable under CO for short periods of time; however the cluster fragments after several days at room temperature. Heating $Ru_3(CO)_{12}$(ads) to 100°C yielded 2 equivalents of CO consistent with the formation of the grafted cluster $HRu_3(CO)_{10}(OSi)$. Furthermore, an additional ten equivalents of CO were expelled when the grafted complex was heated to 500°C. The grafted complex was modeled by the known compound $HRu_3(CO)_{10}(SC_2H_5)$. Based on similar infrared and UV-Vis spectra and CO evolution, the assignment seemed accurate. Fragmentation occurred if the grafted cluster was subjected to an atmosphere of H_2 to produce species of the form $Ru(CO)_y$(ads) where y = 2 or 3. Psaro also reports that when the $Ru(CO)_3$(ads) moieties were produced from $Ru_2(CO)_6Cl_4$ on silica, a shift to higher wave numbers and different relative intensities are seen in the infrared as compared to adsorbed ruthenium tricarbonyls synthesized from $Ru_3(CO)_{12}$. This observation suggested that the oxidation states of the two tricarbonyl fragments are +2 ($Ru_2(CO)_6Cl_4/SiO_2$) and 0 ($Ru_3(CO)_{12}/SiO_2$) respectively.

Bell et al [45] also found that the adsorption of $Ru_3(CO)_{12}$ on silica proceeds through a physisorption process. Once adsorbed, the trimeric cluster can be removed by repeated washings with pentane. The position of the carbonyl infrared stretching frequencies of the supported complex was reported to be the same as that found for $Ru_3(CO)_{12}$ in pentane, only slightly broader. Another piece of evidence for a weak surface to cluster interaction was the position and intensity of the infrared band associated

with the surface hydroxyl groups. No change was observed for the infrared band corresponding to the OH stretch after the adsorption of $Ru_3(CO)_{12}$; therefore, either no interaction or only a very weak interaction existed. Only after time and treatment with vacuum did the bands corresponding to $Ru_3(CO)_{12}$ start to disappear. They found that elevated temperatures and exposure to CO were needed to induce fragmentation which produces mainly adsorbed ruthenium monocarbonyl, Ru(CO)(ads). They also reported a ruthenium dicarbonyl species, but the infrared spectra of these were shifted to much lower wavenumbers than those reported by others for $Ru^o(CO)_2$(ads) on alumina surfaces.

Similarly Evans et al [48] report that the adsorption of $Ru_3(CO)_{12}$ onto silica yields the chemisorbed species $HRu_3(CO)_{10}(\mu\text{-OSi})$. The adsorbed species was characterized by infrared and UV-Vis spectroscopy. The adsorbed ruthenium carbonyl gave similar UV-Vis absorptions as other model ruthenium cluster compounds, thus suggesting the framework remained intact during the adsorption. The adsorbed cluster was reported to be fragmented to the species $[Ru^{+2}(CO)_2]_n$, where n= 2 or 3, upon exposure to air. A metal to metal bond was proposed based on the observation of a UV absorption in the region of 380 nm, which is the region for the $\sigma \dashrightarrow \sigma^*$ transition in a ruthenium to ruthenium bond. The adsorbed trinuclear species was fragmented to $Ru^{+2}(CO)_2$ by vacuum pyrolysis. They report that this new species does not exhibit an UV adsorption in the region of 380 nm, suggesting the species is monomeric.

Pierantozzi et al [14] have shown that the adsorption of $Ru_3(CO)_{12}$ on various inorganic oxides can lead to a wide range of products. When the adsorption is performed on MgO, pretreated at 200°C, both $HRu_3(CO)_{11}^-$ and $Ru_6(CO)_{18}^{-2}$ are observed. This parallels the chemistry observed between $Ru_3(CO)_{12}$ and OH^- in solution, which initially yields $HRu_3(CO)_{11}^-$ and after longer reactions times, $Ru_6(CO)_{18}^{-2}$. The two anions could then be oxidized to $Ru^{+2}(CO)_2$(ads) under an atmosphere of O_2. The carbido cluster $Ru_6C(CO)_{16}^{-2}$ could be synthesized when the two adsorbed anions were reduced under H_2 and CO. Similarly, when $H_4Ru_4(CO)_{12}$ is adsorbed onto MgO and reacted with H_2 and CO the carbido cluster $Ru_6C(CO)_{16}^{-2}$ is formed.

1D SUPPORTED BIMETALLIC CARBONYLS

Bimetallic catalysts have been employed for a wide range of homogeneous and heterogenous reactions [49,50,51]. It has been shown that some bimetallic catalysts have activities and selectivities that are not derived simply form the additive effects of the two metals [52,53]. For these reasons, a great deal of attention has been given to the surface chemistry of supported bimetallic compounds.

One method in the preparation of bimetallic catalyst employs the adsorption of two metal salts onto a support followed by an activation process, usually at an elevated temperature under hydrogen. The obvious drawbacks in this method are the inability to form an alloy during the activation period as well as low dispersions. An alternative route to supported bimetallics has been through the use of bimetallic cluster carbonyl compounds. The premise is that adsorption of a bimetallic cluster will lead to highly dispersed bimetallic particles with the same metal ratio as their precursor. It has been suggested that large bimetallic clusters can be used as models for very small bimetallic alloy particles. For these reasons a great deal of activity has been devoted to the chemistry of supported bimetallic metal carbonyls.

A typical surface reaction is the deprotonation of a neutral bimetallic carbonyl hydride by a hydroxylated surface to yield the corresponding cluster anion, this is illustrated by equation 1.3:

$$HFeCo_3(CO)_{13} + HO\text{-}Al \longrightarrow FeCo_3(CO)_{13}^- + Al^+ + H_2O \qquad 1.3$$

In a deprotonation reaction, the cluster anion is adsorbed at a Lewis acid site and can usually be extracted by a metathesis reaction with a large cation. This is illustrated by the work of Choplin and coworkers [54]. They have studied the adsorption of $H_2FeRu_3(CO)_{13}$, $H_2FeOs_3(CO)_{13}$, and $HFeCo_3(CO)_{13}$ onto hydroxylated MgO. They report that all three compounds are spontaneously adsorbed onto the support from a

CH_2Cl_2 solution with little or no evolution of the gases H_2, CO, or CO_2. Once adsorbed, the surface complexes gave similar infrared spectra to their corresponding anions in solution. Once the anions were synthesized on the surfaces, they could be extracted with [PPN]Cl in CH_2Cl_2 and characterized by classical solution methods. They also report that the adsorbed anions are unstable at elevated temperatures, at temperatures over 100°C large quantities of CO and H_2 are evolved. They do not report whether this is due to a cluster rearrangement or to complete decomposition of the adsorbed cluster.

The bimetallic complex $H_2FeOs_3(CO)_{13}$ has also been adsorbed onto silica gel dehydroxylated at 350°C by Shore and coworkers [55]. They observed that the hydrido cluster is initially physisorbed onto the support and only after exposure to temperatures above 100°C does the cluster chemically react with the surface. When heated to 130°C, the cluster was found to separate to form Fe metal and the surface bound cluster $HOs_3(CO)_{10}$(SURFACE). At temperatures above 200°C, the osmium cluster fragments to form $Os(CO)_2$(ads) species. They also report that decomposed cluster exhibits catalytic activity for Fisher-Tropsch chemistry. The activity and selectivity for the catalysts are best described as the average expected for iron and osmium alone. No evidence for a synergistic effect between the metals was observed.

As seen from these examples, the major problem with supported bimetallic carbonyls is their relative instability. This is further emphasized by the adsorption of $H_2RhOs_3(acac)(CO)_{10}PPh_3$ onto a polymer functionalized with PPh_2. Gates and coworkers [56] report that the adsorption reaction proceeded through a ligand substitution of the cluster's PPh_3 ligand with the polymer bound PPh_2 ligand to form $H_2RhOs_3(acac)(CO)_{10}Ph_2P$--Polymer. The polymer bound cluster was found to be very unstable, fragmentation of the cluster to $Rh(acac)(CO)_2$ and $HOs_3(CO)_{11}^-$ occurred at 60°C and 1 atm of CO.

Kuroda's research group has studied the adsorption and decomposition of $Rh_2Co_2(CO)_{12}$ on partially dehydroxylated alumina[57]. They observe that the initial adsorption proceeds by a physisorption mechanism. They postulate that all three bridging

CO ligands of the adsorbed bimetallic simultaneously interact with surface Lewis acid sites. A shift to lower wavenumbers in the infrared for the bridging carbonyls was the justification for such an interaction. EXAFS data suggest that Rh-Rh bond in the initial cluster was cleaved after submission to a vacuum at 200°C, while the Co-Co bond remained intact. After the activation period, surface oxo groups bridging the Co-Co bond were observed. The resulting surface bimetallic cluster, although structurally different from its precursor, still contained a 1:1 metal ratio. Similar results were observed for $RuCo_3(CO)_{12}$ on Al_2O_3.

CHAPTER 2
EXPERIMENTAL

2A GENERAL

The inorganic oxides used in this study were purchased from the following suppliers Al_2O_3 CATAPAL (Conoco); MgO (STREM); SiO_2 DAVISIL (W. R. Grace); and NaY zeolite (STREM). The supports were then sieved to 200 mesh and calcined at 350°C in flowing O_2 (8 mL/min) to remove any adsorbed organics. Hydroxylated surfaces were prepared by passing N_2 saturated with water vapor over the support at 100°C for 1 hour. The samples were then purged with dry N_2 at 100°C to remove any weakly adsorbed water.

All reagents were either purchased (research grade) or synthesized by literature methods, section 2G, and characterized by chemical analysis. Solvents were distilled from either K/benzophenone or P_2O_5, as appropriate, under an inert atmosphere prior to use. All reactions were carried out under an inert atmosphere using standard Schlenck line techniques unless otherwise stated. Air sensitive compounds were stored in a Vacuum-Atmosphere dry box under and atmosphere of N_2.

The adsorption and reactivity of the ruthenium carbonyls were investigated by two different methods. The first was a batch reaction, this allowed for the extraction of surface species and the quantitation of any evolved gases. The second method involved performing the reactions on a pressed pellet of the desired metal oxide so that the reaction could be monitored in situ with infrared spectroscopy, without exposure of the sample to air.

2B IN SITU INFRARED SPECTROSCOPY

Figure 2.1 shows a diagram of the cell used for the in situ infrared spectroscopy experiments. All infrared spectra were recorded using either a Nicolet 5DX or 5DX-B

a. high vacuum stopcock

b. o-ring seals

c. heater

d. gas inlet

e. 3-way stopcock

f. quartz holder

g. CaF_2 windows

h. gas outlet

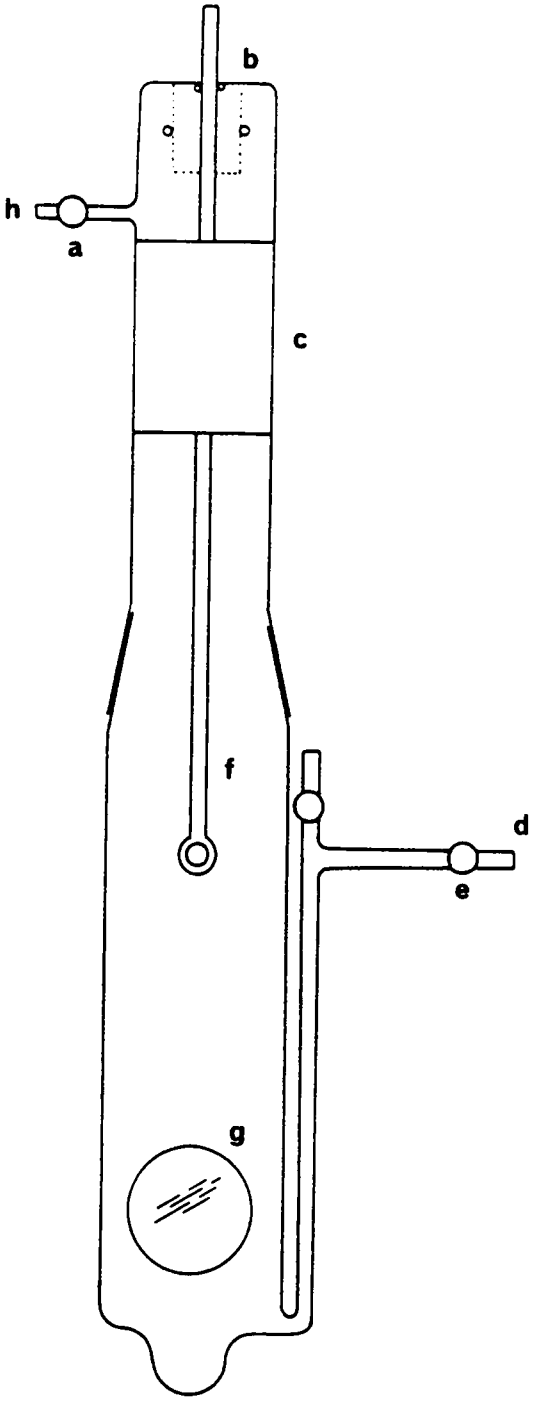

Figure 2.1 Infrared cell used for in situ adsorption experiments.

spectrometer. A typical experiment was performed in the following manner: A 10-15 mg sample of support was pressed into a pellet, 8 mm in diameter and 0.1 mm thick, at 1500 psi for 5 minutes in a standard pellet die. The pellet was then mounted on the quartz holder with stainless steel wire or cemented in place with Alumdum cement. The pellet was then raised into the furnace section of the cell and heated to 100°C while the cell was being purged with ultra pure helium (AIRCO 99.995), dried and deoxygenated over a MnO/SiO_2 catalyst. The cell was judged sufficiently purged when all the CO_2 was flushed from the cell and physisorbed water, from the alumdum cement, was desorbed, as determined by the infrared spectrum of the pellet. This process typically took 0.5 hours. A solution of the desired metal carbonyl was then syringed into the well of the cell, the pellet would be lowered into the solution, and eventually raised into the infrared beam. Weight loadings were judged by the intensity of the carbonyl stretches in the infrared. Higher weight loadings could be achieved by subsequent immersions of the pellet into the solution. For experiments which required co-adsorbents, the pellet would first be immersed into a solution containing the first adsorbent in the well of the cell, followed by raising the pellet to the level of the stopcock on the side of the cell and spraying the pellet with a solution containing the second adsorbent by syringe techniques. The pellet would then be lowered into the beam to record an infrared spectrum. The cell was also equipped with a three way stopcock so that various gases could be used throughout the same experiment, without exposing the sample to air.

2C CO EVOLUTION

Figure 2.2 shows a schematic of the helium flow system used to perform batch reactions. A typical experiment was performed in the following manner. The fused silica reactor was charged with 200 mg of the desired inorganic oxide support by a quartz wool plug. The system was then purged with ultra pure He for one hour. Any traces of oxygen were removed from the helium by a MnO/SiO_2 catalyst just before entering the reactor. A 5 to 10 mL solution of the desired metal carbonyl was then added to the

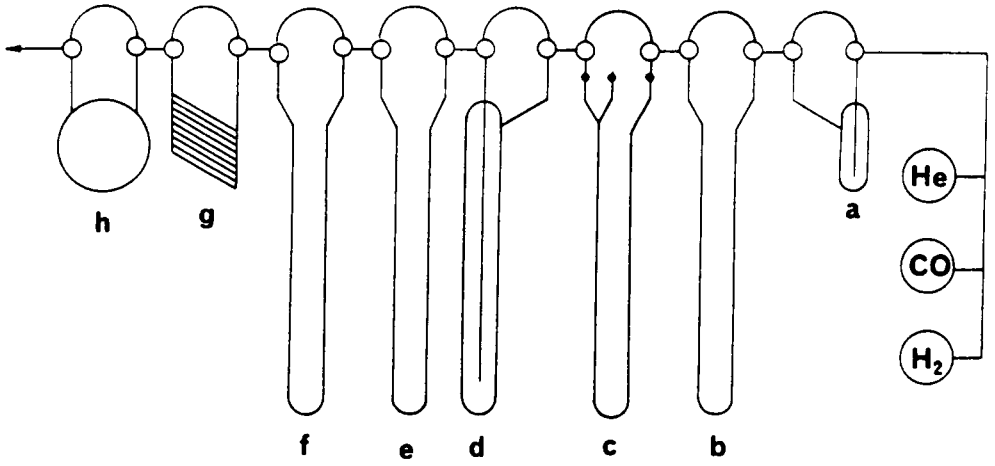

a. water bubbler

b. O_2 trap, MnO on SiO_2

c. reactor

d. solvent trap (-196°C)

e. CO trap, SiO_2 (-196°C)

f. H_2 trap, 5Å (-196°C)

g. column

h. gas chromatograph

Figure 2.2 Helium flow system used for batch adsorption and CO evolution experiments.

reactor via syringe and slurried with the support in flowing helium. The solvent was evaporated by passing helium over the support (40 mL/min) and trapped immediately after the reactor at -196°C. Evolved CO was swept out of the reactor with flowing helium and trapped by adsorption onto SiO_2 cooled to -196°C. The CO was then desorbed from the silica gel by removing the liquid nitrogen dewar from the trap and allowing it to warm to room temperature. Nitrogen which was co-adsorbed on the silica gel trap was separated from CO on a 0.25" x 6' glass column packed with 40-60 mesh 5Å molecular sieve. The CO was quantitated using a Gow-Mac thermal conductivity detector and a Gow-Mac recorder equipped with an integrator. Standard pulses of CO were used to calibrate the GC prior to each experiment.

2D METAL ANALYSIS

Residual metal analyses were determined by DCP, direct current plasma spectroscopy. Digestion of the samples were carried out by fusing the inorganic oxide and LiB_4O_7 followed by acid digestion [58]. A 0.5 g sample of support containing the desired metal was mixed with 5.0 g of LiB_4O_7 in a graphite crucible. The sample was then heated to 1000°C, at which temperature the white powder melted to form a fused glass ball. Once formed, the glass ball was added to a solution of dilute HNO_3 (approx. 100 mL). The solution was stirred vigorously and heated to 90°C in order to dissolve the sample. After 20 minutes any undissolved material, polysilicates, were filtered out. The solution was then concentrated or diluted to a concentration suitable for analysis. Ruthenium and cobalt emissions were monitored at 372.8 and 345.35 nm respectively. Quantitation of 99.5% of the metals could be obtained as determined from experiments with samples of known concentration. All concentrations were determined from solutions prepared from purchased standards (FISHER).

2E X-RAY PHOTOELECTRON SPECTROSCOPY

X-ray photoelectron spectroscopy, XPS, experiments were performed in the

following manner. A 5 to 10 mg portion of the desired sample was mounted on a standard stainless steel XPS mount using double stick tape. The sample was sprinkled onto the tape and smeared with a spatula, any weakly adhered sample was blown off the tape with a stream of dry nitrogen. All spectra were recorded on a Perkin Elmer Phi model 5300 spectrometer using a magnesium anode (K_α = 1253.6 eV) at 250 W. The binding energies were referenced to the Al(2p) photo peak of the support, at 72.6 eV. Unsupported samples were sputtered with gold and referenced to the Au($4f_{7/2}$) photo peak at 83.8 eV. Supported samples referenced to either sputtered gold or the internal standard gave the same ruthenium binding energies.

2F SINGLE CRYSTAL X-RAY DIFFRACTION

The crystal structure of $Ru(CO)_3Cl_2(H_2O)$ was performed on a Nicolet R3m/V X-ray diffractometer. Crystals were first determined to be suitable for single crystal X-ray diffraction by size, shape, and clarity. Once a satisfactory crystal was obtained, it was mounted on the end of a 1 cm quartz fiber using epoxy, the glass fiber was then attached to a standard three way goniometer head. A rotational photograph revealed the quality of the crystal. At this time the crystal was deemed suitable for further analysis. The unit cell was then calculated using 25 reflections. Next a full set of data was collected using an appropriate number of reflections, as determined by the unit cell, using a 2θ scan Refinement of the data was performed using a Nicolet SHELXTL PLUS program on a digital MicroVax II. Parameters of the data collection and refinement are summarized in Appendix 1.

2G SYNTHESIS OF VARIOUS ORGANOMETALLIC REAGENTS

Triruthenium dodecacarbonyl, $Ru_3(CO)_{12}$, was synthesized by Stone's method [5]. A 300 mL autoclave was charged with 5.0 g of $RuCl_3 \cdot 3H_2O$ (19.1 mmol), 50 mL dry MeOH and 2.0 g of zinc shot. Care was taken to use zinc that had a slightly oxidized surface since freshly activated zinc tended to reduce the Ru^{+3} to metallic Ru without

forming the desired cluster. The autoclave was then pressurized to 150 psi with CO and heated to 100°C, working pressure was 190 psi. After 24 hours the autoclave was cooled to room temperature and depressurized. The orange precipitate was filtered and recrystallized from pentane to give 2.45 g of $Ru_3(CO)_{12}$, yield 60%.

Ruthenium tricarbonyl dichloride tetrahydrofuran, $Ru(CO)_3Cl_2(THF)$ was synthesized from $Ru_2(CO)_6Cl_4$ which was synthesized by Colton's method [59]. Ruthenium(+3) chloride trihydrate, $Ru^{+3}Cl_3 \cdot H_2O$ (10.0 g) was refluxed in 300 mL of 1:1 concentrated HCl and HCOOH. During the 30 hour reaction, the solution changed color from red to green to orange and finally to yellow. After the appearance of the yellow color the solution was cooled to room temperature and the solvent was removed by vacuum. The resulting yellow solid was dissolved in 100 mL of THF, upon cooling to 0°C, fine white needles of $Ru(CO)_3Cl_2(THF)$ began to precipitate out of solution, in 80% yield.

Tetracarbonyl cobaltate, $Co(CO)_4^-$, was synthesized as its sodium salt as described by Lyford [60]. A 100 mL flask, equipped with an addition funnel containing 50 mL of THF, was charged with 5.0 g of $Co_2(CO)_8$ (14.6 mmol) and 10.0 g NaOH (250 mmol). As the THF was added drop wise, the $Co_2(CO)_8$ dissolved to give a red-brown solution while the NaOH remained as a white precipitate. The cobalt carbonyl solution was stirred over the NaOH for 1 hour. At this time the solution turned light yellow and the NaOH precipitate purple. The solution was then filtered and the solvent removed under a reduced atmosphere to give 2.27 g of $Co(CO)_4^-Na^+$ as a white air sensitive powder, yield 40% based on total metal.

Ruthenium dicarbonyl dichloride bipyridine, $Ru(CO)_2Cl_2$bipy, was synthesized by Stones method [5]. A solution containing 1.6 g of 2,2'-bipyridine (10.4 mmol) in 5 mL of THF was added drop wise to 3.41 g of $Ru(CO)_3Cl_2(THF)$ (10.4 mmol) dissolved in 5 mL of THF. The resulting solution was stirred for 1 hour at 25°C and cooled to 0°C for 24 hours. The light pink precipitate of $Ru(CO)_2Cl_2$bipy was filtered and dried under vacuum, yield 3.8 g (90%).

Dicobalt ruthenium undecacarbonyl, $RuCo_2(CO)_{11}$, was synthesized as described by Vahrenkamp [7]. A suspension of 300 mg $Ru_2(CO)_6Cl_4$ (0.6 mmol) was stirred in 50 mL of an aqueous solution of $NaCo(CO)_4$ (2.4 mmol) for 1 hour at 25°C. The resulting black precipitate was filtered and recrystallized from hexane to give 450 mg of $RuCo_2(CO)_{11}$, yield 70%.

Tricobalt ruthenium dodecacarbonyl anion, $RuCo_3(CO)_{12}^-$, was synthesized as its PPN^+ salt, by a method similar to Vahrenkamp [10]. A THF (100 mL) solution containing 0.51 g of $Ru_2(CO)_6Cl_4$ (1 mmol) and 1.2 g of $NaCo(CO)_4$ (6 mmol) was stirred for 24 hours at room temperature. The dark red solution was filtered and evaporated under reduced pressure. The red precipitate, crude $RuCo_3(CO)_{12}^-$ was dissolved in 5.0 mL of MeOH and precipitated as its PPN^+ salt by the drop wise addition of 0.9 g of [PPN]Cl (2 mmol) in 5.0 mL of MeOH. This method yielded 1.1 g of $[PPN]RuCo_3(CO)_{12}$, yield 70%.

Tricobalt ruthenium dodecacarbonyl hydride, $HRuCo_3(CO)_{12}$, was synthesized by the protonation of $RuCo_3(CO)_{12}^-$. Approximately 1.0 g of crude $RuCo_3(CO)_{12}^-$ was stirred in 100 mL of 4.0 M H_3PO_4 for two hours. The solution was then filtered and the red solid was dried in vacuo. Recrystallization from pentane yielded between 0.8 and 0.7 g of $RuCo_3(CO)_{12}^-$, approximate yield 80%.

CHAPTER 3

THE SYNTHESIS AND REACTIVITY OF SUPPORTED RUTHENIUM TRICARBONYLS

3A INTRODUCTION

As discussed in Chapter 1, ruthenium carbonyls supported on various inorganic oxides have been studied by several investigators, with the focus of the work being on the adsorption and decomposition of $Ru_3(CO)_{12}$ on Al_2O_3 and SiO_2. It has been well documented that the trinuclear framework of $Ru_3(CO)_{12}$ remains intact during its initial adsorption onto either SiO_2 or Al_2O_3; however, the adsorbed cluster can be fragmented to adsorbed monoruthenium carbonyls after exposure to an oxidative atmosphere and/or thermal treatment. The fragmented ruthenium carbonyls have been described by most authors as $Ru^{+n}(CO)_2(ads)$, where n is believed to be 0, 1, or 2.

Bell [45] and Darensbourg [46] have independently proposed that species of the form $Ru^0(CO)_3(ads)$ are formed from the carbonylation of $Ru^{n+}(CO)_2(ads)$. Basset et al. [47] have also suggested that supported ruthenium tricarbonyl species could be synthesized by the adsorption of $Ru_2(CO)_6Cl_4$ onto silica gel (pretreated at 350°C). Basset's assignment was based on the fact that similar infrared spectra were obtained from the supported carbonyl and its precursor, although this may be due to a physisorption rather then a chemisorption. Basset also postulates that the thermal decomposition of $Ru_3(CO)_{12}$ adsorbed on dehydroxylated silica yields $Ru(CO)_3(ads)$ [47]. In both cases Basset reports infrared spectra for the adsorbed species containing three bands; however, their intensities and positions are dependent of the ruthenium carbonyl precursor. In both Darensbourg's and Bell's study a shift to lower wavenumbers for the adsorbed ruthenium(0) tricarbonyl is seen as compared to either of the infrared spectra reported by Basset for his supported $Ru^{+2}(CO)_3(ads)$ species. In all cases the adsorbed ruthenium tricarbonyl was postulated solely on infrared spectroscopy.

In this chapter, the synthesis and characterization of supported ruthenium

tricarbonyls from the adsorption of $Ru(CO)_3Cl_2(THF)$ onto fully hydroxylated MgO, Al_2O_3, SiO_2, and NaY zeolite will be discussed. It was observed that one of two different ruthenium tricarbonyls were formed on each of the four inorganic oxides. The first, $Ru^{+2}(CO)_3(SURFACE)_3$ was determined to reside on the more basic supports, MgO and Al_2O_3, while $Ru^{+2}(CO)_3Cl_2(SURFACE)$ was determined to reside on SiO_2 and NaY zeolite. These complexes were characterized by in situ infrared spectroscopy, CO evolution and their reactivity towards various reagents.

3B RESULTS

CARBON MONOXIDE EVOLUTION

All of the metal oxides studied, Al_2O_3, MgO, SiO_2, and NaY zeolite spontaneously adsorb the complex $Ru(CO)_3Cl_2(THF)$, **1**, from THF solutions. Maximum metal loadings of up to 0.2% ruthenium could be achieved by spontaneous adsorption onto all four supports. Figure 3.1 summarizes the CO evolution experiments. The adsorption of **1** onto each of the supports at 25°C results in only very small quantities of CO, typically less than 0.1 equivalents per ruthenium at low weight percent loading ruthenium. Neither CO_2 nor H_2 were detected, thus CO is the only evolved gas.

After the adsorption of **1** and removal of excess solvent, the dry solids are typically light tan to pale yellow in color. The supported complexes are stable at room temperature under an inert atmosphere as evidence by the fact that no additional CO is evolved by the dry solids.

The observation of very little evolved CO during the adsorption of $Ru(CO)_3Cl_2(THF)$ onto all four supports is consistent with the retention of the $Ru(CO)_3$ moiety by the adsorbed species on the surface.

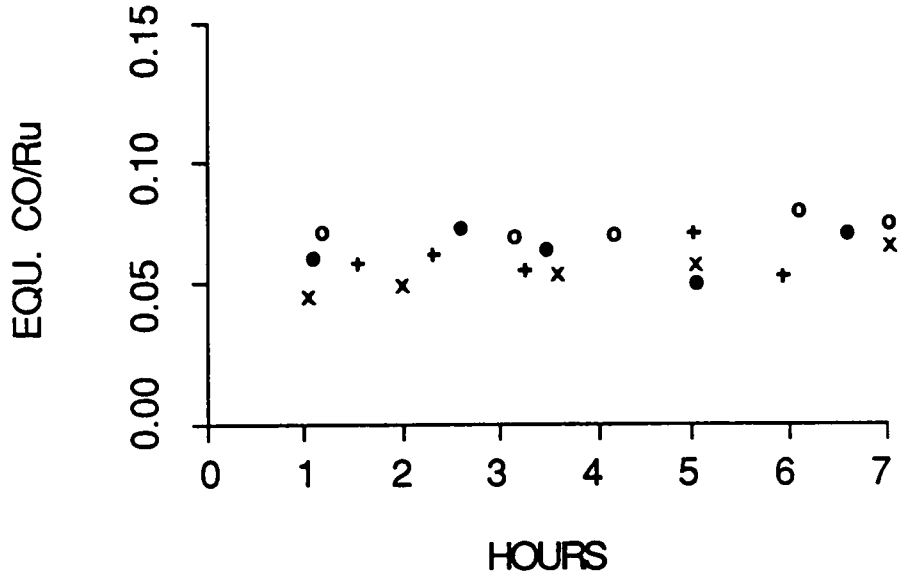

Figure 3.1 CO evolution during the adsorption of $Ru(CO)_3Cl_2(THF)$ onto MgO(o), Al_2O_3(●),SiO_2(x), and NaY zeolite(+).

INFRARED SPECTRUM OF $Ru(CO)_3Cl_2(THF)$ ADSORBED

The in situ infrared spectra obtained from the adsorption of **1** from THF onto MgO and Al_2O_3; and SiO_2 and NaY zeolite respectively are shown in Figures 3.2 and 3.3. All spectra were recorded immediately after a 10 to 20 second immersion of the sample in a 0.1M THF solution of **1**. The spectra were then monitored as a function of time in flowing ultra pure helium. It is important to note that no changes were observed in the infrared spectra over a 3 hour period for each system shown. The spectra for **1**(ads) on MgO and Al_2O_3 are grouped together because of their similarity of the spectra in terms of band position and relative intensity. Likewise the spectra for **1**(ads) on SiO_2 and NaY zeolite are similar in appearance. Furthermore the spectra of this latter group are nearly identical to **1** in THF solution, Figure 3.4.

These spectroscopic and CO evolution results lead to the postulation that one of two different surface species are formed from the adsorption of $Ru(CO)_3Cl_2(THF)$ onto all four supports. On the more acidic metal oxides, SiO_2 and NaY zeolite, a ligand substitution of a coordinated THF for a surface hydroxyl group to yield a surface species with the stoichiometry $Ru(CO)_3Cl_2(SURFACE)$, where surface is a surface hydroxyl group, is believed to be the pathway of adsorption. While on the more basic supports, MgO and Al_2O_3, a chloride abstraction as well as a ligand substitution of a coordinated THF for three surface hydroxyl groups to form $Ru(CO)_3(SURFACE)_3$ is believed to be the pathway of adsorption. The possibility of having physisorbed **1** on the surface is discarded, since no extracted compounds were observed from subsequent washings of the surface with CH_2Cl_2. Several test reagents were chosen to test the validity of these proposed surface species. These surface reagents, bipyridine, $Co(CO)_4^-$, and CO were chosen based on their known reactivity with ruthenium carbonyls in solution (Scheme 1.1).

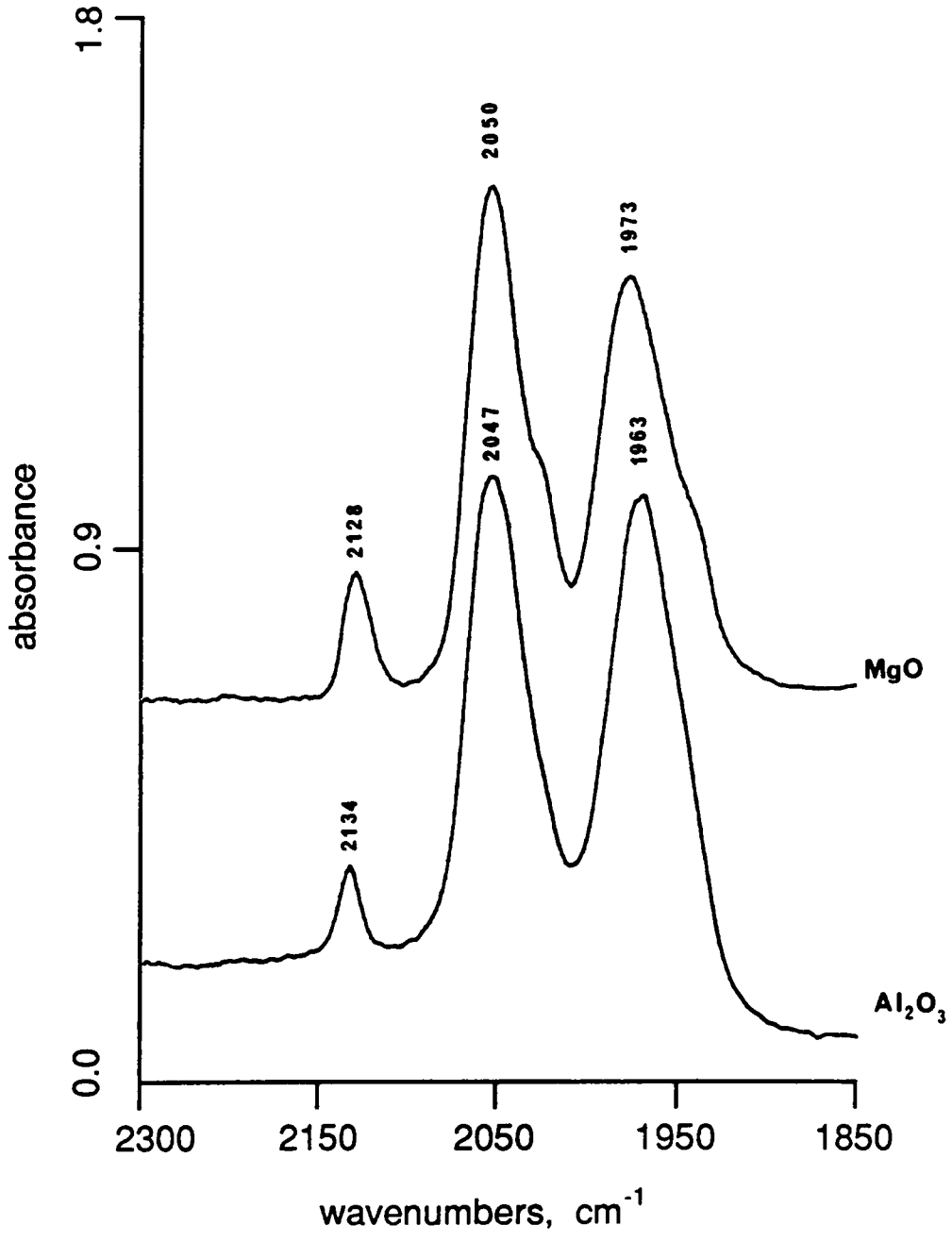

Figure 3.2 The infrared spectra of $Ru(CO)_3Cl_2(THF)$ adsorbed on Al_2O_3 and MgO.

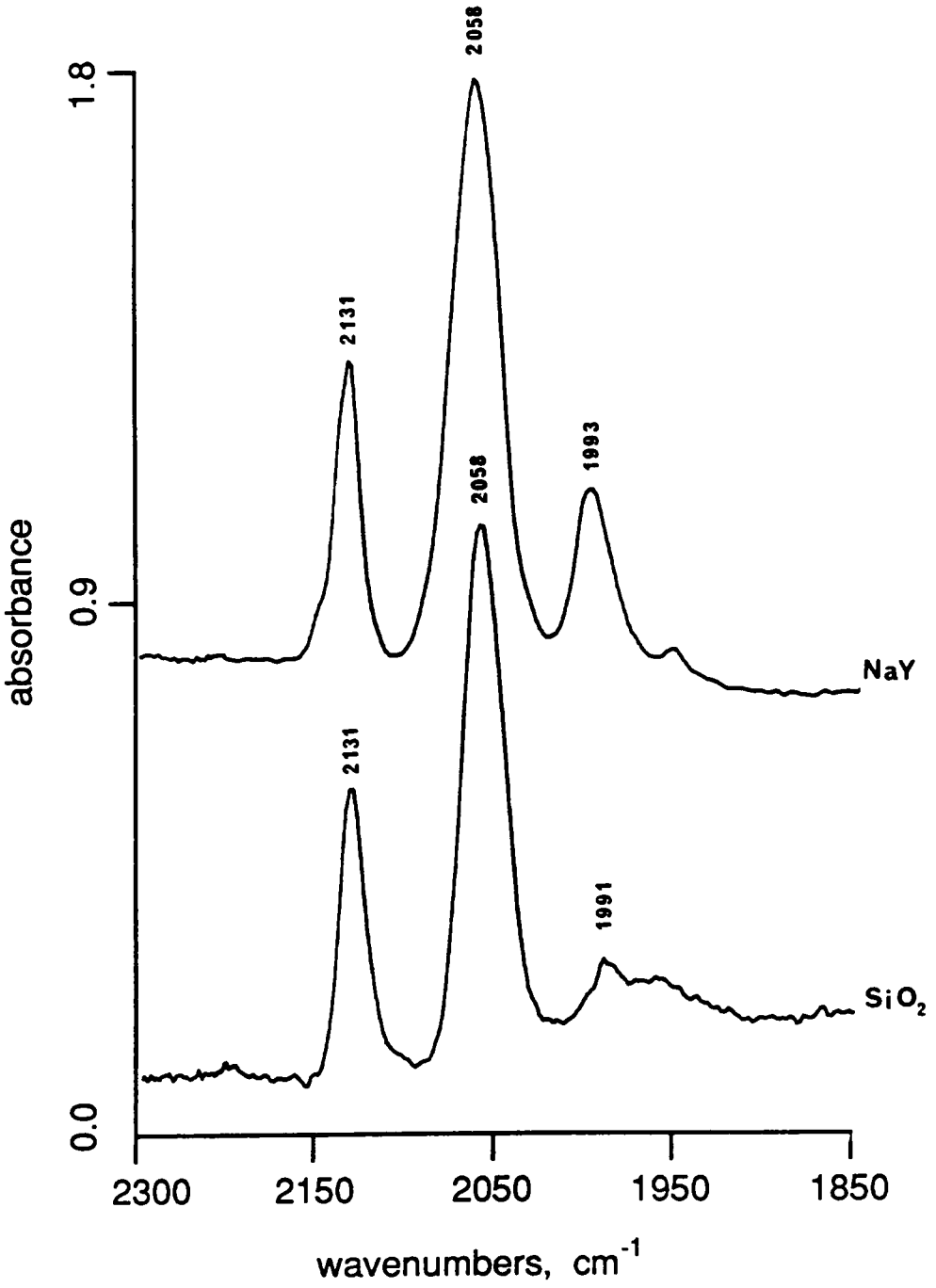

Figure 3.3 The infrared spectra of $Ru(CO)_3Cl_2(THF)$ adsorbed of NaY zeolite and SiO_2.

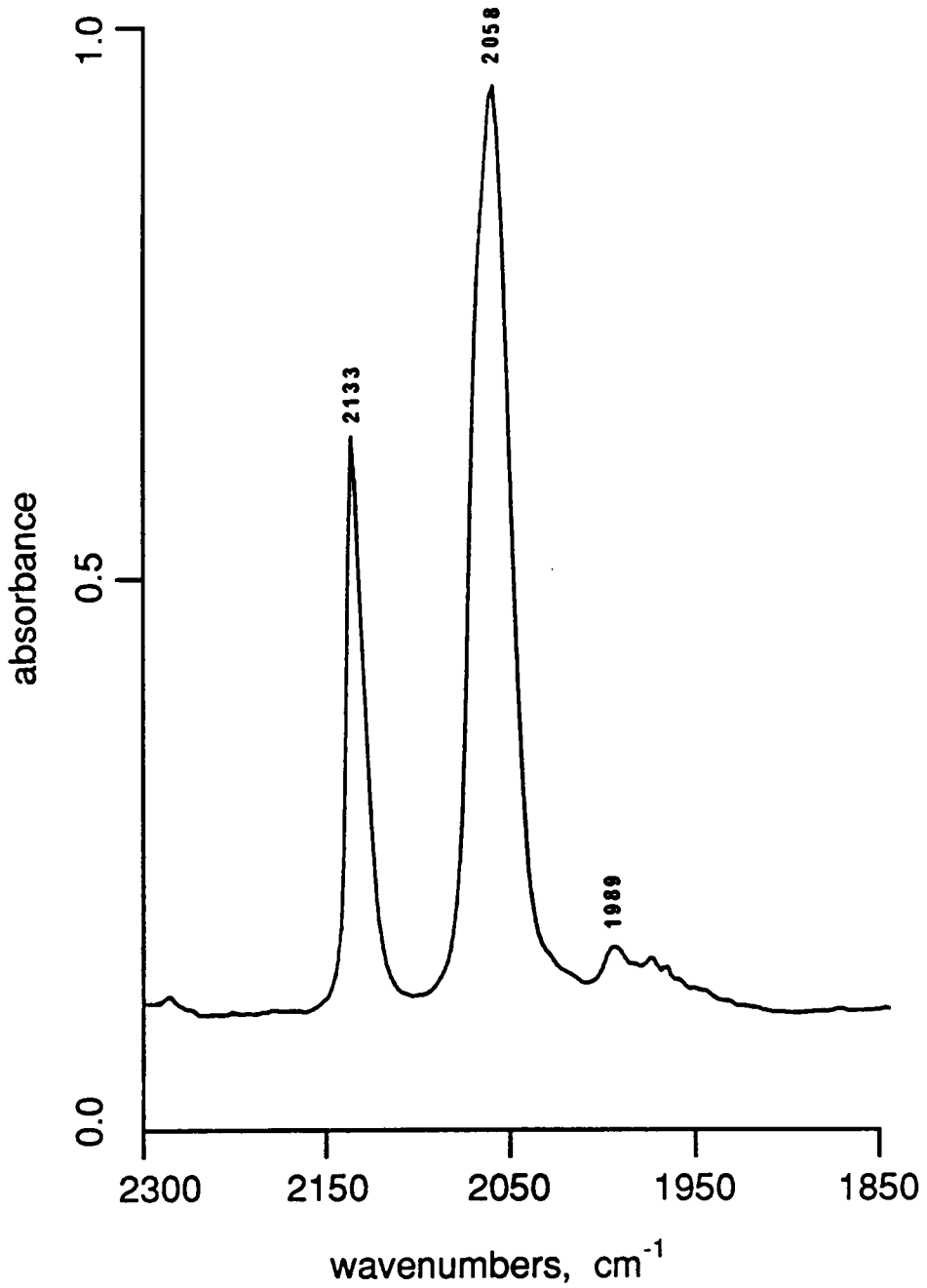

Figure 3.4 The infrared spectrum of $Ru(CO)_3Cl_2(THF)$ in THF.

THE REACTIVITY OF $Ru(CO)_3Cl_2(THF)$(ads) WITH BIPYRIDINE

It is known that the complex $Ru(CO)_2Cl_2$bipy can be synthesized in high yields from **1** and bipyridine, bipy, in THF at room temperature [5]. Bipyridine is also known to react with $Ru_3(CO)_{12}$ supported on SiO_2 to give a very active water-gas shift, WGS, reaction catalyst [61]. Although the exact composition of the catalyst is not known, it has a characteristic two peak infrared spectrum.

The reaction of **1** adsorbed on MgO and Al_2O_3 with bipyridine was monitored by in situ infrared spectroscopy. The results of this reaction on Al_2O_3 are summarized in Figure 3.5. Trace a, in Figure 3.5, shows the infrared spectrum of a ruthenium bipyridine WGS reaction catalyst supported on SiO_2. This was obtained by adsorbing $Ru_3(CO)_{12}$ and bipyridine on SiO_2 followed by heating to 100°C under an atmosphere of helium. During the process the support changed color from yellow to an intense purple, while all the infrared absorbances due to $Ru_3(CO)_{12}$ disappear. Details of this reaction will be described in chapter 5. Trace b, shows **1** adsorbed on Al_2O_3 followed by the addition of bipyridine. Immediately after the adsorption of bipyridine the support turned violet, and the infrared spectrum was recorded, no heating was necessary to generate this spectrum. Also no CO was detected during the reaction of bipyridine and the supported ruthenium carbonyl. When the reaction is performed in the helium flow reactor it appears that a similar ruthenium bipyridine carbonyl species can be synthesized on Al_2O_3 from both $Ru_3(CO)_{12}$ and $Ru(CO)_3Cl_2(THF)$ and bipyridine.

When a THF solution containing bipyridine is brought into contact with **1** adsorbed on NaY zeolite or SiO_2, the support immediately turns light pink and an infrared spectrum, of the supported species, very similar to $Ru(CO)_2Cl_2$bipy is observed. The bipyridine adduct can be extracted from the support with CH_2Cl_2 and gives the identical infrared spectrum as an authentic sample. Once the $Ru(CO)_2Cl_2$bipy complex is formed on NaY zeolite or SiO_2 and heated to 100°C no further reaction takes place. In particular the support does not turn purple in color and the infrared spectrum characteristic of the Ru-CO-bipy complex on Al_2O_3 and MgO is not observed.

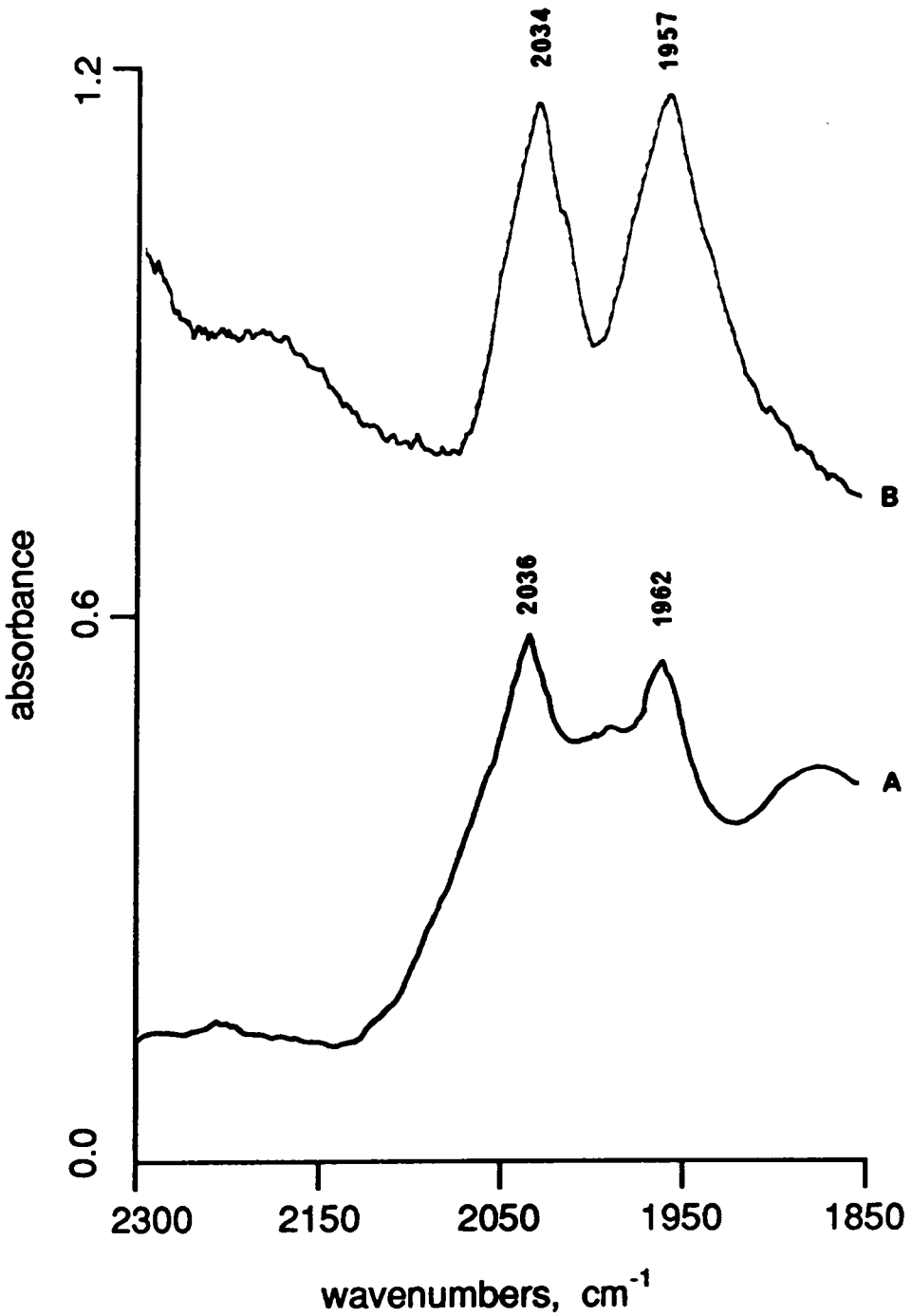

Figure 3.5 A) The infrared spectrum of $Ru_3(CO)_{12}$ and bipyridine co-adsorbed on SiO_2 heated to 100°C. B) The infrared spectrum of $Ru(CO)_3Cl_2(THF)$ and bipyridine co-adsorbed on Al_2O_3.

Furthermore, significant quantities of CO are evolved during the reaction of **1**(ads) and bipyridine on both NaY zeolite and SiO_2. The ability to form $Ru(CO)_2Cl_2$bipy directly from the adsorbed carbonyl on SiO_2 and NaY zeolite suggest that when **1** is adsorbed on on these oxides it retains its ligands.

THE REACTIVITY OF $Ru(CO)_3Cl_2(THF)$ (ads) WITH $Co(CO)_4^-$

It has been shown by Vahrenkamp that the reaction of $Ru_2(CO)_6Cl_4$ and $Co(CO)_4^-$ in water yields $RuCo_2(CO)_{11}$ as a black precipitate [7]. It was found that $Ru_2(CO)_6Cl_4$ can be replaced with **1** with no loss in yield. The bimetallic cluster can then be capped with an additional equivalent of $Co(CO)_4^-$ in THF to form the tetranuclear anion $RuCo_3(CO)_{12}^-$ [8]. Protonation of the anion with H_3PO_4 yields the neutral cluster $HRuCo_3(CO)_{12}$. Tetracarbonyl cobaltate, $Co(CO)_4^-$, is relatively inert to $Ru_3(CO)_{12}$ at room temperature, but is known to cap the metal triangle to form $CoRu_3(CO)_{13}^-$ at elevated temperatures [62].

The reaction of **1**(ads) and $Co(CO)_4^-$ was monitored by in situ infrared spectroscopy by first generating $Ru(CO)_3Cl_2(THF)$(ads) followed by syringing a THF solution of $Co(CO)_4^-$ onto the wafer of inorganic oxide containing **1**(ads).

Figure 3.6 shows the reaction of **1**(ads) with $Co(CO)_4^-$ on Al_2O_3; similar infrared spectra are obtained when the reaction is carried out on MgO. Trace a shows the infrared spectrum resulting from the adsorption of **1** onto Al_2O_3. Trace b is obtained when $Co(CO)_4^-$ in THF is added to this sample. This spectrum contains bands assignable to **1**(ads) at 2134, 2047 and 1963 cm^{-1} and $Co(CO)_4^-$ at 1890 cm^{-1}. No reaction was observed to take place between **1**(ads) and $Co(CO)_4^-$ on either MgO or Al_2O_3. Also, no reaction is observed when the order of adsorption was reversed. For the sample shown in Figure 3.6 the relative amounts of Ru/Co was approximately 2/1 ; the same result, i.e. no reaction, was also observed when an excess of $Co(CO)_4^-$ was used.

A test reaction was performed in order to determine whether the lack of reactivity between $Ru(CO)_3Cl_2(THF)$(ads) and $Co(CO)_4^-$(ads) was the result of the cobalt carbonyl

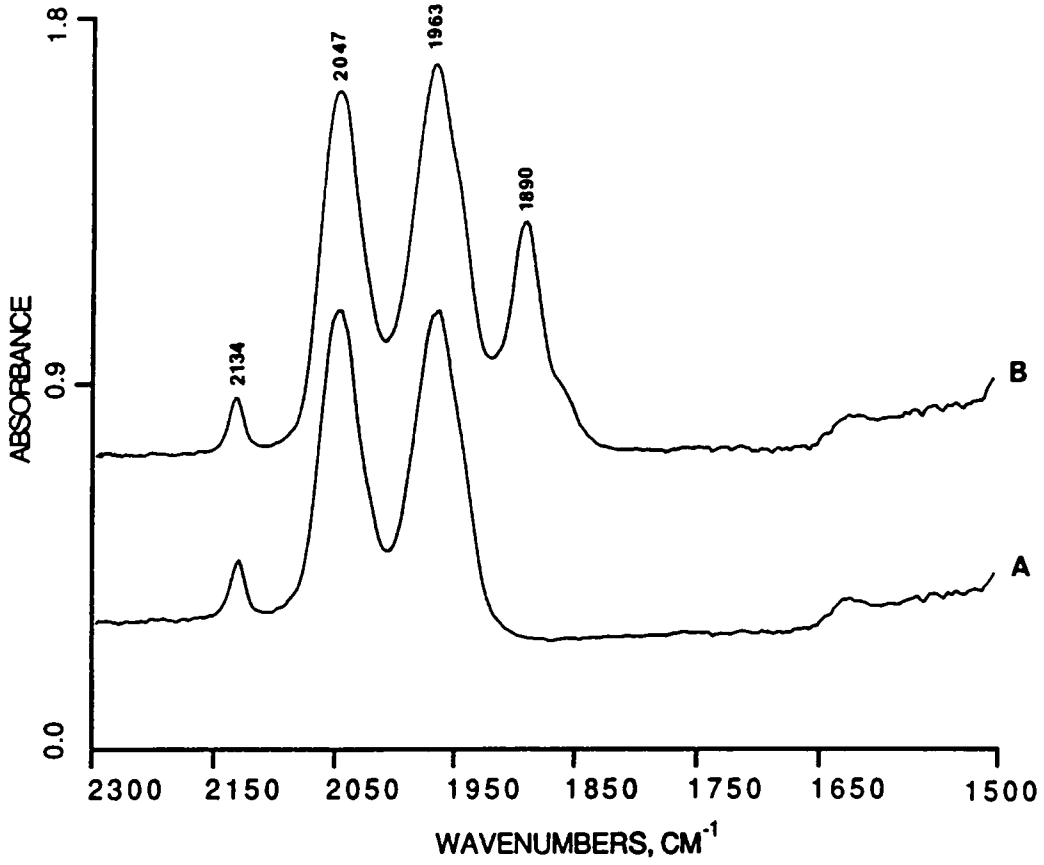

Figure 3.6 A) The infrared spectrum of $Ru(CO)_3Cl_2(THF)$ adsorbed on Al_2O_3. B) The infrared spectrum of $Ru(CO)_3Cl_2(THF)$ and $Co(CO)_4^-$ co-adsorbed on Al_2O_3.

or the ruthenium carbonyl bonding to the surface in such a way that it is unreactive towards the other reagents. It known that in solution CCl_4 reacts with $Co(CO)_4^-$ at room temperature to form a tetranuclear cluster $ClCCo_3(CO)_9$. Therefore if the adsorbed cobalt carbonyl can be transformed into the organometallic cluster, then it is the adsorbed ruthenium carbonyl preventing the formation of a bimetallic cluster.

The in situ reaction between $Co(CO)_4^-$(ads) and CCl_4 was performed by first immersing a pellet of Al_2O_3 or MgO into a THF solution of $Co(CO)_4^-Na^+$ followed by spraying the inorganic oxide with CCl_4. After the CCl_4 wash, the infrared band corresponding to $Co(CO)_4^-$,1890 cm^{-1}, was replaced by bands at 2109, 2062, 2045 cm^{-1}. This is consistent with the formation of the organometallic cluster $ClCCo_3(CO)_9$ [63] on the surface. Therefore it is believed that the ruthenium carbonyl species is bonding to the surface such that it is unreactive and that the cobalt carbonyl anion is only weakly adsorbed on the surface.

The series of infrared spectra shown in Figure 3.7 are generated when **1**(ads) on NaY zeolite is reacted with $Co(CO)_4^-$. Trace a shows the infrared spectrum resulting from the adsorption of **1** onto NaY zeolite. When $Co(CO)_4^-$ in THF is added to this sample trace b is obtained. New bands are now present at 2061, 2014, 2000, 1961, and 1820 cm^{-1}. These are assigned to the tetranuclear cluster anion $RuCo_3(CO)_{12}^-$. An excess amount of $Co(CO)_4^-$ is present in this sample as determined by the band at 1890 cm^{-1}. Stoichiometric amounts of $Co(CO)_4^-$ and **1** were difficult to achieve because the experiment is performed in situ by syringing a solution of $Co(CO)_4^-$ onto the wafer of inorganic oxide containing **1**(ads). When an excess of **1** was used, the infrared bands due to both **1**(ads) and $RuCo_3(CO)_{12}^-$ could not be fully resolved. Therefore, for the sake of clarity, only the infrared spectrum from the experiment utilizing an excess of $Co(CO)_4^-$ is shown. The absorption at 1640 cm^{-1} is assigned to physisorbed water which could not be removed during the pretreatment.

An adsorbed compound can reside in one of three places on a faujasitic zeolite: 1. on the surface, 2. in the channels between the α cages, or 3. in the α cages. The

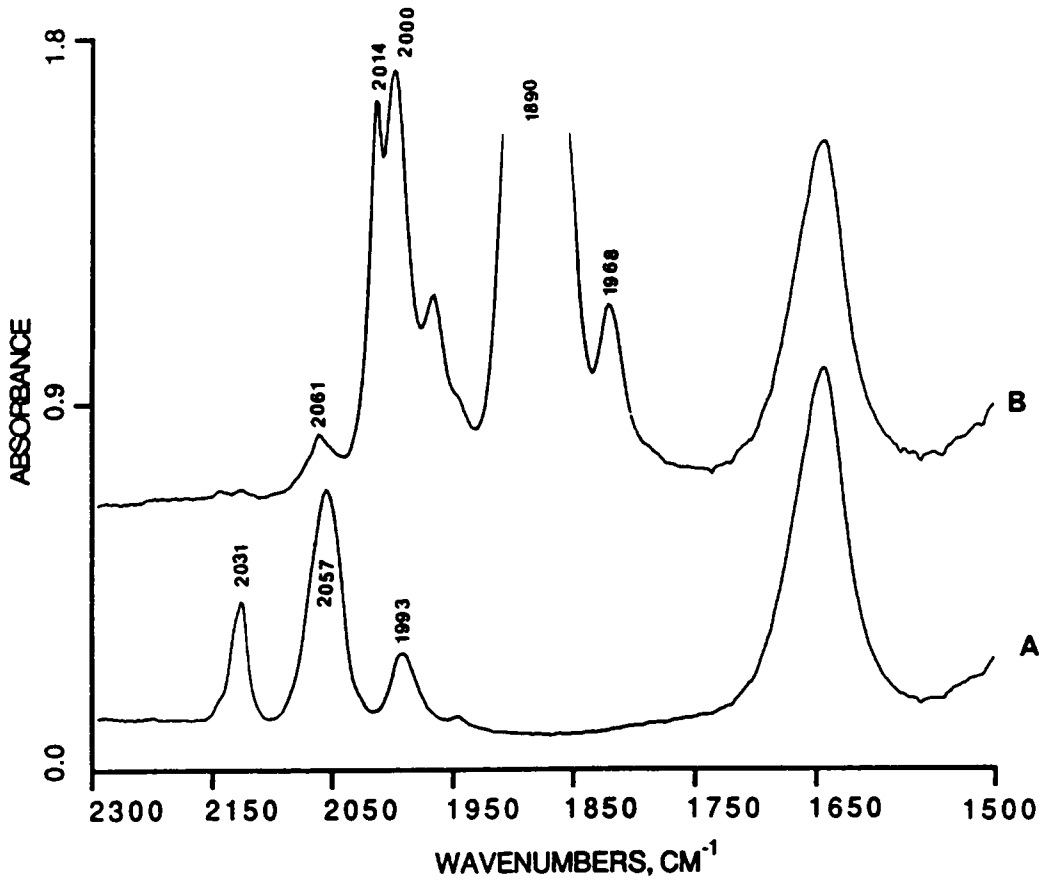

Figure 3.7 A) The infrared spectrum of $Ru(CO)_3Cl_2(THF)$ adsorbed on NaY zeolite. B) The infrared spectrum of $Ru(CO)_3Cl_2(THF)$ and $Co(CO)_4^-$ adsorbed on NaY zeolite.

average spacial diameter for tetranuclear compounds is approximately 9.5Å, as determined by molecular models, which is small enough to fit in the 13Å α cages but larger then than the 8.1Å kinetic pore diameter of NaY zeolites [64].

The most common method for determining the position or the adsorbed compound is by reacting it with phosphines of various sizes [65]. If the supported compound reacts with a phosphine with a smaller spacial diameter then the pore of the zeolite, but not with one with a larger spatial diameter, then it is very likely that the compound resides in the α-cages of the zeolite. If the adsorbed compound reacts with both a large and small phosphine, then the adsorbed compound is believed to reside on the surface of the zeolite.

When the anion $RuCo_3(CO)_{12}^-$ was synthesized as described above and reacted with a neat solution of PEt_3, infrared bands corresponding to the bimetallic anion disappear and bands corresponding to $Co(CO)_4^-$ appeared. The spectrum also contained several unassignable bands, between 1950 and 2200 cm^{-1}, which are most likely due to cobalt and/or ruthenium carbonyl phosphine cations [66,67]. No reaction was observed when the same reaction was performed with a large phosphine such as $P(tBu)_3$. This does not prove that the bimetallic anion is in the α cages since no reaction was observed by infrared spectroscopy between $RuCo_3(CO)_{12}^-$ and $P(tBu)_3$ in a THF solution. Furthermore $RuCo_3(CO)_{12}^-$ does not react with any other large phoshine, PPh_3 or PPh_2R R= Me, Et, or t-Bu or large amines, $N(tBu)_3$ or NPh_3. Thus the location of the cluster on the zeolite could not be concluded using this method, therefore an indirect method had to be employed. This consisted of determining whether the reactants were contained in the α cages or on the surface. This is based on the assumption that if the reactants, **1**(ads) and $Co(CO)_4^-$(ads), reside in the α cages then the resulting product, $RuCo_3(CO)_{12}^-$, must also be contained in the α cages.

When **1**(ads) was reacted with a phosphine, whether large or small, a two peak infrared spectrum corresponding to $Ru(CO)_2Cl_2(PR_3)_2$ [68] was observed. Since the ruthenium-phosphine was synthesized from both large and small phosphines, it is believed that **1**(ads) resides on the surface of the zeolite. In the case of $Co(CO)_4^-$(ads), addition

of phosphines did not change its composition or the infrared spectrum. Nor did the addition of phosphines to a THF solution of $Co(CO)_4^-$ produce any new species. As was performed on Al_2O_3 and MgO, $Co(CO)_4^-$(ads) was first transformed to $ClCCo_3(CO)_9$ by the addition of CCl_4. The organometallic cluster was then fragmented to $Co(CO)_4^-$(ads) by the addition of P-tBu_3 or PEt_3, thus suggesting that the cobalt carbonyl anion resides on the surface of the zeolite. Since both reactants are present only on the surface of the zeolite it is most likely the tetranuclear anion also resides on the surface.

Furthermore if the cluster was synthesized inside the α cages it would be very unlikely that it could be extracted from the zeolite. When $RuCo_3(CO)_{12}^-$ is synthesized in situ and extracted from the NaY zeolite with [PPN]Cl in CH_2Cl_2, the infrared spectrum of the resulting solid contains no bands in the carbonyl region; thus all of the anion was removed from the support, Both the reactivity and extraction results support the conclusion that the anion resides on the surface and not within the large α cages of the zeolite.

THE REACTIVITY OF $Ru(CO)_3Cl_2(THF)$(ads) WITH CARBON MONOXIDE

When the adsorption of **1** onto hydroxylated Al_2O_3 is performed under an atmosphere of carbon monoxide or when the surface species generated above is placed under an atmosphere of carbon monoxide a new reaction takes place. Figure 3.8 shows the infrared spectra obtained in situ during the adsorption of **1** onto Al_2O_3 under CO as a function of time. The first spectrum, trace a, represents the sample immediately after adsorption. Initially the surface species is the same as described in section 3B which is identified by its major bands at 2044 and 1962 cm^{-1}. With time new bands at 2012, 1987, and 1951 cm^{-1} increase in intensity as the bands due to the starting material, 2044 and 1962 cm^{-1}, decrease in intensity. After 30 minutes the bands corresponding to the starting material have completely disappeared and major bands at 2012, 1987, 1951, and 1731 cm^{-1} are seen. This spectrum is assigned to $HRu_3(CO)_{11}^-$(ads). The bands for the

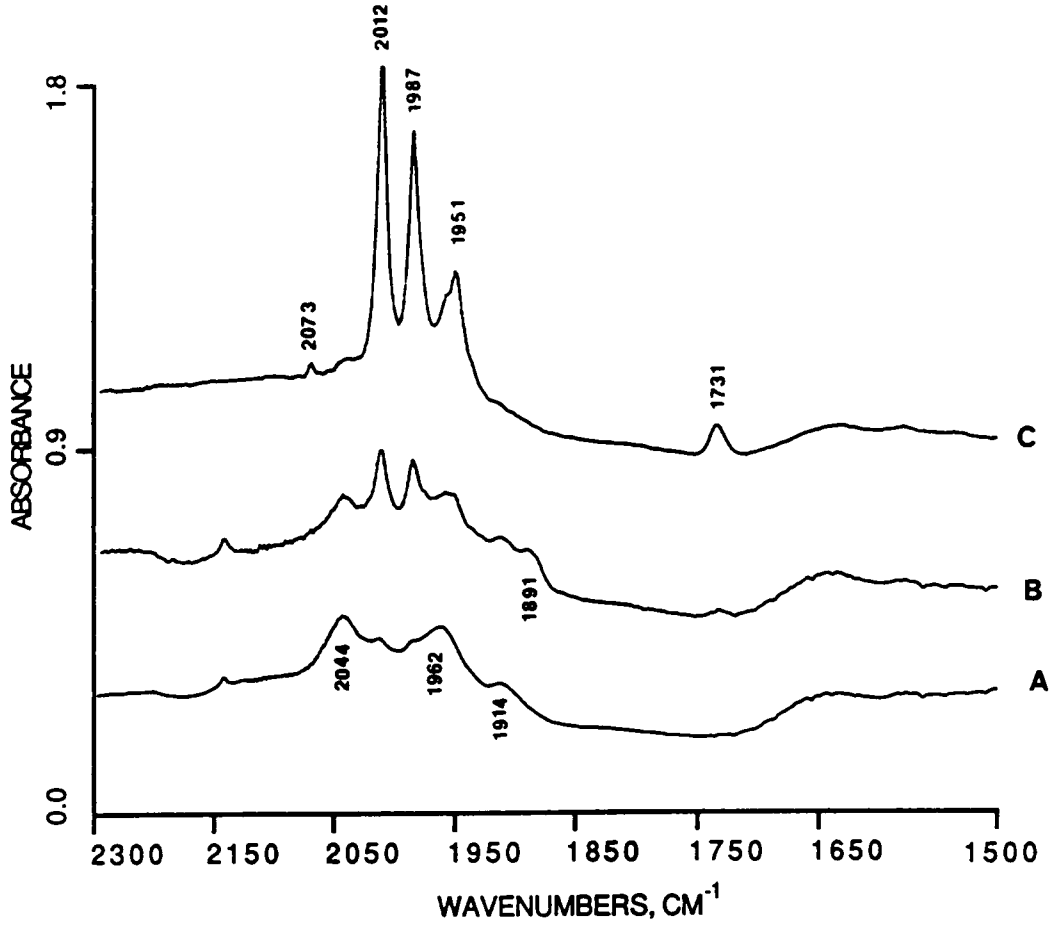

Figure 3.8 The infrared spectra of $Ru(CO)_3Cl_2(THF)$ adsorbed on Al_2O_3 under an atmosphere of CO as a function of time, trace a t=0 min., b t=7 min. and c t=30 min.

surface anion generated from the ruthenium carbonyl chloride correspond well to those reported for $HRu_3(CO)_{11}^-$ with PPN^+ or NEt_4^+ cations in THF [69]. The adsorption at 2148 cm^{-1} is a result of the subtraction of gas phase CO from the sample. In solution the position of the bridging band is very sensitive to the nature of the cation. The spectra shown by Darensbourg[46] for the supported cluster are significantly different than observed here. A well defined bridging carbonyl is not seen by Darensbourg [46], or others [41,45], for $Ru_3(CO)_{12}$ adsorbed on aluminum oxide. However it should be noted that the solvent used in this study, namely THF, interacts strongly with alumina surfaces and may poison Lewis acid sites. This would prevent any bridging carbonyl from forming a Lewis acid-base adduct on the surface. Thus when synthesized in the presence of THF on the surface the bridging carbonyl band of $HRu_3(CO)_{11}^-$ is readily seen while in the absence of a coordinating solvent the bridging carbonyl band may be shifted to a lower wave-number. This suggests that $HRu_3(CO)_{11}^-$(ads) is synthesized on Al_2O_3 is only weakly adsorbed.

When $HRu_3(CO)_{11}^-$ is generated on the surface from $Ru(CO)_3Cl_2(THF)$ under batch conditions, it is easily extracted from the surface as its PPN^+ salt in CH_2Cl_2. The extracted cluster anion is identified as $[PPN]HRu_3(CO)_{11}$ by infrared spectroscopy and comparison with an authentic sample [69]. Digestion of the support and analysis by direct current plasma, DCP, following the extraction shows 10% of the total ruthenium remains on the alumina. The extraction can be made more quantitative by using the binary solvent system THF/CH_2Cl_2 plus [PPN]Cl. Under these conditions no ruthenium is detected on the alumina following the extraction.

When 1(ads) on MgO is placed under an atmosphere of CO at 25°C for 1 hour, the support changes color from light yellow to orange. Figure 3.9 shows the infrared spectrum of the resulting orange support. This spectrum contains absorptions assigned to 1(ads) (2133, 2048, and 1900 cm^{-1}) as well as an additional peak at 2022 cm^{-1}. Additional exposure to CO did not generate larger quantities of the new species. This new band could be consistent with the formation of the cluster $HRu_6(CO)_{18}^-$. Since

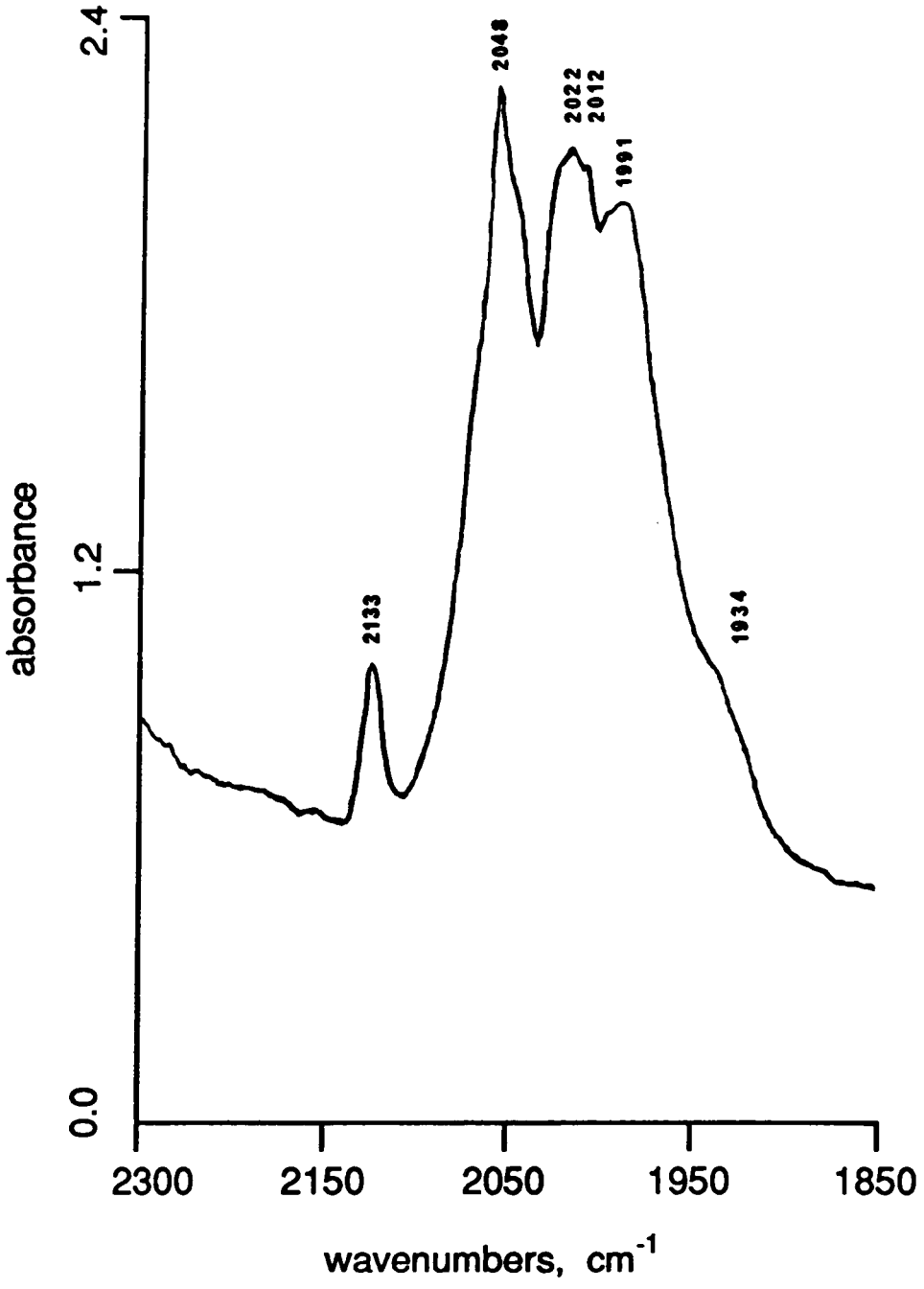

Figure 3.9 The infrared spectrum of $Ru(CO)_3Cl_2(THF)$ adsorbed on MgO under an atmosphere of CO.

extraction with [PPN]Cl in CH_2Cl_2 did not yield any identifiable ruthenium carbonyl complexes an exact assignment of the peak can not be made. Pierantozzi et al [14] have reported the formation of the deprotonated cluster $Ru_6(CO)_{18}^{-2}$ from the carbonylation of $Ru_3(CO)_{12}$ adsorbed on partially dehydroxylated MgO (200°C vacuum). If the anion $Ru_6(CO)_{18}^{-2}$ was formed by the carbonylation of **1**(ads), it is quite possible that any physisorbed water on the surface would have protonated the cluster. Gates et al [70] report that the cluster $Ru_6C(CO)_{18}^{-}$ can be synthesized from $RuCl_3$ on MgO with $CO:H_2$ (10 atm) at 225°C. However this carbido cluster contains three characteristic infrared bands, of which, none are present in the spectrum generated from **1**(ads) on MgO under CO. It should be noted that structural assignments based only on infrared band positions are sometimes inaccurate especially when extraction of the surface species followed by characterization using other analytical techniques cannot be performed.

When **1** supported on NaY zeolite or SiO_2 was placed under an atmosphere of CO at 25°C no reaction was observed. Even exposures of CO (1 atm) for 24 hours did not alter the infrared spectrum of the adsorbed species.

3C DISCUSSION

The observation of very little evolved CO during the adsorption of **1** onto all four supports is consistent with the formation of a "$Ru(CO)_3$" species adsorbed on the surface. Furthermore the spontaneous adsorption from solution suggests that the adsorption proceeds via a substitution of the Cl^- and/or THF ligands by surface hydroxyl groups.

As shown in Figures 3.2 and 3.3, the infrared spectra of **1** supported on SiO_2 and NaY zeolite and in solution are very similar. This, along with the spontaneous adsorption from solution, implies that coordinated THF has been replaced by a surface hydroxyl group. Three bands in the infrared spectrum are also observed for **1** supported on MgO and Al_2O_3, although these bands have different relative intensities and a shift of up to 30 cm^{-1} as compared to **1**(ads) on SiO_2 or NaY zeolite. A simple ligand substitution of THF by a surface hydroxyl group can not be used to explain the differences observed in the

infrared spectrum, therefore it is believed that the chloride ligands are abstracted by the support during the adsorption.

Darensbourg [46] and Bell [41] have independently generated infrared spectra of a surface species, synthesized by the decomposition of $Ru_3(CO)_{12}$ on Al_2O_3 followed by recarbonylating with CO, that are very similar to the infrared spectrum of 1(ads) on Al_2O_3 and MgO. They speculate that the surface species generated is $Ru^{\circ}(CO)_y$(ads) y= 3 or 4. A tri- or tetra- carbonyl species seems like a reasonable assignment since it has been well established that the adsorption and decomposition of $Ru_3(CO)_{12}$ on Al_2O_3, under similar conditions, yields ruthenium dicarbonyls and recarbonylation would lead to a species containing three or more carbonyl ligands. The assignment of a ruthenium tri- or tetra- carbonyl species was made by each author strictly on infrared analysis, CO evolution during the decomposition and CO uptake during the recarbonylation was not quantified. For these reasons, the formation of two different surface bound $Ru(CO)_3$ species are postulated for the adsorption of **1** onto all four supports.

The adsorption of **1** onto MgO and Al_2O_3, and SiO_2 and NaY zeolite are shown in Scheme 3.1.

The first reaction, in Scheme 3.1, is an example of a ligand substitution of THF for a donor ligand (surface hydoxyl group). There is a great deal of precedent for this type of reaction in the chemical literature as evidence by the synthesis of compounds, of the form $Ru(CO)_3Cl_2L$ (L= PPh_3 or pyridine) the displacement of THF in **1** [5]. The second reaction can also be classified as a ligand substitution, although a chloride abstraction must occur prior to the substitution. An important feature is that the more basic metal oxides, MgO and Al_2O_3, apparently act as a halide acceptor. As stated in Chapter 1, it has been suggested by Psaro et al. that MgO acts as a chloride acceptor during the adsorption of $Os(CO)_3Cl_2$ to form $Os(CO)_3$(ads) [71]. Basset et al [47] have postulated that a $Ru(CO)_3$ species can be generated from the adsorption of $Ru_2(CO)_6Cl_4$ onto partially dehydroxylated SiO_2 (225°C in vacuo) however the authors do not present data demonstrating that the chloride ligands were actually abstracted, e.g. XPS or EXAFS

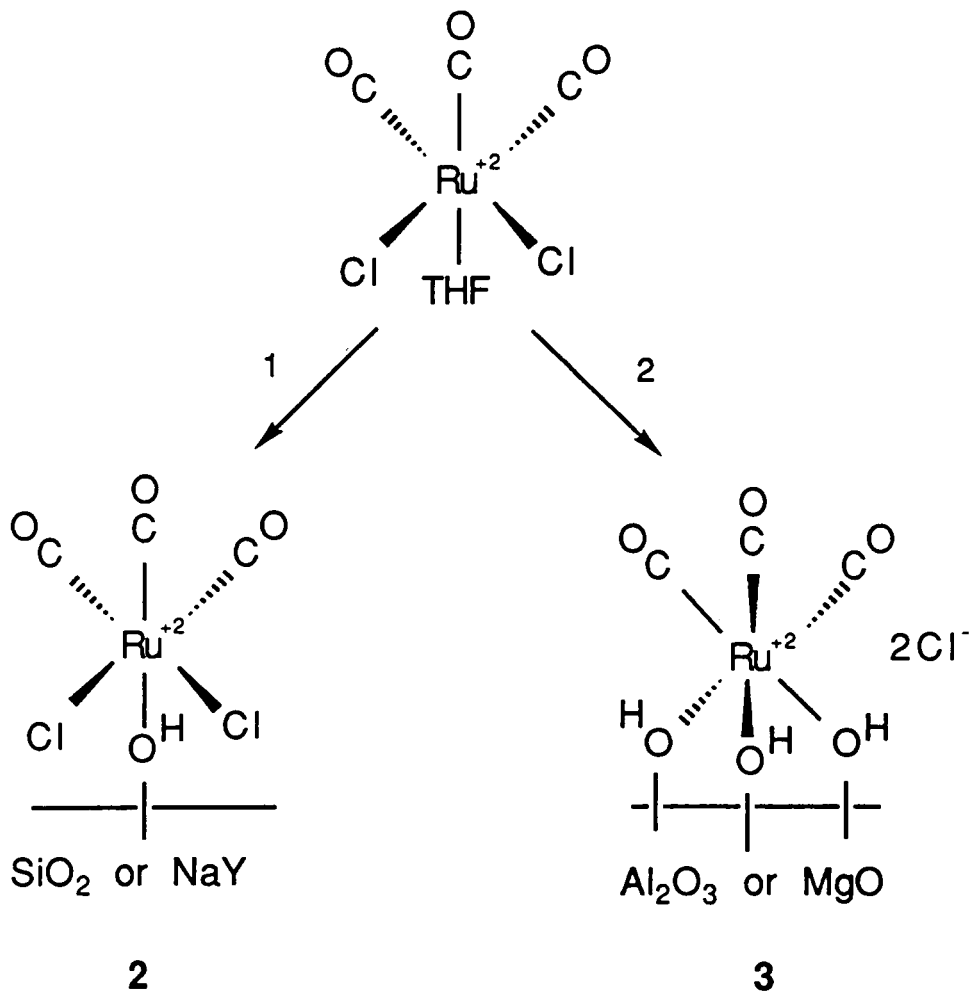

Scheme 3.1 Surface species generated from the adsorption of $Ru(CO)_3Cl_2(THF)$ on MgO, Al_2O_3, SiO_2 and NaY zeolite.

spectra or the reactivity of the surface species. The infrared spectrum of the his adsorbed ruthenium tricarbonyl species is virtually the same as its ruthenium carbonyl chloride precursor. Therefore a simple physisorption would be more accurate to describe the adsorption taking place in Basset's experiment.

It could be suggested that the metal to surface bond in **3** is through a surface oxo group (-OAl) rather then a hydroxyl group (HOAl). In this study there was no way of distinguishing the difference between the two. If the bond was through a hydroxyl group, then a shift in the infrared OH stretch should be observed, also if the bond was through an oxo group then there should be a decrease in the OH infrared stretch following the adsorption. Since neither phenomenon was observed, it can not be concluded at this time whether the bonding takes place through a surface oxo group on the surface. The stabilization of Ru^{+2} tricarbonyls appears to be unique to inorganic oxide surfaces since no molecular compounds of the form $Ru^{+2}(CO)_3L_2L'$ where L= a neutral donor ligand and L' is a neutral or anionic ligand, are known.

The reactivity of the adsorbed species towards the various reagents, presented in the results section, were investigated in order determine if the adsorption of **1** involved the abstraction of the chloride ligands by the metal oxide.

The retention of coordinated Cl^- by the surface species can be best shown by the reaction of **2** and bipyridine. In solution bipyridine reacts with **1** to expel one equivalent of CO and THF to form $Ru(CO)_2Cl_2bipy$ [5]. The observation of $Ru(CO)_2Cl_2bipy$ on the surface along with the evolution of CO during the reaction clearly demonstrates that the $Ru(CO)_3Cl_2$ moiety resides on the surface of SiO_2 and NaY zeolite. The reaction of **3** and bipyridine is evident by the appearance of an intense purple color of the support. During the reaction no additional CO was evolved. The infrared spectrum of this new surface species does not correspond well with any known ruthenium carbonyl bipyridine complexes namely, $Ru(CO)_2Cl_2bipy$ [5], $Ru_3(CO)_{10}bipy$ [72,73], $Ru(CO)_2bipy_2$ [74], $Ru(CO)bipy_2H$ [75]. The same ruthenium carbonyl bipyridine complex can be synthesized on both SiO_2 and Al_2O_3 from bipyridine and ruthenium carbonyls which

contain no chloride ligands, such as $Ru(CO)_5$ and $Ru_3(CO)_{12}$, this is consistent with the postulation that the ruthenium in **3** does not contain chloride ligands.

It is clear that the reaction of **2** and $Co(CO)_4^-$ yields the adsorbed anion $RuCo_3(CO)_{12}^-$, which is also observed for **1** in solution. No reaction was observed between **3** and the cobalt carbonyl anion. This second reaction neither proves nor disproves the presence of a chloride ligand. If **3** does not contain chloride ligands, consistent with all previous results, then the failure to synthesize $RuCo_3(CO)_{12}^-$ from **3** suggests that the surface hydroxyl groups of MgO and Al_2O_3 are poorer leaving groups than chloride ligands.

The reactivity of **2** towards CO is also consistent with the solution chemistry of **1** ; for both, no reaction is observed. This is not surprising since the formation of ruthenium carbonyl clusters from **1** and CO only occur in the presence of a halide acceptor and reducing agent. Elevated temperatures and pressures were not used because $Ru_3(CO)_{12}$ can be synthesized from **1** in yields less than 10%, at high pressures of CO and elevated temperatures.

When **3** on Al_2O_3 was exposed to CO the cluster anion $HRu_3(CO)_{11}^-$ was readily observed. The same anion is also observed from the direct adsorption of $Ru_3(CO)_{12}$ on hydroxylated Al_2O_3. Ruthenium carbonyl chlorides are known to react with CO at atmospheric pressure in the presence of zinc to yield $Ru_3(CO)_{12}$ [6]. Therefore two pathways for the formation of the adsorbed anion $HRu_3(CO)_{11}^-$ can be postulated, they are described by equations 3.1 and 3.2.

$$3\ Ru^{+2}(CO)_3(SURFACE)_3 \xrightarrow{CO} Ru_3(CO)_{12} \xrightarrow{Al_2O_3} HRu_3(CO)_{11}^- \qquad 3.1$$

$$3\ Ru^{+2}(CO)_3(SURFACE)_3 \xrightarrow[Al_2O_3]{CO} HRu_3(CO)_{11}^- \qquad 3.2$$

In equation 3.1, **1**(ads) is first transformed to $Ru_3(CO)_{12}$ which then reacts with the

hydroxylated alumina to produce the cluster anion. While in equation 3.2, 1(ads) is transformed directly to the $HRu_3(CO)_{11}^-$ in the presence of CO. Since infrared bands due to $Ru_3(CO)_{12}$ are not observed in the series of spectra in Figure 3.8, either $Ru_3(CO)_{12}$ is synthesized and reacts with the Al_2O_3 faster than can be detected by infrared spectroscopy or the anion is generated directly from the adsorbed $Ru^{+2}(CO)_3$ surface species without forming the intermediate $Ru_3(CO)_{12}$.

The anion $HRu_3(CO)_{11}^-$ is not observed when **1** adsorbed on MgO is exposed to an atmosphere of CO, however a new species in addition to 1(ads) is present. No exact assignment has been made for this species.

3D Summary

In summary the adsorption of **1** onto MgO and Al_2O_3 yields the surface species $Ru^{+2}(CO)_3(SURFACE)_3$ however when **1** is adsorbed onto SiO_2 or NaY zeolite the surface species $Ru^{+2}(CO)_3Cl_2(SURFACE)$ is formed. These assignments are based not only on CO evolution and infrared spectroscopy, but also the reactivity of the adsorbed species towards various reagents.

The reactivity of 1(ads) on SiO_2 or NaY zeolite was observed to be the same as **1** in solution. The reaction of 1(ads) and bipyridine produced $Ru(CO)_2Cl_2$bipy, no ruthenium carbonyl clusters were formed from the exposure of 1(ads) to CO and the bimetallic cluster, and $RuCo_3(CO)_{12}^-$, was readily synthesized from 1(ads) and $Co(CO)_4^-$.

The reactivity of 1(ads) on Al_2O_3 or MgO was observed to be very different then that of 1(ads) on SiO_2 or NaY zeolite. The reaction of 1(ads) and bipyridine produced a compound which contained no chloride ligands, the formation of ruthenium carbonyl clusters on Al_2O_3 from 1(ads) and CO and the inability to form the cluster $RuCo_3(CO)_{12}^-$ from 1(ads) and $Co(CO)_4^-$ indicates that a surface species coordinatively different from **1** is formed. Specifically, a ruthenium carbonyl without coordinating chloride resides on the surface as $Ru^{+2}(CO)_3(SURFACE)_3$.

CHAPTER 4

THE SYNTHESIS AND CHARACTERIZATION OF MOLECULAR MODELS OF $Ru(CO)_3Cl_2$(SURFACE) AND $Ru(CO)_3$(SURFACE)$_3$

4A INTRODUCTION

Many times the results from a combination of several indirect surface analytical techniques are needed to characterize a supported organometallic compound. An available tool in this case was the synthesis of molecular analogs, model compounds, of the supported complex. As mentioned in Chapter 1, ideal model compounds for supported metal carbonyls incorporate ligands containing oxygen, such as ethers or alkoxides, to emulate the oxygen sites present on the surface of inorganic oxides. The objective in designing model compounds is to synthesize a compound which is believed to be structurally similar to its supported counterpart. Once synthesized, the molecular analog can be characterized by classical methods, such as infrared and mass spectroscopy, x-ray diffraction and chemical analysis. If both the molecular analog and supported complex have similar spectroscopic properties and reactivity patterns, then the supported complex can be suggested to have a similar structure.

The objective of the work presented in this chapter is, to synthesize and characterize ruthenium carbonyl compounds that are coordinatively similar to the surface species $Ru(CO)_3Cl_2$(SURFACE) and $Ru(CO)_3$(SURFACE)$_3$, formed by the adsorption of $Ru(CO)_3Cl_2$(THF) on SiO_2 or NaY and Al_2O_3 or MgO respectively.

The compound $Ru(CO)_3Cl_2(H_2O)$ was synthesized to model the surface species $Ru(CO)_3Cl_2$(SURFACE); water was used as a ligand to best emulate the surface hydroxyl group. The literature contains several examples for the synthesis of compounds of the form $Ru(CO)_3Cl_2L$ where L= THF, PR_3, or pyridine [5,75], however this is the first time the water adduct, L= H_2O, has been reported [77].

Since there were no known molecular analogs of $Ru(CO)_3$(SURFACE)$_3$, a synthetic strategy incorporating the substitution of both the chloride and THF ligands of

$Ru(CO)_3Cl_2(THF)$ for oxygen and/or phosphorous donor ligands was used. Silver triflate, $AgSO_3CF_3$, was used to abstract the chloride ligands and various donor ligands such as water, ethers and phosphines were used to model the surface hydroxyl groups.

4B EXPERIMENTAL

The compound $Ru(CO)_3Cl_2(H_2O)$ was synthesized from $Ru(CO)_3Cl_2(THF)$ by a ligand substitution of THF for H_2O in the following manner. A 100 ml flask was charged with 200 mg of $Ru(CO)_3Cl_2(THF)$, 10 μL of H_2O, and 50 mL of diglyme, the solution was then stirred at room temperature for 1 hour, after which time it was stored at -10°C. After three weeks a small amount of transparent crystals were present on the walls of the flask. Filtration of the solution yielded approximately 10 mg of $Ru(CO)_3Cl_2(H_2O)$ crystals, approximately 4% yield. Removal of the solvent, from the mother liquor, under vacuum yielded $Ru_2(CO)_6Cl_4$ as a cream colored noncrystalline solid. Crystals suitable for single crystal X-ray diffraction analysis were determined by size, shape, and clarity.

Solution 200 MHz ^1H NMR spectra were obtained using an IBM WP200 NMR spectrometer. All NMR spectra were referenced to the residual proton resonance of the deuterated solvent.

The reaction between silver triflate, Agtrif, and $Ru(CO)_3Cl_2(THF)$ was performed as follows. A solution of Agtrif 154 mg (.6 mmol) and $Ru(CO)_3Cl_2(THF)$ 100 mg (.3 mmol) in 50 mL of CH_2Cl_2 was stirred, at room temperature, for 1 hour under an inert atmosphere. The flask was also covered with aluminum foil to prevent the photo reduction of the silver chloride produced. Blank experiments demonstrated that stirring AgTrif in CH_2Cl_2 did not produce any AgCl. The white precipitate of silver chloride was separated from the solution by a canula with one end wrapped with a piece of filter paper. This allowed for the filtration of the AgCl and the transfer of the air sensitive liquid to be performed under nitrogen. The receiving flask contained 0.9 mequ of the desired donor ligand under an inert atmosphere. The solution containing the ruthenium

carbonyl and donor ligand was then stirred for 30 minutes, at this time the solutions were typically light yellow. Removal of the solvent under a reduced atmosphere yielded an air sensitive oil. The resulting white paste of AgCl was washed with 10 ml of CH_2Cl_2 to remove any residual ruthenium carbonyl. The silver chloride was washed out of the flask with water and collected on filter paper, dried and weighed.

4C RESULTS AND DISCUSSION

THE CHARACTERIZATION OF $Ru(CO)_3Cl_2(H_2O)$

Infrared absorptions in the carbonyl region for $Ru(CO)_3Cl_2(H_2O)$ and related compounds are presented in Table 4.1. As evidence by its infrared spectrum, the compound $Ru(CO)_3Cl_2(H_2O)$ is a good molecular model of $Ru(CO)_3Cl_2(THF)$ adsorbed on SiO_2 and NaY zeolite. Both the model compound and the supported species contain three absorptions at virtually the same wavenumbers and relative intensities when the infrared was recorded in the solid state as a mull or KBr pellet.

The position of the infrared bands corresponding to $Ru(CO)_3Cl_2(H_2O)$ are very sensitive to the matrix used when obtaining the infrared spectrum. When the infrared spectrum was recorded as a KBr pellet, two strong bands were observed at 2133 and 2052 cm^{-1}, however; when the infrared was recorded in parrafin oil as a mull, three bands were observed at 2135, 2053, and 1996 cm^{-1}. When the infrared spectrum was recorded as a CH_2Cl_2 solution, only two bands were observed at 2142 and 2060 cm^{-1}. Upon standing for 24 hours, the two absorptions shift to higher wavenumbers, 2144 and 2083 cm^{-1}. At this time the infrared spectrum was indistinguishable from the infrared spectrum of $Ru_2(CO)_6Cl_2$ in CH_2Cl_2.

These infrared results were consistent with the dimerization of $Ru(CO)_3Cl_2(H_2O)$ to $Ru_2(CO)_6Cl_4$. In fact the dimerization of $Ru(CO)_3Cl_2(THF)$ in methylene chloride is used to synthesize highly pure $Ru_2(CO)_6Cl_4$ [5]. When $Ru(CO)_3Cl_2(H_2O)$ was dissolved in THF an infrared indistinguishable from $Ru(CO)_3Cl_2(THF)$ was observed. This was not very surprising since THF could easily displace the water ligand.

Table 4.1

Carbonyl infrared stretching frequencies for compounds of the form $Ru(CO)_3Cl_2L$, where L = a donor ligand.

L	MATRIX	ν (CO) cm^{-1}		
NaY	a	2134s	2058s	1984w
SiO_2	a	2131s	2058s	1990w
H_2O				
	KBr	2133s	2052s	
	Nujol	2135s	2053s	1996w
	THF	2133s	2058s	1991w
	CH_2Cl_2	2142s	2060s	
THF				
	THF	2133s	2058s	1991w
	CH_2Cl_2	2142s	2060s	

a. Similar spectra where obtained from either a nujol mull or from a free standing pellet.

The dimerization of $Ru(CO)_3Cl_2(H_2O)$ was also seen in a series of ^1H NMR spectra recorded over 20 hours, Table 4.2. When a proton NMR was obtained from a freshly prepared solution of $Ru(CO)_3Cl_2(H_2O)$ in $CDCl_3$, resonances due to coordinated water and dissolved water were observed at 6.09 and 1.64 PPM respectively (referenced to $CHCl_3$ at 7.2 ppm). Also present in the spectrum were resonances due to diglyme at 3.41 and 3.72 PPM, these resonances are assigned to the methyl and methylene hydrogens respectively. The relative integrated intensities of total water hydrogens to diglyme hydrogens was 1 to 7, which is expected for $Ru(CO)_3Cl_2(H_2O)\cdot C_6H_{14}O_3$. With time the resonance assigned to coordinated water decreases while the resonance due to dissolved water increases. After 24 hours the resonance due to coordinated water disappeared while a single resonance for dissolved water remains. At this time the integration of water protons to diglyme protons was still 1 to 7.

The dimerization process was not observed to be reversible. When a ^1H NMR of a chloroform solution of H_2O and $Ru_2(CO)_6Cl_4$ was recorded, a resonance due solely to dissolved water was present. Additional amounts of water produced resonances due to dissolved and bulk water at 4.81 ppm. Similarly infrared bands due only to $Ru_2(CO)_6Cl_4$ were observed in the carbonyl region for a methylene chloride solution of $Ru_2(CO)_6Cl_4$ and H_2O. Also present in the infrared spectrum was a broad peak at 3400 cm^{-1} assigned to dissolved H_2O.

The compound $Ru(CO)_3Cl_2(H_2O)$ was structurally characterized by X-ray crystallography. A structure determination summary is included in the appendix. In the molecular analog, a water molecule (HOH) was incorporated on the ruthenium carbonyl chloride to model the hydroxylated surface (HOM), where M= Si or Al, of the inorganic oxides. In both the model compound and the adsorbed species, the bonding is through the lone pair of electrons on the oxygen, as opposed to binding through a hydroxide (HO-) or a surface oxo (MO-) group.

A thermal ellipsoid plot of $Ru(CO)_3Cl_2(H_2O)$ is shown in Figure 4.1. Also present in the crystal structure is one equivalent of diglyme, from which the crystal was

Table 4.2

Proton NMR resonances for $Ru(CO)_3Cl_2(H_2O)\cdot$Diglyme in chloroform.

^1H NMR RESONANCE	ASSIGNMENT	RELATIVE INTEGRATION t=0	t=12h	t=24h
1.64	dissolved H_2O	.6	.3	1
3.41	CH_3	3	3	3
3.72	CH_2	4	4	4
6.09	coor. H_2O	.4	.2	0

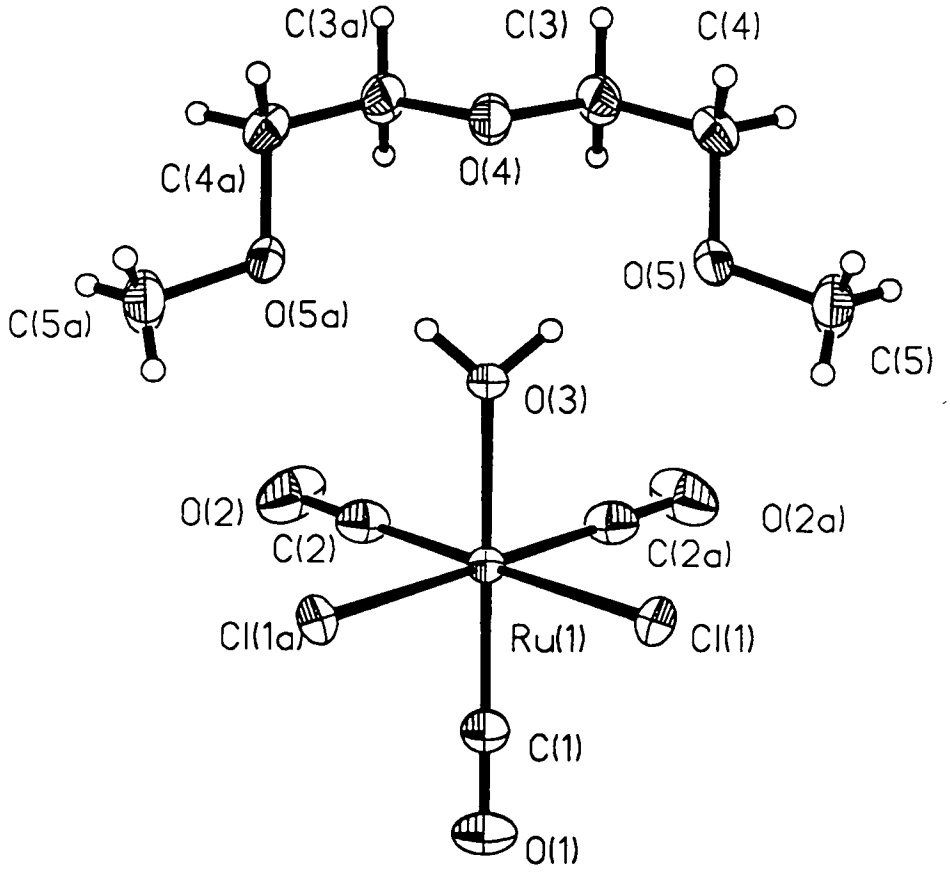

Figure 4.1 The crystal structure of $Ru(CO)_3Cl_2(H_2O)\cdot$diglyme, shown as a thermal ellipsoid plot.

grown, which co-crystallized with the ruthenium carbonyl chloride. The co-crystallization of a solvent molecule is not uncommon [78] however in this case the diglyme has adopted a configuration that is strained, as compared to non bonded diglyme. Using the molecular design program Chem-X 88, bond lengths and angles as well as repulsion energies were calculated for non bonded diglyme and diglyme in the conformation found in the crystal structure. The repulsion energy calculated for diglyme in the configuration shown in Figure 4.1 was approximately 195 kcal/mol while the most stable configuration of free diglyme was calculated to have a repulsion energy of 98 kcal/mol. It should be noted that these are relative and not absolute energies. These results are consistent with hydrogen bonding between the water protons and the diglyme oxygens.

Typically hydrogen bond lengths found in crystal structures are 1.7Å to 2.6Å [79,80,81]. The intermolecular distance between the methoxy oxygens (O5 and O5A) in the diglyme and the hydrogens on the water ligand are 1.8Å, which is within the range of hydrogen bonding. A hydrogen bond is also suggested from the infrared spectrum. If such an interaction is present, then a shift to lower wavenumbers for the O-H stretch should be observed. The OH stretch in $Ru(CO)_3Cl_2(H_2O)$ (KBr) was observed as a broad absorption at 3150 cm^{-1} which was shifted from 3450 cm^{-1} which was observed for non hydrogen bonding H_2O.

All bond lengths and angles reported in the crystal structure are comparable to literature values for similar compounds [82,83,84]. Stone [5] has reported that the THF adduct of this compound, $Ru(CO)_3Cl_2(THF)$, also has a facial arrangement of CO ligands. Stones's assignment was based on the number of infrared absorptions and symmetry arguments since an X-ray crystal structure was not available for this compound.

MODEL COMPOUNDS OF $Ru(CO)_3(SURFACE)_3$

A ligand substitution of THF in $Ru(CO)_3Cl_2(THF)$ for H_2O was used to synthesize a molecular analog of the adsorbed species $Ru(CO)_3Cl_2(SURFACE)$ however, to

synthesize a molecular analog of $Ru(CO)_3(SURFACE)_3$ a ligand substitution of both the THF and Cl^- ligands for donor ligands had to be employed. Silver triflate, AgTrif, was used to abstract the chloride ligands and donor ligands such as ethers and phosphines were used to model the surface hydroxyl groups of MgO and Al_2O_3.

When a methylene chloride solution of $Ru(CO)_3Cl_2(THF)$ and Agtrif was stirred at room temperature, a white precipitate of AgCl readily appears, maximum precipitation occurred after 1 hour. The formation of a white precipitate, AgCl, was not observed when a CH_2Cl_2 solution of Agtrif was stirred for 24 hours. Therefore all the AgCl produced was the result of the removal of coordinated Cl^- from the ruthenium carbonyl chloride. It was determined gravimetrically that 1.5 to 2.0 equivalents of Cl^- could be removed. Furthermore, no observable quantities of CO were produced when the ruthenium carbonyl solution came into contact with the donor ligand, thus eliminating the possibility that a ligand substitution of CO for the donor ligand occurred. The infrared spectrum of the resulting pale yellow solution contained two absorptions at 2150 and 2090 cm^{-1}. Attempts to isolate the product results in an impure yellow oil. If the above reaction was performed under an atmosphere of CO, the neutral species $Ru_3(CO)_{12}$ is formed.

Once the Ru-CO-trif species was synthesized the methylene chloride solution containing Ru-CO-trif was filtered and added to a solution of the desired donor ligand. In some cases the solution turned a darker shade of yellow when added to the solution containing the donor ligands. When H_2O was used as the donor ligand, the solution rapidly forms a brown precipitate while large quantities of CO were evolved. Furthermore an infrared spectrum of the brown solid reveled no infrared absorbances due to CO ligands. Table 4.3 lists the infrared carbonyl stretching frequencies of several compounds synthesized in this fashion.

The infrared spectrum of all the species listed in table 4.3 were very similar to the surface species $Ru(CO)_3(SURFACE)_3$ in terms of relative intensities and band positions.

All the compounds except for the phosphine 1,1,1 (tris(diphenylphoshinomethyl)ethane

Table 4.3

Carbonyl infrared stretching frequencies of compounds of the form $Ru^{+2}(CO)_3L_3$, where L = a donor ligand.

L	MATRIX		ν (CO) cm^{-1}	
Al_2O_3	a	2133w	2047s	1963s
MgO	a	2128w	2050s	1973s
PMe_3	CH_2Cl_2	2137w	2055s	1998s
PEt_3	CH_2Cl_2	2123w	2044s	1978s
$(PPh_2CH_2)_3CCH_3$	CH_2Cl_2	2148w	2072s	2010s
EtOH	CH_2Cl_2	2137w	2070s	2000s

a. Similar spectra were obtained from either a nujol null or from a free standing pressed pellet.

,tripod, adduct were isolated as an air sensitive impure oil as determined by ^{1}H and ^{13}C NMR and ^{31}P NMR where acceptable. Attempts to purify these compounds by liquid chromatography or fractional crystallization failed. Attempts to grow single crystals of the tripod adduct for an X-ray crystal structure produced crystals of inferior quality and purity.

When the tripod adduct was recrystallized from hot toluene, orange crystals of $Ru_3(CO)_{12}$ precipitated on the walls of the flask, also suggesting that no chloride ligands were present on the ruthenium carbonyl tripod adduct.

It clear that the AgTrif was acting as a chloride acceptor when reacted with $Ru(CO)_3Cl_2(THF)$. This is obvious from the following facts; 1.5 to 2.0 equivalents of AgCl were produced during the reaction and by the production of $Ru_3(CO)_{12}$ when the reaction was performed under CO. The formation of $Ru_3(CO)_{12}$ from a ruthenium carbonyl chloride at room temperature, only occurs in the presence of a halide acceptor. What is not clear is the composition and structure of the model compounds of $Ru(CO)_3(SURFACE)_3$. Elemental analysis and ^{13}C and ^{31}P NMR suggest several possibilities. Currently the model compounds are postulated to be fac-$Ru(CO)_3L_3$, where L is a donor ligand. This structure is based on the facts that two equivalents of Cl^- can be removed from $Ru(CO)_3Cl_2(THF)$, no apparent quantities of CO are produced during the reaction, and the assumption that a facial to meridian rearrangement does not occur during the chloride abstraction. This seems like a reasonable assumption since the ligand TRIPOD can coordinate to a metal center, only, in a facial arrangement.

CHAPTER 5

THE CHARACTERIZATION OF A SUPPORTED RUTHENIUM CARBONYL BIPYRIDINE COMPLEX

5A INTRODUCTION

As mentioned in chapter 3, the reaction between $Ru_3(CO)_{12}$ and bipyridine on silica yields an active water-gas shift reaction (WGSR) catalyst (equ 5.1).

$$CO + H_2O \text{ ----> } H_2 + CO_2 \qquad 5.1$$

Pakkanen and coworkers first reported the synthesis of this catalyst in 1986 [85]; however, the structure of the ruthenium carbonyl bipyridine surface species is still not known. Pakkanen et al. report that the catalyst is insoluble in polar and nonpolar solvents and bonds very strongly to the silica support and the glass walls of the reaction vessel. They also observe that spectroscopic and catalytically similar species can be synthesized from other nitrogen containing aromatics.

In the process of characterizing $Ru(CO)_3Cl_2(THF)$ adsorbed on Al_2O_3 and MgO it was discovered that a species spectroscopically similar to Pakkanen's WGSR catalyst can be synthesized from mononuclear and polynuclear ruthenium carbonyls and bipyridine on Al_2O_3 and SiO_2. Experiments are currently being conducted in conjunction with Pakkanen's laboratory to determine whether the species generated from the various ruthenium carbonyls are catalytically the same.

The objective of the work presented in this chapter is to characterize the ruthenium carbonyl bipyridine complex generated from the reaction of $Ru(CO)_3Cl_2(THF)$ and bipyridine adsorbed on Al_2O_3. This was performed using FTIR, CO evolution diffuse reflectance UV-Vis spectroscopy, and reaction stoichiometry.

5B EXPERIMENTAL

CO EVOLUTION

A typical carbon monoxide evolution reaction was performed in the following manner. The helium line reactor was charged with 200 mg of the desired support and 10 mL of a CH_2Cl_2 solution containing 8.4 mg of $Ru_3(CO)_{12}$ (1.3×10^{-2} mmol) and 12.4 mg of bipyridine (8.0×10^{-2} mmol). Precipitation of the reactants onto the support was achieved by evaporating the CH_2Cl_2 with a stream of helium. The resulting support was light yellow. Metal loadings were determined to be 2 weight percent. A bipyridine to Ru ratio of 2 to 1 was used in all experiments. The physisorbed species were activated by heating the support to 100°C for five minutes in flowing helium, during the activation period the support turned dark purple. Evolved gases were swept out of the reactor with flowing helium and quantified as described in Chapter 2. If extraction of the surface species was to be performed, a solution containing the appropriate counter anion was then added to the reactor. After 1 minute of agitation of the sample with flowing helium, a 1 mL portion of the solution was removed via syringe and analyzed by infrared spectroscopy.

5C RESULTS

The compounds $Ru_3(CO)_{12}$ and 2,2'-bipyridine, bipy, were co-adsorbed onto Al_2O_3 from CH_2Cl_2 by the method of incipient wetness, to yield a light yellow support. No reaction was observed between $Ru_3(CO)_{12}$ and bipyridine in CH_2Cl_2 at room temperature during the adsorption. The metal loading was determined to be 2 weight percent ruthenium. A Ru/bipy ratio of 1/2 was used to insure complete conversion of $Ru_3(CO)_{12}$ to the Ru-CO-bipy surface species. Triruthenium dodecacarbonyl, $Ru_3(CO)_{12}$, was precipitated onto the silica, since the maximum weight obtainable by spontaneous adsorption onto Al_2O_3 from solution was 1 weight percent. Experiments were not conducted to determine whether bipyridine has spontaneously adsorbed onto the support, hence it is assumed also to be adsorbed by precipitation.

Figure 5.1, trace a, shows the infrared spectrum of $Ru_3(CO)_{12}$ and bipyridine physisorbed onto Al_2O_3. This spectrum was recorded immediately after adsorption. Bands at 2062, 2033, and 2012 cm^{-1} are assigned to physisorbed $Ru_3(CO)_{12}$ and bands present at 1589 and 1563 cm^{-1} are assigned to bipyridine. Both sets of infrared absorptions are in good agreement with their solution values [86,87]. Trace b, in Figure 5.1, was obtained immediately after heating the sample (trace a) at 100°C for 5 minutes in flowing He. During this activation period the support underwent a color change from yellow to dark purple. All bands corresponding to $Ru_3(CO)_{12}$ disappeared and two new absorptions at 2036 and 1971 cm^{-1} emerge. Infrared absorptions corresponding to bipyridine are not shifted nor are there any new absorptions assignable to coordinated bipyridine present. Pakkanen and coworkers have reported when the same reaction is performed on SiO_2 the resulting supported Ru-CO-bipy complex is an active Water Gas Shift reaction catalyst, with turnover numbers as high as 2400 mol H_2/mol Ru [81]. It has been reported by Darensbourg that the adsorbed anion $HRu_3(CO)_{11}^-$ can be readily synthesized from $Ru_3(CO)_{12}$ supported on hydroxylated Al_2O_3 [46], however, there are no infrared bands assignable to the anion present in the spectrum nor are there any infrared bands assignable to any other polynuclear ruthenium carbonyl cluster [88,89,90]. Furthermore more the infrared spectrum of the supported Ru-CO-bipy complex does not correspond well with any known ruthenium carbonyl bipyridine complexes, namely, $Ru_3(CO)_{10}$bipy [72,73], $Ru^{+2}(CO)_2(bipy)_2$ [74], or $Ru^{+2}(CO)H(bipy)_2$ [75]. Surface species spectroscopically similar to the above mentioned can also be generated from other ruthenium carbonyls, such as $Ru(CO)_5$, $Ru_3(CO)_{12}$, and $H_4Ru_4(CO)_{13}$.

The Ru-CO-bipy complex was also synthesized on Al_2O_3 under the same reaction conditions, these results are summarized in Table 5.1.

The purple Ru-CO-bipy surface species could be synthesized from $Ru(CO)_3Cl_2(THF)$ and bipyridine on Al_2O_3, but not on SiO_2. As discussed in Chapter 3, the reaction of $Ru(CO)_3Cl_2(THF)$ and bipyridine on SiO_2 yields the physisorbed species $Ru(CO)_2Cl_2$bipy. When $Ru(CO)_2Cl_2$bipy supported on SiO_2 was heated to 100°C

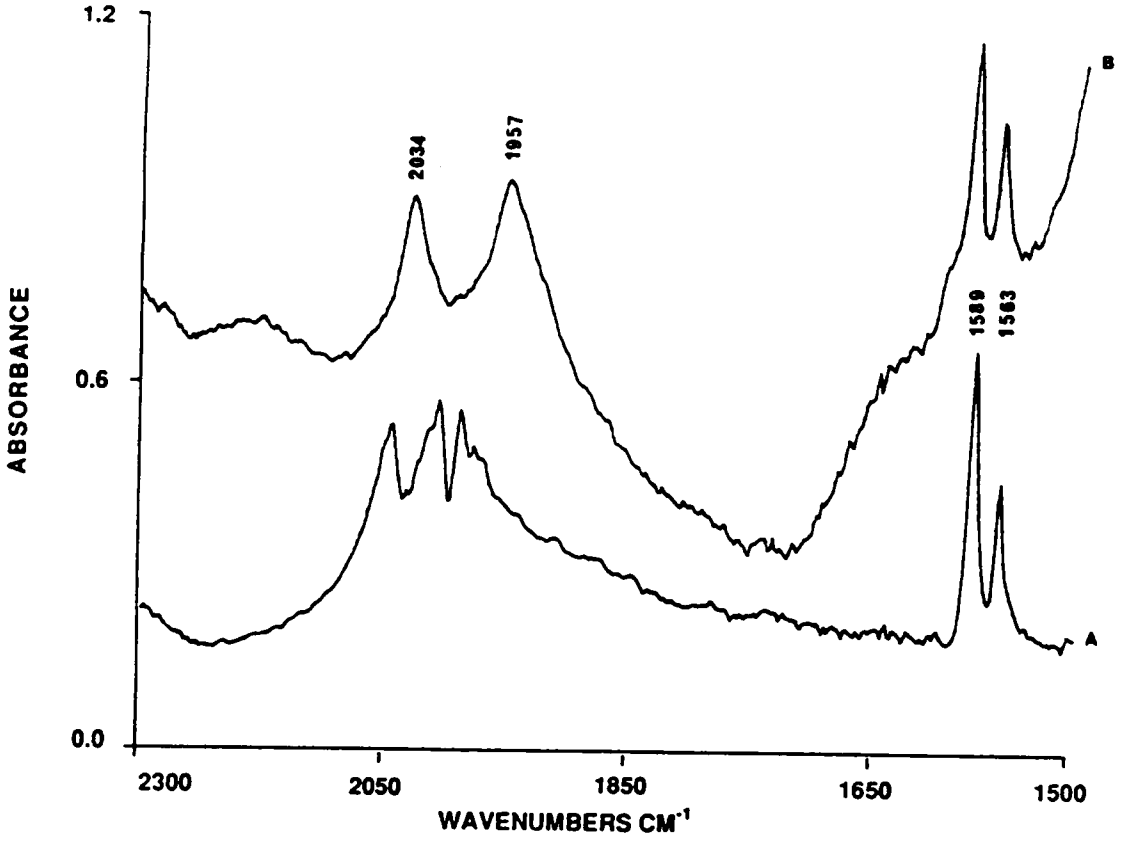

Figure 5.1 A) The infrared spectrum of $Ru_3(CO)_{12}$ and bipyridine co-adsorbed on Al_2O_3. B) The infrared spectrum of $Ru_3(CO)_{12}$ and bipyridine co-adsorbed on Al_2O_3 heated to 100°C for 10 min in He.

Table 5.1

Ruthenium carbonyl precursors used to synthesize the Ru-CO-bipy surface species.

RUTHENIUM CARBONYL	Al_2O_3	SiO_2
$H_2Ru_4(CO)_{13}$	n.t.	Y
$Ru_3(CO)_{12}$	Y	Y
$Ru(CO)_5$	Y	Y
$Ru(CO)_3Cl_2(THF)$	Y	Y
$Ru(CO)_2Cl_2(bipy)$	N	N

Y = Yes, is a precursor to Ru-CO-bipy

N = No, is not a precursor to Ru-CO-bipy

n.t. = not tried

neither the dark purple color nor the characteristic infrared spectrum was observed. The Ru-CO-bipy complex was not observed even after the addition of more bipyridine and further heating. The compounds $Ru(CO)_3Cl_2(THF)$ and bipyridine were not adsorbed onto Al_2O_3 from the same solution since the two would readily react to form $Ru(CO)_2Cl_2$bipy in solution. Instead $Ru(CO)_3Cl_2(THF)$ was adsorbed onto the surface of Al_2O_3 from CH_2Cl_2, and, only after the aluminum oxide extracted all the ruthenium carbonyl and the methylene chloride was removed, was the bipyridine precipitated onto the surface from CH_2Cl_2. The Ru-CO-bipy complex was not observed if $Ru(CO)_2Cl_2$bipy was adsorbed onto the aluminum oxide and heated. Also additional amounts of bipyridine and subsequent heatings did not generate the Ru-CO-bipy surface species. Infrared absorptions for the Ru-CO-bipy surface species generated from the various ruthenium carbonyls are presented in Table 5.2.

A bipy/Ru ratio of 2 was used to generate the Ru-CO-bipy surface species for all the ruthenium carbonyl precursors. At bipy/Ru ratios less than 1.5 complete conversion to the Ru-CO-bipy complex did not occur, as determined by infrared spectroscopy, even though the dark purple color was observed during the activation period. The infrared spectrum of the surface species generated at bipy/Ru ratios less then 1.5 contained several unassignable bands in addition to those of the Ru-CO-bipy complex. Therefore in order to insure the complete conversion of the ruthenium carbonyl to the Ru-CO-bipy species, bipy/Ru ratios of at least 2 were used.

Extraction of the Ru-CO-bipy complex were attempted with the following solvents: THF, MeOH, acetone, and CH_2Cl_2. Co-solvents were also employed to poison any possible Lewis acid sites present on the support. Counter ions were also added in anticipation that the surface species was an anion or a cation. The large cation PPN^+ (bis(triphenylphosphine)imine(+1)) was dissolved in CH_2Cl_2 or a CH_2Cl_2/THF mixture as its Cl^- salt, the resulting solution was used to extract any surface anions by a metathesis reaction. A solution of $Na^+BF_4^-$ in MeOH or $K^+PF_6^-$ in acetone was used to extract any cations from the surface. All attempts to extract the Ru-CO-bipy surface

Table 5.2

Carbonyl infrared stretching frequencies for Ru-CO-bipy generated on Al_2O_3 or SiO_2 from various ruthenium carbonyls.

RUTHENIUM CARBONYLS	$Al_2O_3(cm^{-1})$	$SiO_2(cm^{-1})$
$H_2Ru_4(CO)_{13}$	n.t.	2036 1971
$Ru_3(CO)_{12}$	2034 1957	2036 1971
$Ru(CO)_5$	2042 1969	2038 1970
$Ru(CO)_3Cl_2(THF)$	2041 1971	----

n.t. = not tried

--- = could not be synthesized

species as a neutral, cationic, or anionic species failed. These extraction results suggest either a very strong interaction between the surface and the Ru-CO-bipy surface species exist and perhaps a direct bond from the Ru-CO-bipy complex to the surface.

The results from carbon monoxide evolution experiments for the adsorption of $Ru_3(CO)_{12}$ and $Ru(CO)_3Cl_2(THF)$ in the presence of bipyridine are summarized in Table 5.3. Approximately two equivalents of evolved CO are observed during the reaction of $Ru_3(CO)_{12}$ and bipyridine on either SiO_2 or $Al2O_3$. This implies the formation of a surface species with the stoichiometry $(Ru(CO)_{3.3}bipy_x)_n$, where $n \leq 3$ and $x \leq 2$. Very little CO is evolved , < 0.1 equivalents, when $Ru(CO)_3Cl_2(THF)$ is used as the carbonyl precursor adsorbed on Al_2O_3. When $Ru(CO)_3Cl_2(THF)$ is adsorbed on Al_2O_3, 0.1 equ of CO is evolved, therefore, no CO evolution is detected during the formation of the Ru-CO-bipy from $Ru(CO)_3Cl_2(THF)$. This corresponds to a surface species with the formula $(Ru(CO)_3bipy_x)_n$ where $x \leq 2$ and n is unknown. Similarly, Pakkanen etal report a heptane solution of $Ru_3(CO)_{12}$ and bipyridine heated to 80°C evolves two equivalents of CO to produce a purple precipitate of $Ru_3(CO)_{10}bipy$ [72]. However the infrared spectrum of $Ru_3(CO)_{10}bipy$ contains several additional bands as compared to the Ru-CO-bipy surface species.

As mentioned above, the formation of the Ru-CO-bipy surface species is accompanied by the color change of the support from yellow to an intense purple. The purple color is not observed when bipyridine alone is adsorbed onto SiO_2 or Al_2O_3 followed by thermal treatment at 100°C. Nor is it observed by heating $Ru_3(CO)_{12}$ adsorbed on SiO_2 or Al_2O_3 to 100°C. Furthermore the infrared spectra of the latter samples do not have the characteristic two peak pattern of the Ru-CO-bipy species, although bands due to physisorbed $Ru_3(CO)_{12}$ and $HRu_3(CO)_{11}^-$ are present. When the Ru-CO-bipy surface species is synthesized on SiO_2 and exposed to a vacuum at 100°C the support rapidly turns yellow. The infrared spectrum of the resulting yellow complex is relatively the same as its purple precursor, Figure 5.2, both contain absorptions at 2038 and 1960 cm^{-1}, the adsorption at 1860 cm^{-1} is assigned to the silica support. If the Al_2O_3

Table 5.3

CO evolution during the formation of Ru-CO-bipy from $Ru_3(CO)_{12}$ and $Ru(CO)_3Cl_2(THF)$ and bipyridine on Al_2O_3 and SiO_2.

RUTHENIUM CARBONYL	**Al_2O_3**	**SiO_2**
$Ru_3(CO)_{12}$	1.9	2.1
$Ru(CO)_3Cl_2(THF)$	0.1	---

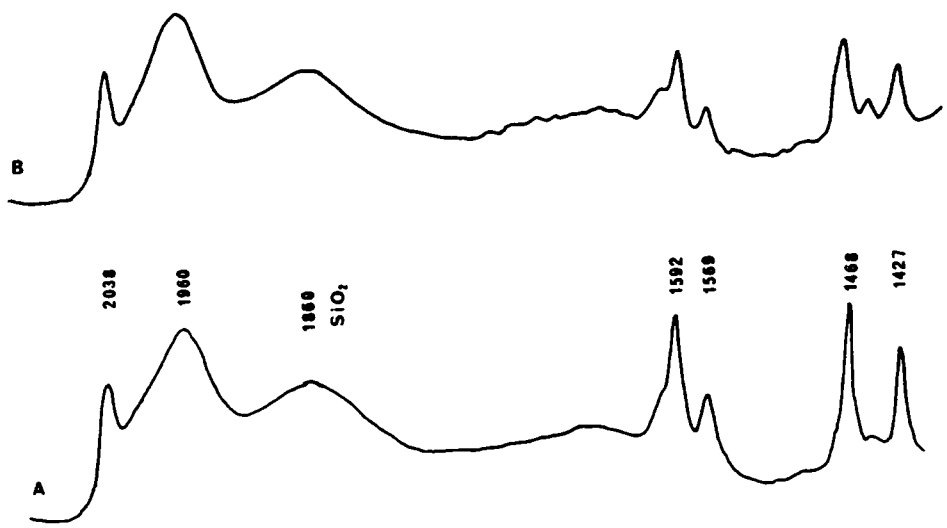

Figure 5.2 A) The infrared spectrum of $Ru_3(CO)_{12}$ and bipyridine adsorbed on SiO_2 heated to 100°C. B) The infrared spectrum of $Ru_3(CO)_{12}$ and bipyridine adsorbed on SiO_2 heated to 100°C under vacuum.

supported Ru-CO-bipy complex is exposed to oxygen at room temperature the support turned a brown color, however, the infrared spectrum of this sample did not change. A change in the infrared spectrum was observed only after exposure to oxygen for more than 1/2 hour; the new species contained absorptions at 2062 and 2040 cm^{-1}. The SiO_2 supported complex was found to be more oxygen sensitive than its Al_2O_3 analog. A color change from purple to brown is observed after exposure to only trace amounts of oxygen. A shift in the infrared bands from 2036 and 1970 cm^{-1} (for the purple support) to 2062 and 2040 cm^{-1} (for the brown support) is also observed for Ru-CO-bipy supported on SiO_2. Pakkenan reports that this new species (2062 and 2040 cm^{-1}) is inactive as a WGSR catalyst [91].

The generation of the purple color could be the result of a radical of bipyridine on the support. If such a radical did exist then a signal should be present in the Electron spin resonance, ESR, spectrum. Figure 5.3 shows the electron spin resonance spectrum of the purple Ru-CO-bipy complex generated from $Ru_3(CO)_{12}$ on Al_2O_3. This signal is very broad but its position (g=2.03) is close to that expected for an organic radical (g=2.00) [91]. If the signal was generated on the bipyridine then hyperfine coupling should exist. Since the signal is so broad it is not possible to conclusively state that there is no hyperfine coupling. Blank experiments with Al_2O_3 demonstrate that this signal is generated by an adsorbed species and not the support.

Figure 5.4 shows the diffuse reflectance UV-VIS spectrum for the synthesis of the Ru-CO-bipy complex on SiO_2. Trace a was recorded immediately after the adsorption of $Ru_3(CO)_{12}$ and bipyridine from CH_2Cl_2. The absorption at 291 nm is assigned to the $\pi \rightarrow \pi^*$ transition in bipyridine and the broad absorption at 398 nm is assigned to the $\sigma \rightarrow \sigma^*$ transition in $Ru_3(CO)_{12}$. Both values correspond well to their reported solution values [93,94]. Trace b was recorded after the activation of the sample used to generate trace a. A 10 nm bathochromic shift and a broadening of the adsorption is observed for the $\pi \rightarrow \pi^*$ band. Absorptions in the visible region due to possible $\sigma \rightarrow \sigma^*$ transitions in metal to metal bonds are masked because of the 340 nm cut off of

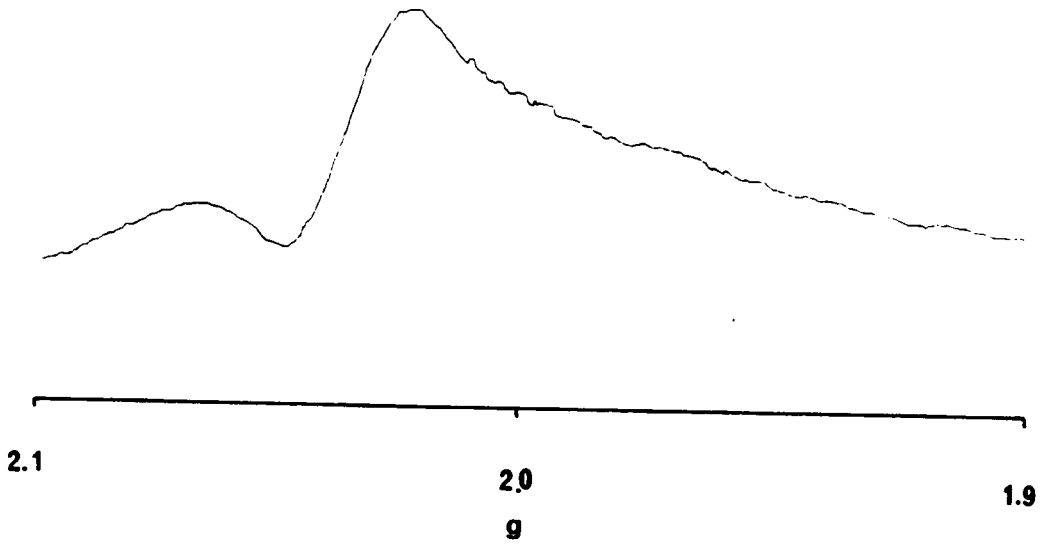

Figure 5.3 The electron spin resonance spectrum of $Ru_3(CO)_{12}$ and bipyridine heated to 100°C on Al_2O_3.

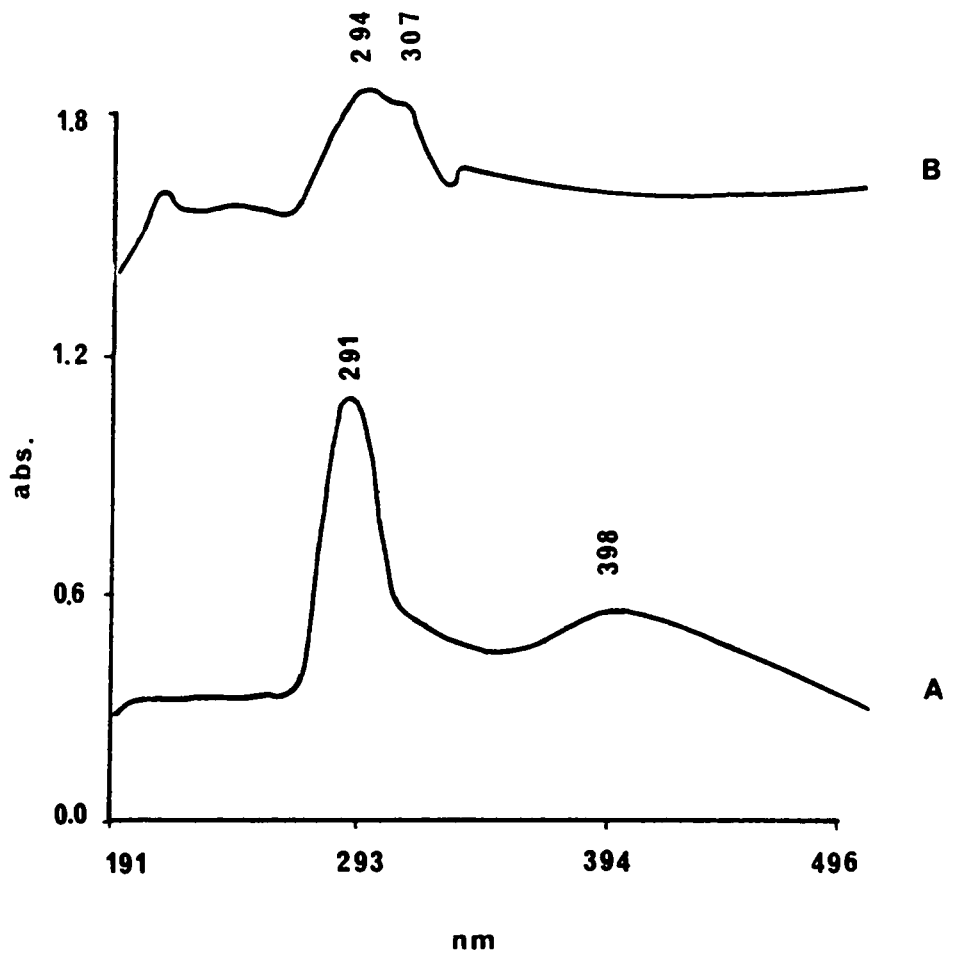

Figure 5.4 The diffuse reflectance UV-Vis spectra of, A. $Ru_3(CO)_{12}$ and bipyridine adsorbed on SiO_2. B. after heating the sample used to generate A to 100°C.

the sample.

X-ray Photoelectron Spectroscopy, XPS, was used to determine the oxidation state of the ruthenium in the Ru-CO-bipy surface species. Figure 5.5 shows the $3d_{5/2}$ binding energy peak for the Ru-CO-bipy surface species generated from $Ru_3(CO)_{12}$ and bipyridine on Al_2O_3. The infrared spectrum of the Ru-CO-bipy surface species taken before and after XPS analysis was the same, thus the Ru-CO-bipy species was not transformed to another species during the analysis. The only difference observed between the two samples was the change in color from purple to brown upon exposure to the atmosphere. During the experiment the Ru $3p_{3/2}$ and Ru $3d_{5/2}$ peaks were monitored. The Al (2p) photo peak from the support was used as an internal standard. The XPS spectrum of $Ru(CO)_2Cl_2$bipy and 1(ads) on NaY zeolite was also recorded as a reference, these results and peak positions for other ruthenium compounds in various oxidation states are reported in Table 5.4 [95,96].

5D DISCUSSION

As seen in Table 5.1, the Ru-CO-bipy complex could be synthesized from a variety of mononuclear and polynuclear ruthenium carbonyls. These carbonyl precursors were chosen for their varying Ru to CO ratios.

Ruthenium carbonyls with Ru/CO ratios as high as 1/5 for $Ru(CO)_5$ and as low as 1/2 for $Ru(CO)_2Cl_2$bipy were employed. The most significant observation is that the Ru-CO-bipy species could only be synthesized from ruthenium carbonyl containing at least three carbonyl ligands per ruthenium. Also the Ru-CO-bipy species could be synthesized from both ruthenium anions and cations.

The Ru-CO-bipy surface species was synthesized from $Ru(CO)_3Cl_2$(THF) and bipy on $Al2O_3$ but not on SiO_2. As described in Chapter 3, a surface species containing no chloride ligands is formed by the adsorption of $Ru(CO)_3Cl_2$(THF) on Al_2O_3. The adsorbed ruthenium carbonyl can then react with bipyridine to yield the purple Ru-CO-bipy complex. When $Ru(CO)_3Cl_2$(THF) adsorbed on SiO_2 is reacted with

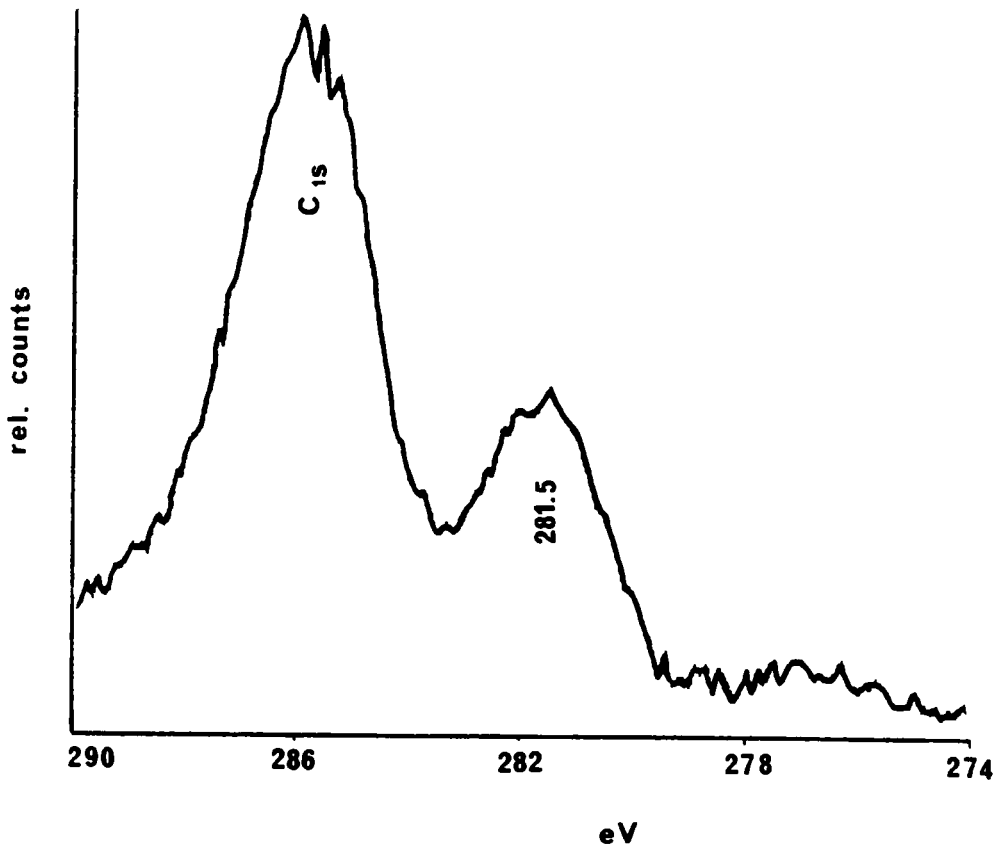

Figure 5.5 The X-ray photoelecton spetra of $Ru_3(CO)_{12}$ and bipyridine co-adsorbed onto Al_2O_3 heated to 100°C.

Table 5.4

X-ray photoelectron spectroscopy binding energies for various ruthenium compounds.

Compound	3 $p_{3/2}$	3 $d_{5/2}$
Ru°(metal)[95]	462.2	278.1
$[Ru^{+2}(NH_3)_5(CH_3CN)]Br_2$[96]	---	281.0
$[Ru^{+3}(NH_3)_5(CH_3CN)]Br_2$[96]	---	283.1
$Ru_3(CO)_{12}/Al_2O_3$[a]	462.9	278.0
$Ru^{+2}(CO)_2Cl_2$bipy[a]	463.0	281.7
$Ru^{+2}(CO)_3Cl_2$(SURFACE)[a,b]	462.8	281.5
Ru-CO-bipy[a]	463.1	281.7

[a] = This work

[b] = SURFACE = NaY zeolite

bipyridine the compound $Ru(CO)_2Cl_2bipy$ is formed and not the desired Ru-CO-bipy complex nor is the purple color of the support associated with the formation of the Ru-CO-bipy species observed. The Ru-CO-bipy complex could not be generated from $Ru(CO)_2Cl_2bipy$ on SiO_2 or Al_2O_3. This observation is not surprising since hydroxylated SiO_2 is not known to abstract chloride ligands in similar reactions. On the basic supports such as MgO and Al_2O_3 abstraction of chloride ligands from organometallic complexes is postulated to occur [20,97] and still the formation of the Ru-CO-bipy species from $Ru(CO)_2Cl_2bipy$ is not observed. Therefore it is postulated that the surface species contains three CO ligands per ruthenium.

The same ruthenium to CO ratio can be rationalized from CO evolution data. When $Ru_3(CO)_{12}$ is used as the ruthenium carbonyl precursor, for the synthesis of the Ru-CO-bipy surface species, approximately two equivalents of CO were evolved, regardless of the support used. This suggests that the stoichiometric composition of the Ru-CO-bipy compound is $(Ru(CO)_{3.3}bipy_x)_n$ where $n \leq 3$ and $x \leq 2$. When the Ru-CO-bipy surface complex is synthesized from $Ru(CO)_3Cl_2(THF)$ on Al_2O_3, less then 0.1 equivalents of CO were evolved, which is also observed for the adsorption of **1** on Al_2O_3. Again implying the surface species contains three CO ligands per ruthenium.

As described above, the surface species was assigned the structure $(Ru(CO)_3bipy_x)_n$. Metal to metal bonds would be present only if n is greater then one. If any metal to metal bonds were present an UV-Vis absorption due to a $\sigma \rightarrow \sigma^*$ transition, in the metal to metal bond, in the region of 390 nm would be observed. As shown in Figure 5.4 trace a, $Ru_3(CO)_{12}$ adsorbed on silica has an absorption at 398 nm which is assigned to the $\sigma \rightarrow \sigma^*$ transition. However the UV-Vis spectrum of the Ru-CO-bipy surface species (trace b) has a cut off at 340 nm, thus any absorptions due to Ru-Ru bonds could not be observed. Therefore the number of ruthenium atoms in the surface species had to be determined indirectly.

The Ru-CO-bipy surface species can be synthesized from the mononuclear ruthenium carbonyl precursors $Ru(CO)_5$ and $Ru(CO)_3Cl_2(THF)$, as well as the

polynuclear ruthenium carbonyls, $Ru_3(CO)_{12}$ and $H_4Ru_4(CO)_{13}$ (Table 5.1). There is precedent in the literature for the transformation of $Ru(CO)_5$ to $Ru_3(CO)_{12}$ [28] on the surface of inorganic oxides however cluster synthesis from ruthenium (+2) species, in solution or on support, only occur in the presence of a reducing agent [6]. Since reducing agents are not present the formation of a cluster from an adsorbed Ru^{+2} species seems to be very unlikely. Furthermore there is precedent for the fragmentation of polynuclear ruthenium carbonyls on SiO_2 and Al_2O_3 [45,46,47] under the same conditions used to generate the Ru-CO-bipy species. For these reasons it is postulated that the Ru-CO-bipy surface species is a mononuclear ruthenium compound.

Carbon monoxide evolution observed during the synthesis of the Ru-CO-bipy complex from $Ru_3(CO)_{12}$ and bipyridine ,on SiO_2 or Al_2O_3, indicates a surface species with the stoichiometry $Ru_3(CO)_{10}$bipy; however, the infrared of the surface species is not in good agreement with $Ru_3(CO)_{10}$bipy [72,73]. This type of structure is further discounted by the fact that a stoichiometry of at least 1.5 bipyridine per Ru is needed to synthesize the surface species. Therefore Ru-Ru bonds would have to be broken to obtain a compound with at least one bipyridine per Ru atom in the triangle with the retention of ten CO ligands.

The XPS data is consistent with ruthenium in the +2 oxidation state for the surface species. The position and the width of the Ru $3p_{3/2}$ and $3d_{5/2}$ peaks are in good agreement with other Ru^{+2} compounds. Since the peaks are very symmetrical it is unlikely that ruthenium in other oxidation states are present. Furthermore the infrared spectrum of the sample was the same (2034 and 1957 cm^{-1}) before and after XPS analysis. This indicates neither oxidation nor reduction of the sample occurs during the XPS analysis.

The surface species represented by Ru-CO-bipy is assigned the structure shown in Figure 5.6, $Ru(CO)_3$bipy(SURFACE).

The assignment was based on the following, Ru in the +2 oxidation state from XPS data, three CO ligands per Ru from carbon monoxide evolution, a Ru to surface

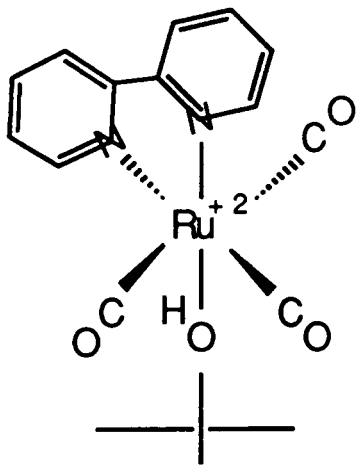

Figure 5.6 The proposed structure of the Ru-CO-bipy surface species

bond from the inability to extract any compounds from the surface, and one bipyridine per Ru from reaction stoichiometry. The Ru-CO-bipy species is not believed to be a cluster since Ru in the +2 oxidation state would require 2 Ru-Ru bonds as well as five two electron donor ligands to satisfy its coordination sphere which is unlikely.

It is easy to postulate a mechanism for the formation of the surface species from $Ru(CO)_3Cl_2(THF)$ and bipyridine on Al_2O_3 ,equation 5.1. The carbonyl chloride can first react with the Al_2O_3 to form $Ru^{+2}(CO)_3(SURFACE)_3$ as described in Chapter 3. After the addition of bipyridine to the supported ruthenium carbonyl, two coordinated surface hydroxyl groups can be substituted for a bipyridine.

$$Ru^{+2}(CO)_3Cl_2(THF) \xrightarrow{---Al_2O_3-->} Ru^{+2}(CO)_3(HO\text{-}Al)_3 \qquad 5.1$$

$$\downarrow \text{bipy}$$

$$Ru^{+2}(CO)_3bipy(HO\text{-}Al)$$

A more complex mechanism is needed to describe the synthesis of the Ru-CO-bipy complex from $Ru_3(CO)_{12}$ and bipy.

$$Ru_3(CO)_{12} + 3\ HOM + 3\ \text{bipyridine} \longrightarrow$$

$$3\ Ru^{+2}(CO)_3bipy(HO\text{-}M) + 3H_2 + 6\ ^-O\text{-}M \qquad 5.2$$

The ruthenium carbonyl is oxidized by the surface to Ru^{+2} while producing six oxo groups and three equivalents of H_2. The six surface oxo groups generated during the redox reaction provide the charge balance. Similar reaction pathways have been proposed for the formation of ruthenium carbonyl cations from $Ru_3(CO)_{12}$ adsorbed on Al_2O_3 and SiO_2 by several authors [41,45]. This seems like a logical synthetic pathway since no other oxidizing agents are present during the reaction, however no H_2 was observed during the reaction.

Evolved hydrogen was quantified by gas chromatography, by first converting it

to H_2O. This was performed by passing any evolved H_2 over CuO at 400°C. This signal was usually broad and had a bad base line also the quantities of H_2 that would be produced in equation 5.2 were 10% greater then the limit of detection, so it is possible that the H_2 went undetected. An alternative route to the Ru^{+2} surface species would be a disproportionation of the ruthenium cluster. This second argument is quickly eliminated since only Ru^{+2} is present on the surface as determined by XPS analysis.

As demonstrated by the experiment shown in Figure 5.2, the purple color associated with the formation of the Ru-CO-bipy surface species is not necessarily the color of the complex. Although to date, the Ru-CO-bipy complex has not been generated without the appearance of the purple color. Virtually no change is observed in the infrared spectra for the purple and yellow supports. This suggests that the compound responsible for the purple color had infrared absorptions overlapping with those of bipyridine and/or it has a very large UV-Vis extinction coefficient and existed in quantities small enough that detection by infrared could not be done.

When synthesizing the Ru-CO-bipy species 1.5 equivalent of bipyridine per Ru were used yet the surface species is postulated to contain only one bipyridine per ruthenium. When ratios less then 1.5 were used the purple color was observed as well as other infrared absorptions in the carbonyl region. Therefore the extra 0.5 equivalent of bipyridine needed to generate the Ru-CO-bipy surface species exclusively is believed to be producing the purple color.

The ESR spectrum, figure 5.3, of the purple Ru-CO-bipy surface species contains a signal at 2.03 g. There are two possible situations where such an ESR signal would occur. (1) an unpaired electron on the Ru in the surface species and (2) an unpaired electron on the bipyridine. If an unpaired electron was present on the ruthenium, then the ruthenium would have to be in the +1 or +3 oxidation states. Since XPS results indicate the ruthenium is in the +2 oxidation state, it is not very likely that the signal was generated from the ruthenium. Ruthenium in the +2 oxidation state would be in a low spin d^8 configuration and would not generate such a signal, therefore the ESR signal

is believed to be generated from the bipyridine. Radicals of bipyridine are known; however, the 2,2'-bipyridine radical is orange and the 4,4'-bipyridine radical is violet. A rearrangement to 4,4'-bipyridine does not seem reasonable since the infrared spectrum of $Ru(CO)_3$bipy(SURFACE) is consistent with 2,2'-bipyridine [87]. Therefore, it is not clear at this time what is generating the ESR signal.

Jacobs et al [16,98] report a similar observation from a water-gas shift reaction catalyst derived from $Ru(NH_3)_6^{3+}$ supported on HX zeolite. In their study they activated the catalyst by passing CO (1 atm) at 280°C over the Ru zeolite. During the WGS reaction a color change from white to blue to yellow and finally to brown for the deactivated catalyst was observed. They found that maximum activity (18 mol H_2/ mol Ru 24 h) occurs when the catalyst is blue and yellow. They assign the formula $Ru(CO)_z(OH)(NH_3)_x^{n+}$ (where z and x are unknown and n= 1 or 2) for the surface species. When bipyridine is substituted with tetramethylethylenediamine in the synthesis of the Ru-Co-bipy species the intense purple color is not observed nor is the characteristic two peak infrared spectrum observed. Also Pakkanen observes the purple color as well as catalytic activity only when the catalyst is synthesized in the presence of other aromatic amines [91].

5E SUMMARY

The adsorbed ruthenium carbonyl bipyridine complex was determined to be $Ru^{+2}(CO)_3$bipy(SURFACE). This assignment was based on XPS, FTIR, CO evolution, reaction stoichiometry, and ESR spectroscopy. The compound or compounds generating the violet color could not be determined. It is known that the $Ru(CO)_3$bipy(SURFACE) complex is not yellow; however, it could not be synthesized without generating the violet color. It is suggested by ESR spectroscopy that the violet complex may be a bipyridine or a bipyridine derivative radical.

CHAPTER 6

THE IN SITU SYNTHESIS OF RUTHENIUM-COBALT BIMETALLICS ON HYDROXYLATED ALUMINA

6A INTRODUCTION

It is known that the reaction between $Ru(CO)_3Cl_2(THF)$ and $Co(CO)_4^-$ is solvent dependent [7,8] (equations 6.1 and 6.2).

$$Ru(CO)_3Cl_2(THF) + 3\ Co(CO)_4^- \xrightarrow{THF} RuCo_3(CO)_{12}^- \qquad 6.1$$

$$Ru(CO)_3Cl_2(THF) + 2\ Co(CO)_4^- \xrightarrow{H_2O} RuCo_2(CO)_{11} \xrightarrow[THF]{+\ Co(CO)_4^-} RuCo_3(CO)_{12}^- \qquad 6.2$$

In equation 6.1, the reaction between $Ru(CO)_3Cl_2(THF)$ and $Co(CO)_4^-$ in THF at room temperature yields a brick red solution of $RuCo_3(CO)_{12}^-$ with a yield of 60%, based on total metal. The reaction can be stopped at the trinuclear neutral bimetallic, by performing the reaction in water, equation 6.2. This reaction affords a black precipitate of $RuCo_2(CO)_{11}$ in 50% yield, based on total metal. The trinuclear cluster can be capped with a third equivalent of $Co(CO)_4^-$ in THF to form the anion $RuCo_3(CO)_{12}^-$.

The chemistry of $RuCo_2(CO)_{11}$ supported on Al_2O_3 was studied in attempt to synthesize the adsorbed anion $RuCo_3(CO)_{12}^-$, since the tetranuclear bimetallic could not be synthesized on Al_2O_3 from $Ru(CO)_3Cl_2(THF)$ and $Co(CO)_4^-$.

In this chapter the results from the adsorption of $RuCo_2(CO)_{11}$ and $HRuCo_3(CO)_{12}$ on hydroxylated alumina will be discussed. The various adsorbed bimetallic compounds were characterized by in situ infrared spectroscopy, CO evolution and extraction of the surface species which were characterized by infrared, mass and UV-Vis spectroscopy.

6B RESULTS

The adsorption of $RuCo_2(CO)_{11}$ on hydroxylated alumina was followed by in situ infrared spectroscopy. Figure 6.1 shows the solution infrared spectrum of $RuCo_2(CO)_{11}$ in pentane. The adsorption of $RuCo_2(CO)_{11}$ onto hydroxylated alumina as a function of time is shown as Figure 6.2. The bottom spectrum in Figure 6.2 was recorded immediately following the adsorption of the trinuclear ruthenium-cobalt carbonyl. There are no bands in this spectrum that can be assigned to any of the starting cluster which may be physisorbed onto the surface. The top spectrum of Figure 6.2 was recorded 1 hour after the adsorption. All the bands in the top trace have been replaced with two new bands. These are in the terminal region and occur at 2027 and 1973 cm^{-1}. No further changes were observed once this spectrum is generated.

When $RuCo_2(CO)_{11}$ is adsorbed onto the surface of hydroxylated alumina significant quantities of CO are evolved, up to one equivalent per cluster in the first three hours after the adsorption, with most of that evolved in the first 15 minutes, Figure 6.3. After one hour the adsorbed cluster loses CO very slowly;thus after ten hours a total of 1.4-1.5 equivalent of CO/cluster is detected.

Given the quantitative removal of the cluster from a pentane solution, close to one equivalent of CO evolved during the initial adsorption, and the simplicity of the final infrared spectrum, two terminal bands and no bridging carbonyls, generated in the in situ adsorption experiment, it is possible to describe the surface species as "$RuCo_2(CO)_{10}$" bonded to a surface hydroxyl group. The infrared spectra generated immediately after adsorption of the cluster are quite complex. The band at 1882 cm^{-1} suggest the possible presence of $Co(CO)_4^-$, during the adsorption although this band disappears as the intermediate spectrum is obtained (trace b). There is no evidence for the presence of $Co(CO)_4^-$ on the surface by infrared spectroscopy once the intermediate infrared spectrum is obtained.

The identity of the surface specie or species responsible for the top trace in Figure 6.2 is difficult to assign from the infrared spectrum. It does not correspond well

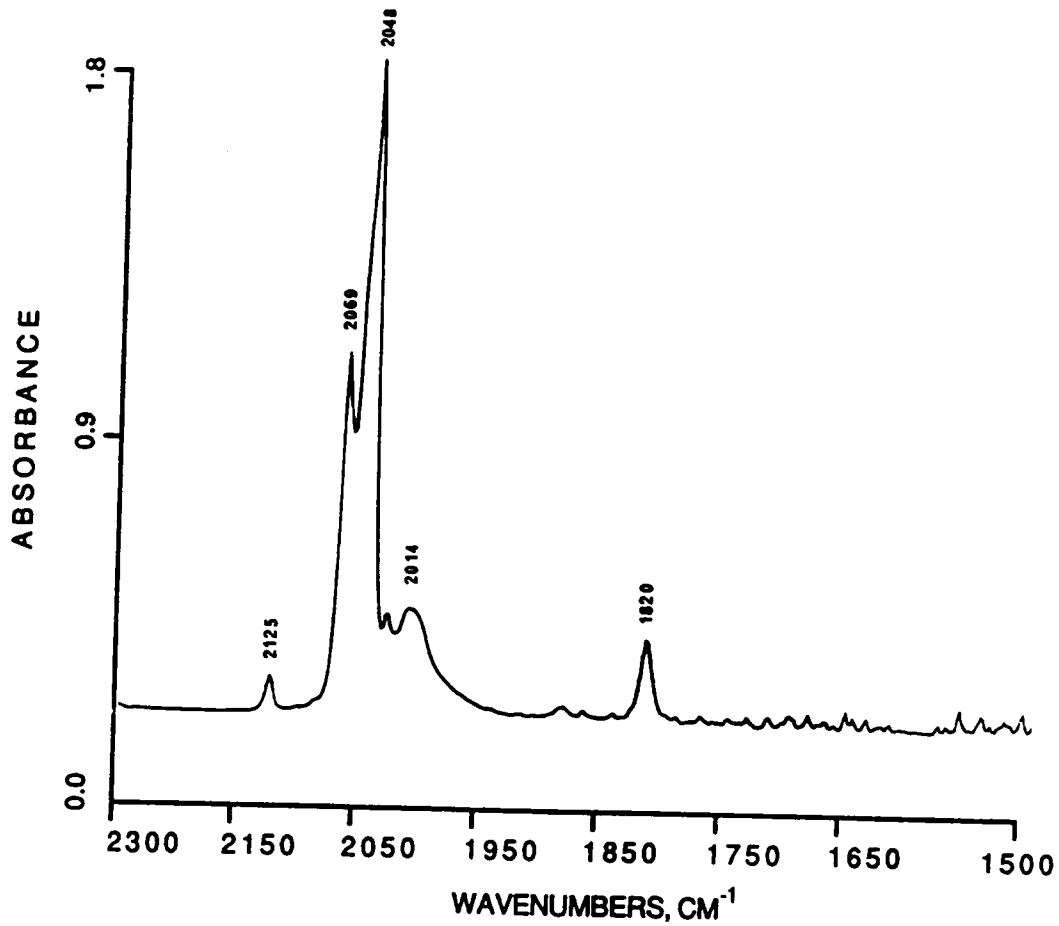

Figure 6.1 The solution infrared spectrum of $RuCo_2(CO)_{11}$ in pentane.

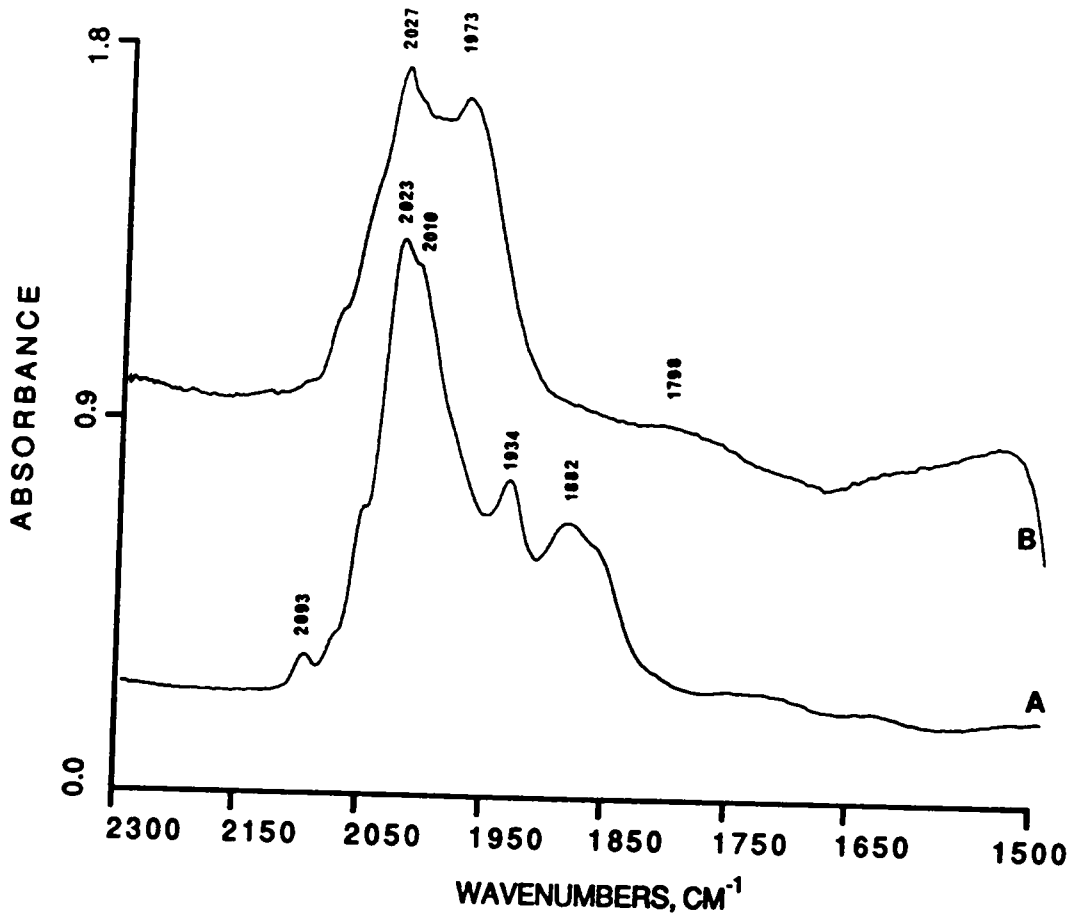

Figure 6.2 The infrared spectra of $RuCo_2(CO)_{11}$ adsorbed on Al_2O_3 as a function of time: trace a, t = 1 min and trace b, t = 1 hour.

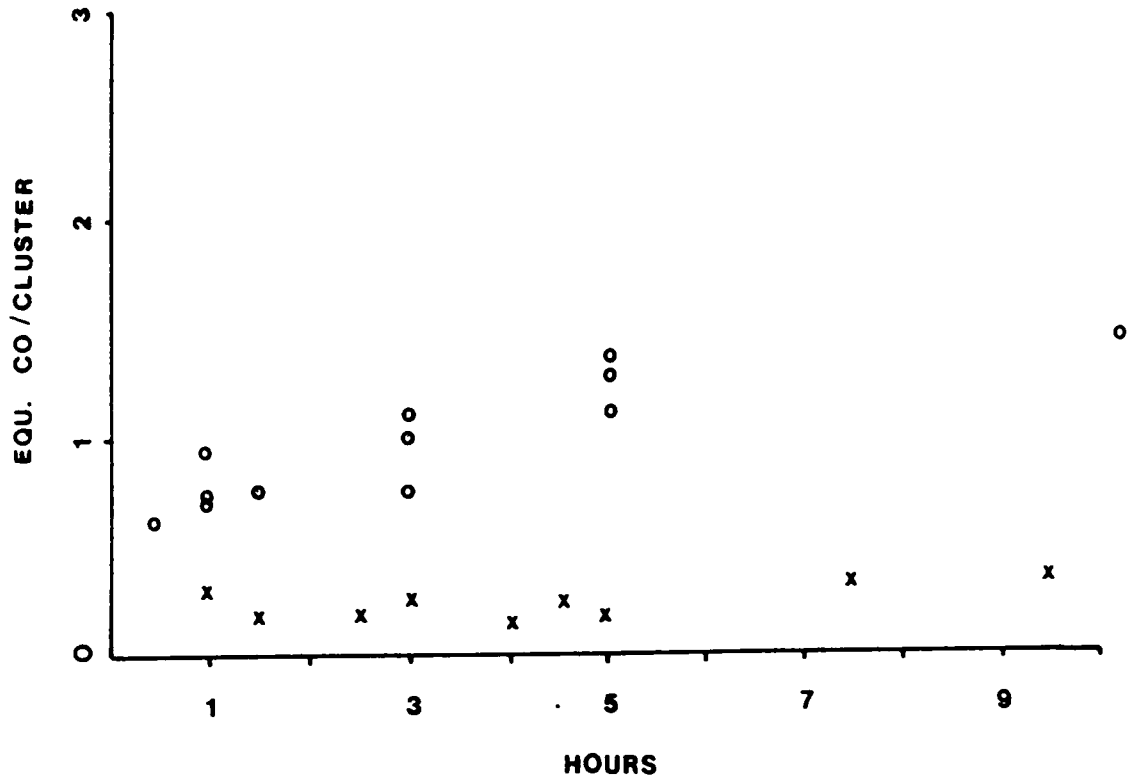

Figure 6.3 CO evolution during the adsorption on $RuCo_2(CO)_{11}$ (o) and $HRuCo_3(CO)_{12}$ (x) on hydroxylated alumina.

to the solution spectrum of any known ruthenium-cobalt clusters that have been reported in the literature, such as, $RuCo_2(CO)_{11}$ [7], $Ru_2Co_2(CO)_{12}$ [7], $Ru_3Co(CO)_{13}^-$ [62], $RuCo_3(CO)_{12}^-$ [99], or simple substituted or capped derivatives[8]. Nor is the spectrum similar to either $Co_4(CO)_{12}$ [100] or $Ru_3(CO)_{12}$ [41,46] adsorbed on hydroxylated alumina.

The trinuclear cluster is well known to be unstable in solution, and in fact its decomposition, forms the basis for the preparation of $Ru_2Co_2(CO)_{12}$ [7]. Nucleophilic solvents such as tetrahydofuran of diglyme were used to model the reactivity of the alumina surface. When $RuCo_2(CO)_{11}$ is stirred in THF or diglyme for 24 hours all infrared bands corresponding to $RuCo_2(CO)_{11}$ are replaced by ones corresponding to the anion $RuCo_3(CO)_{12}^-$. After the solvent is removed the resulting black solid can be protonated with H_3PO_4 to yield the neutral species $HRuCo_3(CO)_{12}$. This was confirmed by infrared and mass spectroscopy. During the decomposition traces of $RuCo_3(CO)_{12}^-$ and $Co_4(CO)_{12}$ in solution are also observed. The concentration of $Co_4(CO)_{12}$ is less than 5% of $RuCo_3(CO)_{12}^-$ as determined by the intensities of the infrared absorptions of the bridging carbonyls.

Following the initial adsorption of $RuCo_2(CO)_{11}$ onto alumina, attempts were made to extract the surface species with [PPN]Cl. The extraction experiments are summarized in Table 6.1. The products extracted from the surface were found to be dependent on the solvents used for the extraction. When [PPN]Cl in CH_2Cl_2 is used to extract surface species, the major product is $Co(CO)_4^-$. If the surface is first washed with an ether solvent such as THF or diglyme, then the tetranuclear cluster $RuCo_3(CO)_{12}^-$ can be extracted with [PPN]Cl in CH_2Cl_2. The extracted cluster yielded an infrared spectrum identical to an authentic sample. Furthermore the anion could also be protonated with H_3PO_4, to yield the neutral cluster $HRuCo_3(CO)_{12}$. This also was characterized by UV-Vis, infrared, and mass spectroscopy. Analysis of the support and extracted species by DCP, direct current plasma, spectroscopy shows that the bimetallic cluster anion can be synthesized and extracted in 60% yield based on total metal of the starting cluster,

Table 6.1

Attempted extractions of surface species following the adsorption of $RuCo_2(CO)_{11}$

1st wash	2nd wash	extracted species	surface metal complex (determined by IR)	% metal remaining
CH_2Cl_2	n.p.	no carbonyls	"$RuCo_2(CO)_{10}$"	n.p.
THF	n.p.	no carbonyls	$RuCo_3(CO)_{12}^-$	n.p.
THF	[PPN]Cl/ CH_2Cl_2	$RuCo_3(CO)_{12}^-$ + trace $Co(CO)_4^-$	no IR bands in carbonyl region	2% Co 40% Ru
[PPN]Cl/ CH_2Cl_2	n.p.	$Co(CO)_4^-$ + trace $RuCo_3(CO)_{12}^-$	no IR bands in carbonyl region	55% Co 96% Ru

n.p. = not performed

$RuCo_2(CO)_{11}$.

When $RuCo_3(CO)_{12}^-$ is extracted with $THF/CH_2Cl_2/PPNCl$, some $Co(CO)_4^-$ is present in the extract. Since $Co(CO)_4^-$ is not present on the surface prior to extraction, Figure 6.2, it seems likely that the anion $RuCo_3(CO)_{12}^-$ decomposes during the extraction or the surface species is decomposed to form the bimetallic anion. If $RuCo_2(CO)_{11}$ is stirred in a solution of [PPN]Cl in CH_2Cl_2, the anion $RuCo_3(CO)_{12}^-$ is formed very rapidly, however when $RuCo_2(CO)_{11}$ is stirred in CH_2Cl_2, no infrared evidence for the formation of $RuCo_3(CO)_{12}^-$ is found after one hour. The addition of ether solvents to the surface species apparently initiates a transformation to yield $RuCo_3(CO)_{12}^-$(ads). In all the attempted extractions additional carbon monoxide evolution is observed during the extraction, no other gases, such as CO_2 or H_2 are detected.

The formation of the anion $RuCo_3(CO)_{12}^-$ on hydroxylated alumina is confirmed by the infrared experiment shown in Figure 6.4. The trinuclear cluster, $RuCo_2(CO)_{11}$, is adsorbed on hydroxylated alumina from pentane to give an infrared spectrum as shown in the top trace of Figure 6.2. When THF is added to this sample, the top trace in Figure 6.4 is obtained. A bridging band is now observed at 1820 cm^{-1}, and well defined terminal bands are observed at 2014, 2000, and 1966 cm^{-1} . For comparison the infrared spectrum of $RuCo_3(CO)_{12}^-$ adsorbed on Al_2O_3 as its $[PPN^+]$ salt in THF is shown in the bottom trace of Figure 6.4. The major bands present on the surface are accounted for by postulating presences of the tetranuclear anion. However, there are broad shoulders in the infrared spectrum shown in the top trace of Figure 6.2, that remain unassigned. This is not surprising since a disproportionation reaction to yield $RuCo_3(CO)_{12}^-$ must be very complex; for example, the formation of either ruthenium or cobalt containing cations is expected [66,67].

The direct adsorption of $HRuCo_3(CO)_{12}$ on to hydroxylated alumina yields an infrared spectrum that is identical with the spectrum of $RuCo_3(CO)_{12}^-$ in THF. Very little CO is evolved during this adsorption: (0.15 $\pm$ 0.03) CO per cluster, Figure 6.3, consistent with a simple deprotonation reaction. This provides confirmation for the

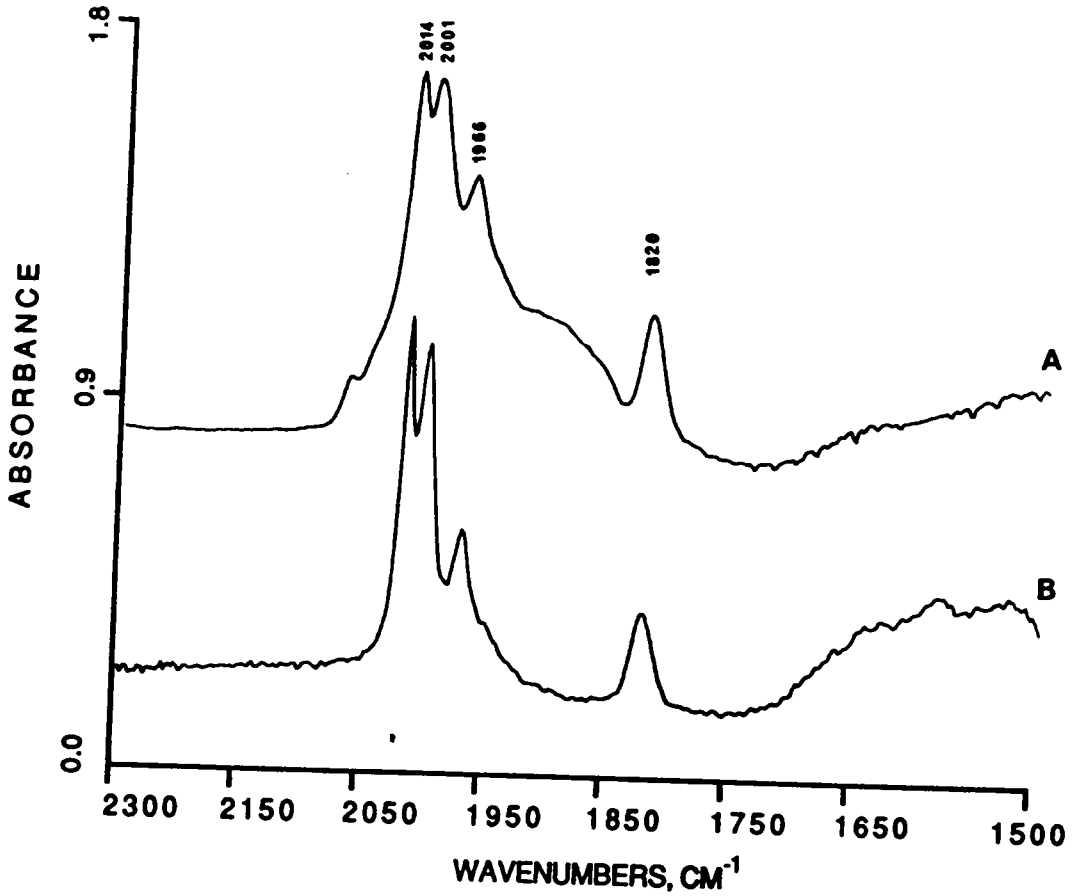

Figure 6.4 A) The infrared spectrum of $RuCo_2(CO)_{11}$ adsorbed on Al_2O_3 followed by the addition of THF. B) The infrared spectrum of $RuCo_3(CO)_{12}^-$ adsorbed on Al_2O_3 from THF.

presence of $RuCo_3(CO)_{12}^-$(ads) from the reaction of $RuCo_2(CO)_{11}$ with hydroxylated alumina following the addition of THF. Figure 6.5 shows the in situ infrared spectra obtained upon adsorption of $HRuCo_3(CO)_{12}$ onto alumina from pentane solution. The bridging carbonyl band is lost during the adsorption; after 3 hours the band at 1820 cm^{-1} has nearly disappeared. This band is regenerated upon the addition of THF; after the addition of THF the spectrum is virtually identical with the spectrum of $RuCo_3(CO)_{12}^-$ in THF and with the spectrum obtained after the addition of THF to adsorbed on alumina shown as trace b in Figure 6.3.

6C DISCUSSION

The adsorption of and $HRuCo_3(CO)_{12}$ onto hydroxylated alumina can be represented by equations 6.3 and 6.4.

$$RuCo_2(CO)_{11} \text{ ---> } A + CO \text{ -----> } [RuCo_3(CO)_{12}^-](ads,solv) + CO + B \quad 6.3$$

$$HRuCo_3(CO)_{12} \text{ -----> } RuCo_3(CO)_{12}^-(ads) \text{ ---> } [RuCo_3(CO)_{12}^-](ads,solv) \quad 6.4$$

The second reaction is an example of cluster deprotonation which is well documented for the adsorption of cluster hydrides[54,55]. The adsorbed species $RuCo_3(CO)_{12}^-$(ads) shows no bridging carbonyl in the infrared spectrum. The bridging carbonyl band appears only upon the addition of solvent; thus a distinction is made between two types of adsorbed $RuCo_3(CO)_{12}^-$. After the addition of solvent the infrared spectrum is indistinguishable from that observed in solution; for this reason the cluster anion is referred to as solvated. Addition of solvent alone, however, does not extract any metal carbonyls; thus the surface species adsorbed.

The reappearance of the bridging bands upon addition of THF may be consistent with poisoning of the Lewis acid sites. This last explanation is often used for surface metal carbonyls, and often there is good evidence for this interaction. However, in the present case we do not find bands below 1600 cm^{-1} which can be assigned to such an

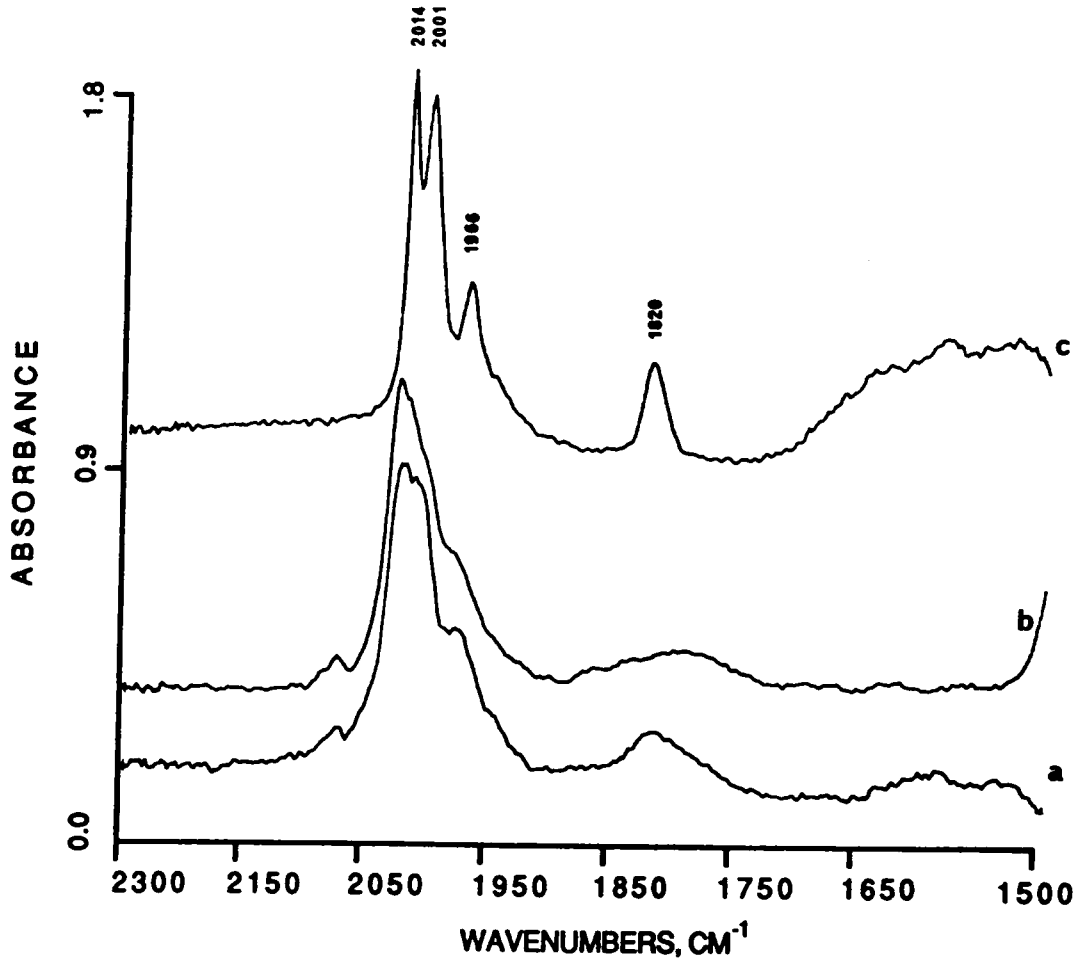

Figure 6.5 The infrared spectra of $HRuCo_3(CO)_{12}$ adsorbed on Al_2O_3 as a function of time: trace a, t = 0 min, trace b, t = 1 hour, trace c, t = 1 hour plus the addition of THF.

interaction. Also, it is difficult to imagine how all three of the bridging carbonyls in $RuCo_3(CO)_{12}^-$ could interact simultaneously with the surface. Another explanation is that an alternative isomeric form of $RuCo_3(CO)_{12}^-$ which has no bridging CO's is stabilized on the surface. Such isomers for $M_4(CO)_{12}$ systems have been discussed by Lauher[101].

In the reactions represented by equation 6.3 above it is clear that predominantly $RuCo_3(CO)_{12}^-$(ads,solv) is formed as the major product following the addition of THF. The stoichiometry of the transformation, however, it is not clear. Other products, B in equation 6.3, must be formed. Broad peaks are observed in the infrared spectrum, Figure 6.4, are consistent with other products which are not assigned. The reaction of A with THF to yield $RuCo_3(CO)_{12}^-$on the surface is described as a disproportionation since other possible reduction pathways with CO as the reductant must generate CO_2, and this is not observed either in the gas phase or on the surface as carbonate.

The species represented by A in this scheme is characterized by the following facts: (1) It is formed with the apparent stoichiometry $RuCo_2(CO)_{10}$. (2) It decomposes in the presence of [PPN]Cl to give predominantly $Co(CO)_4^-$. (3) It is converted predominantly to $RuCo_3(CO)_{12}^-$(ads,solv) upon addition of THF. (4) Its infrared spectrum is very simple consisting of only two terminal bands. Without being able to model this compound with a known molecular analogue, the assignment is proposed to be $RuCo_2(CO)_{10}$(ADS) in which a surface hydroxyl group occupies a bridging position between two cobalt atoms.

CHAPTER 7

SUMMARY

It was demonstrated in Chapter 3 that the adsorption of $Ru(CO)_3Cl_2(THF)$ onto the hydroxylated supports MgO, Al_2O_3, SiO_2 and NaY zeolite yields two different surface species. On the more Lewis basic supports, MgO and Al_2O_3, a ruthenium tricarbonyl containing no chloride ligands was formed, $Ru(CO)_3(SURFACE)_3$ where SURFACE is a surface hydroxyl group. While on the neutral supports, SiO_2 and NaY zeolite, the ruthenium tricarbonyl retains its chloride ligands during the adsorption, to form $Ru(CO)_3Cl_2(SURFACE)$. These two surface species were characterized by in situ infrared spectroscopy, CO evolution and their reactivity towards various reagents.

The adsorbed species $Ru(CO)_3(SURFACE)_3$ was modeled with several ruthenium carbonyl coordination compounds; however, these could not be structurally characterized. Both the model compound and the adsorbed species gave similar infrared spectra.

Schemes 7.1 and 7.2 summarizes the reactions of $Ru(CO)_3Cl_2(SURFACE)$ and $Ru(CO)_3(SURFACE)_3$ with $Co(CO)_4^-$, bipyridine, and CO respectively. The reactivity of $Ru(CO)_3Cl_2(SURFACE)$ was observed to parallel the reactivity of similar compounds in solution, while a different reactivity pattern was observed for $Ru(CO)_3(SURFACE)_3$.

The adsorbed ruthenium carbonyl on SiO_2 or NaY could be transformed in situ into the bimetallic cluster $RuCo_3(CO)_{12}^-$(ads) when it was reacted with $Co(CO)_4^-$. No reaction was observed when the same reaction was performed on Al_2O_3 or MgO. This lack of reactivity in the latter case is attributed to the surface hydroxyl groups of $Ru(CO)_3(SURFACE)_3$ being poorer leaving groups then the Cl^- ligands of $Ru(CO)_3Cl_2(SURFACE)$. The bimetallic cluster $RuCo_3(CO)_{12}^-$ could be synthesized in situ on Al_2O_3 from the precursor $RuCo_2(CO)_{11}$. The species initially formed from the adsorption of $RuCo_2(CO)_{11}$ on Al_2O_3 is best described as "$RuCo_2(CO)_{10}$". Only after the addition of a nucleophilic solvent, such as THF, is the adsorbed species disproportionated to $RuCo_3(CO)_{12}^-$.

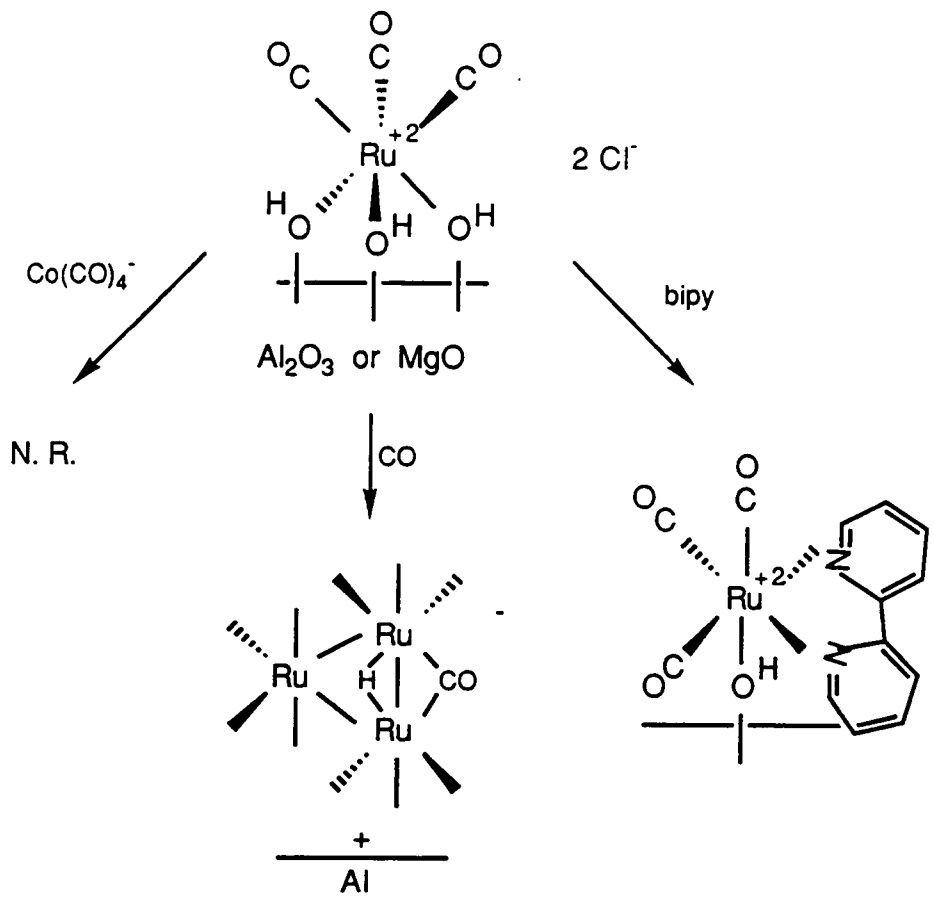

Scheme 7.1 The reactivity of $Ru(CO)_3Cl_2(THF)$ on Al_2O_3 and MgO.

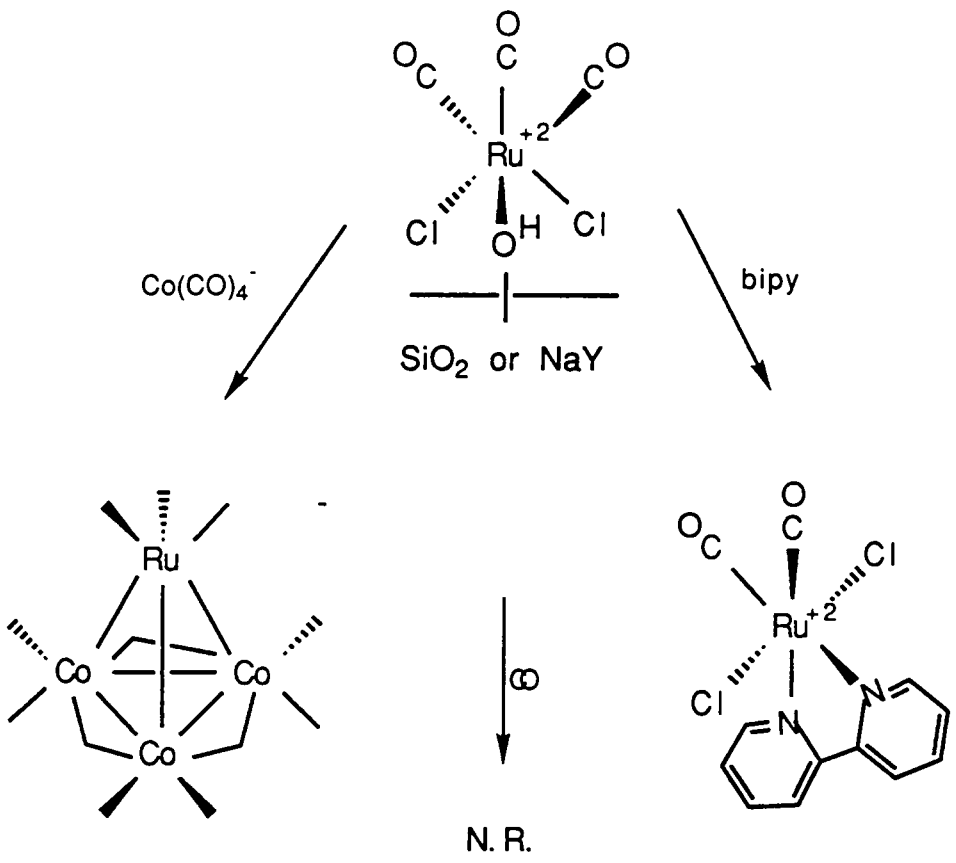

Scheme 7.2 The reactivity of $Ru(CO)_3Cl_2(THF)$ on SiO_2 and NaY zeolite.

The surface species $Ru(CO)_3(SURFACE)_3$ was transformed to $HRu_3(CO)_{11}^-$ on Al_2O_3 under relatively mild conditions (1 atm CO and 25°C). When the same reaction was performed on MgO a new species is formed in addition to $Ru(CO)_3(SURFACE)_3$; however, this second species has not been fully characterized. No reaction was observed when $Ru(CO)_3Cl_2(SURFACE)$ is exposed to an atmosphere of CO.

The coordination complex $Ru(CO)_2Cl_2bipy$ was readily synthesized on SiO_2 or NaY zeolite from $Ru(CO)_3Cl_2(SURFACE)$ and bipyridine. While on Al_2O_3 or MgO the complex $Ru(CO)_3(bipy)(SURFACE)$ could be synthesized from $Ru(CO)_3(SURFACE)_3$ and bipyridine. The species $Ru(CO)_3(bipy)(SURFACE)$ could also be synthesized on SiO_2, but only from ruthenium carbonyl containing no chloride ligands. The ruthenium carbonyl bipyridine complex was characterized by infrared, UV-Vis, X-ray photoelectron and electron spin resonance spectroscopies, CO evolution and reaction stoichiometry.

The adsorbed species $Ru(CO)_3Cl_2(SURFACE)$ was modeled by the complex $Ru(CO)_3Cl_2(H_2O)$. The ruthenium carbonyl aqua complex was characterized by single crystal x-ray diffraction, ^1H NMR, and infrared spectroscopy. It was observed from the crystal structure, that the model compound contains a tricarbonyl functionality in a facial arrangement. Also one equivalent of diglyme co-crystallized with the ruthenium carbonyl such that the two methoxy oxygens, of the diglyme, participate in hydrogen bonding to the water's protons. Both the model compound and the adsorbed species gave similar infrared spectra.

APPENDIX

STRUCTURE DETERMINATION SUMMARY

CRYSTAL DATA

Empirical Formula	$C_9H_{16}O_7Cl_2Ru$
Color;Habit	Clear, Cubic
Crystal Size (mm)	.3 X .3 X .3
Crystal System	Orthorhombic
Space Group	Pnma
Unit cell Dimensions	$\underline{a}$ = 9.453(9) Å $\underline{b}$ = 15.312(13) Å $\underline{c}$ = 11.075(16) Å b = 90.000(0)°
Volume	1603(3) $Å^3$
Z	4
Formula weight	408.2
Density (calc.)	1.691 Mg/m^3
Absorption Coefficient	1.315 mm^{-1}
F (000)	816

DATA COLLECTION

Diffractometer used	Nicolet R3m/V
Radiation	MoK_α (=0.71073)
Temperature (K)	152
Monochromator	Highly oriented graphite crystal
2θ Range	3.5 to 55.0°
Scan Type	2θ-θ
Scan Speed	Variable; 10.10 to 19.50°/min in 2θ
Scan Range (w)	1.20° plus K_α-separation
Background Measurement	Stationary crystal and stationary counter at beginning and end of scan, each for 25.0% of total scan time
Standard Reflections	3 measured every 200 reflections
Index Ranges	$-4 \leq H \leq 12$, $-19 \leq k \leq 4$, $-4 \leq l \leq 14$
Reflections Collected	5235
Independent Reflections	1915 (R_{int}=2.25%)
Observed Reflections	1790 ($F > 3.0\ \sigma(F)$)
Absorption Correction	N/A

SOLUTIONS AND REFINEMENT

System used	Nicolet SHELXTL PLUS (MicroVax II)
Solution	Direct Methods
Refinement Method	Full-Matrix Least Squares
Quantity Minimized	$\Sigma\ w(F_o - F_c)^2$
Absolute Configuration	N/A
Extinction Correction	N/A
Hydrogen Atoms	Riding Model, fixed isotropic U
Weight Scheme	Unit weights
Final R indices (obs. data)	R= 2.92% wR= 3.3%
R Indicies (all data)	R = 3.22%, wR = 3.51%
Goodness-of-Fit	3.51%
Largest and Mean Δ /σ	0.007, 0.000
Data-to-Parameter Ratio	19.0 : 1
Largest Difference Peak	0.55 $\AA e^{-3}$
Largest Difference Hole	-0.64 $e\AA e^{-3}$

Table 1. Atomic coordinates (X 10^4) and equivelent isotropic displacement coefficients ($Å^2$ x 10^3)

	x	y	z	U (eq)
Ru(1)	2400(1)	2500	1131(1)	17(1)
C(1)	2207(5)	2500	2829(4)	24(1)
Cl(1)	4160(1)	1392(1)	1400(1)	24(1)
O(3)	2979(4)	2500	-702(3)	23(1)
O(2)	263(3)	3955(2)	703(3)	49(1)
C(2)	1043(4)	3403(3)	880(3)	31(1)
O(5)	2439(3)	969(2)	-1839(2)	31(1)
C(3)	1250(4)	1735(2)	-3401(3)	31(1)
O(4)	2041(4)	2500	-3200(3)	29(1)
C(4)	2151(4)	960	-3098(3)	31(1)
C(5)	3165(5)	208(2)	-1458(4)	42(1)
O(1)	2270(4)	2500	3850(3)	35(1)

* Equivelent isotropic U defined as one third of the trace of the orthogonalized U_{ij} tensor.

Table 2. Bond lengths (Å)

Ru(1)-C(1)	1.889 (5)	Ru(1)-Cl(1)	2.395 (3)
Ru(1)-O(3)	2.103 (4)	Ru(1)-C(2)	1.906 (5)
Ru(1)-Cl(1A)	2.395 (3)	Ru(1)-C(2A)	1.905 (5)
C(1)-O(1)	1.133 (6)	O(2)-C(2)	1.139 (5)
O(5)-C(4)	1.420 (5)	O(5)-C(5)	1.416 (5)
C(3)-O(4)	1.407 (5)	C(3)-C(4)	1.499 (5)
O(4)-C(3A)	1.407 (5)		

Table 3. Bond Angles (°)

C(1)-Ru(1)-Cl(1)	86.8(1)	C(1)-Ru(1)-O(3)	170.4(2)
Cl(1)-Ru(1)-O(3)	86.5(1)	C(1)-Ru(1)-C(2)	94.6(2)
Cl(1)-Ru(1)-C(2)	178.0(1)	O(3)-Ru(1)-C(2)	92.0(1)
C(1)-Ru(1)-Cl(1A)	86.8(1)	Cl(1)-Ru(1)-Cl(1A)	90.2(1)
O(3)-Ru(1)-Cl(1A)	86.5(1)	C(2)-Ru(1)-Cl(1A)	88.4(1)
C(1)-Ru(1)-C(2A)	94.6(2)	Cl(1)-Ru(1)-C(2A)	88.4(1)
O(3)-Ru(1)-C(2A)	92.0(1)	C(2)-Ru(1)-C(2A)	93.0(2)
Cl(1A)-Ru(1)-C(2A)	178.0(1)	Ru(1)-C(1)-O(1)	171.4(4)
Ru(1)-C(2)-O(2)	177.7(3)	C(4)-O(5)-C(5)	112.1(3)
O(4)-C(3)-C(4)	108.7(3)	C(3)-O(4)-C3A	112.6(4)
O(5)-C(4)-C(3)	108.7(3)		

Table 4. Anisotropis displacement coefficients ($Å^2*10^3$)

	U_{11}	U_{22}	U_{33}	U_{23}	U_{13}	U_{12}
Ru(1)	18(1)	17(1)	16(1)	0	-1(1)	0
C(1)	21(2)	29(2)	24(2)	0	-1(2)	0
Cl(1)	29(1)	17(1)	27(1)	3(1)	-1(1)	4(1)
O(3)	35(2)	19(1)	14(1)	0	-1(1)	0
O(2)	48(2)	57(2)	42(2)	12(1)	4(1)	36(2)
C(2)	32(2)	38(2)	23(2)	-1(1)	1(1)	2(2)
O(5)	47(1)	17(1)	27(1)	-4(1)	-9(1)	5(1)
C(3)	38(2)	24(2)	32(2)	-3(1)	-14(2)	-5(1)
O(4)	35(2)	20(2)	31(2)	0	-8(2)	0
C(4)	41(2)	24(2)	29(2)	-7(1)	-5(2)	-2(2)
C(5)	57(3)	19(2)	51(2)	-3(2)	-22(2)	6(2)
O(1)	34(2)	52(2)	21(2)	0	1(2)	0

The anisotropic dissplacement exponent takes the form :

$-2\pi^2(h^2a^{*2}U_{11} + \ldots + 2hka^*b^*U_{12})$

Table 5. Hydrogen atom coordinates (X 10^4) and isotropic displacement coefficients ($Å^2$ x 10^3)

	x	y	z	U
H(3B)	395	1725	-2835	50
H(3A)	856	1717	-4210	50
H(4B)	2998	948	-3606	50
H(4A)	1566	454	-3247	50
H(5C)	3935	150	-1947	50
H(5b)	3456	288	-834	50
H(5A)	2639	-210	-1592	50
H(1)	2772	2079	-1183	50

REFERENCES

1. Theolier, A.; Smith, A.K.; Leconte, M.; Basset, J.M.; Zanderighi, G.M.; Psaro, R.; Ugo,R. *J.Organometallic Chem.* **1980**, *191*, 415.

2. Rode, E.J.; Davis, M.E.; Hanson, B.E.; *J. Catal.* **1985**, *96*, 574.

3. Chini, P. *Rev. Appl. Chem.* **1970**, *23*, 489.

4. Hugues, F.; Smith, A.K.; Taarit, Y.B.; Basset, J.M. *J. Chem. Soc. Chem. Comm.*. **1980**, 68.

5. Bruce, M.I.; Stone, F.G.A. *J. Chem. Soc. (A)* **1967**, 1238.

6. Mantovani, A.; Cenini, S. *Inorg. Synthesis.* **1976**, *16*, 47.

7. Roland, E.; Vahrenkamp, H. *Angew. Chem.,Int. Ed. Engl.* **1981**, *20*, 679.

8. Roland, E.; Vahrenkamp, H. *Organometallics* **1983**, *2*, 1048.

9. Iwasawa, Y. in *"Tailored Metal Catalysts"* Y. Iwasawa, ed. D. Reidel, Boston **1986**.

10. Budge, J.R.; Lucke, B.F.; Gates, B.C.; Toran, J.; *J. Catal.* **1985**, *91*, 272.

11. Beck, A.; Dobos, S.; Guczi, L. *Inorg. Chem.* **1988**, *27*, 3220.

12. Simpson, A.F.; Whyman, R. *J. Organometallic Chem.* **1981**, *213*, 157.

13. Ferkul, H.E.; Stanton, D.J.; McCowan, J.D.; Baird, M.C. *J. Chem. Soc. Chem. Comm.* **1982**, 955.

14. Pierantozzi, R.; Valagene, E.G.; Nordquist, A.F.; Dyer, P.N. *J. Mol. Catal.* **1983**, *21*, 189.

15. Doi, Y.; Miyake, H.; Yokota, A.; Soga, K. *J. Catal.* **1985**, *95*, 293.

16. Verdonck, J.J.; Jacobs, P.A.; Uytterhoeven, J.B. *J. Chem. Soc. Chem. Comm.* **1979**, 181.

17. Lausarot, P.M.; Vaglio, G.A.; Valle, M.; *J Organometallic Chem.* **1984**, *275*, 233.

18. Ballivet-Tkatchenko, D.;Coudrier, G. *Inorg. Chem.* **1979**, *18*, 558.

19. Tessier-Youngs, C.; Correa, F.; Pioch, D.; Burwell Jr., R.L.; Shriver, D.F. *Organometallics* **1983**, *2*, 898.

20. Bergmeister, J.J.; Hanson, B.E. *J. Organometallic Chem.* **1988**, *352*, 367.

21. Brenner, A.; Burwell Jr.,R.L. *J. Catal.* **1978**, *52*, 353.

22. Guglielminotti, E.; Osella D.; Stanghellini, P.L. *J. Organometallic Chem.* **1985**, *281*, 291.

23. Huges, F.; Basset, J.M.; Taarit, Y.B.; Choplin, A.; Primet, M.; Rojas, D.;

Smith, A.K. *J. Am. Chem. Soc.* **1982**, *104*, 7020.

24. Hanson, B.E.; Bergmeister, J.J.; Petty, J.T.; Connaway, M.C. *Inorg. Chem.* **1986**, *25*, 3089.

25. Lamb, H.H.; Gates, B.C. *J. Am. Chem. Soc.* **1986**, *108*, 81.

26. Nakamura, R.; Oomura, A.; Okada, N.; Echigoya, E. *Chem. Lett.* **1982**, 1463.

27. Smith, A.K.; Hugues, F.; Theolier, A.; Basset, J.M.; Ugo, R.; Zanderighi, G.M.; Bilhou, J.L.; Bilou-Bougnol, V.; Graydon, W.F. *Inorg. Chem.* **1979**, *18*, 3104.

28. Bein, T.; Jacobs, P.A. *J. Chem. Soc. Faraday Trans. 1* **1983**, *79*, 1819

29. Connaway, M.C.; Hanson, B.E. *Inorg. Chem.* **1986**, *25*, 1445.

30. Mantovani, E.; Palladino, N.; Zanobi, A. *J. Mol. Catal.* **1978**, *3*, 285.

31. Herron, N.,;Stucky, G.D.; Tollman, C.A. *Inorg. Chem. Acta.* **1985**, *100*, 135.

32. Goodwin Jr., J.G.;Naccache, C. *J. Mol. Catal.* **1982**, *14*, 259.

34. Cooney, R.P.; Curthoys, G.; Tam, U.T.; *Adv. in Catal.* **1975**, *24*, 293.

35. Doi, Y.; Soga, K.; Yano, K.; Ono, Y. *J. Mol. Catal.* **1983**, *19*, 359.

36. Doi, Y.; Yanko, K. *Inorg. Chem. Acta.* **1983**, *76*, L71.

37. Roberts, M.W. *Adv Catal.* **1980**, *29*, 55.

38. Bart, J.C.J; Vlaic, G. *Adv. Catal.* **1987**, *35*, 1.

39. Wagner, G.W. PhD. dissertation, Virginia Polytechnic Institute and State University Blacksburg VA, **1987**.

40. Theolier, A.; Choplin, A.;D'Ornelas, L.; Basset, J.M.; Zanderighi, G.; Sourisseau, C. *Polyhedron* **1982**, *2*, 219.

41. Zecchina, A.; Guglielminotti, E.; Bosi, A.; Camia, M. *J. Catal.* **1982**, *74*, 225.

42. Asakura, K.; Yamada, M.;Iwasawa, Y.;Kuroda, H. *Chem. Lett.* **1985**, 511

43. Hastings, W.R.; Cameron, C.J.; Thomas, M.J.; Baird, M.C. *Inorg. Chem.* **1988**, *27*, 3024.

44. Hunt, D.J.;Moyes, R.B.; Wells, P.B.; Jackson, S.D.; Whyman, R. *J. Chem. Soc. Faraday Trans.* **1986**, *82*, 189.

45. Kuznetsov, V.L.; Bell, A.T.; Yermakov, Y.I. *J. Catal.* **1980**, *65*, 374.

46. Darensbourg, D.J.; Ovalles, C. *Inorg. Chem.* **1986**, *25*, 1603.

47. Zanderighi, G.M.; Dossi, C.;Ugo, R.;Psaro, R. Theolier, A.; Choplin, A. D'Ornelas, L.;Basset, J.M. *J. Organometallic Chem.* **1985**, *296*, 127.

48. Evans, J.; McNulty, G.S. *J. Chem. Soc. Dalton Trans.* **1984**, 1123.

49. Budge, J.R.; Scott, J.P.;Gates, B.C. *J. Chem. Soc. Chem. Comm.* **1983**, 342.

50. Hemmerich, R.;Keim, W.; Roper, M. *J. Chem. Soc. Chem. Comm.* **1983**, 428.

51. Anderson, J.R.;Elmes, P.S., Howe, R.F.; Mainwaring, D.E. *J. Catal.* 1977, *50*, 508.

52. Sinfelt, J.H. *Acc. Chem. Res.* **1977**, *10*, 15.

53. Ichikawa, M. *J. Catal.* **1979**, *59*, 67.

54. Choplin, A.; Huang, L.; Basset, J.M.; Mathieu, R.; Siriwardane, U.;Shore, S.G. *Organometallics* **1986**, *5*, 1547.

55. Choplin, A.; Leconte,M.; Basset, J.M.;Shore, S.G.; Hsu, W.L.; *J. Mol. Catal.* **1983**, *21*, 389.

56. Lieto, J.; Wolf, M.; Matrana, B.A.; Prochazka, M.; Tesche, B.;Knozinger, H.; Gates, B.C. *J. Phys. Chem.* **1985**, *89*, 991.

57. Yokoyama, T.;Yamazaki, K.; Kosugi, N.;Kuroda,H.; Ichikawa, M.; Fukushima, T. *J. Chem. Soc. Chem. Comm.* **1984**, 962.

58. Wilson, M.J.; *"A Handbook of determination Methods in Clay Minerology"*, Chapman and Hall: NewYork **1987**, pp. 61-63.

59. Colton, R.; Farthing, R.H. *Aust. J. Chem.* **1971**, *24*, 903.

60. Edgell, W.F.; Lyford IV, *Inorg. Chem.* **1970**, *9*, 1932.

61. Venalainen, T.; Pakkanen, T.A.; Pakkanen, T.T.; Iiskola, E. Finn Pat. 69620

62. Steinhardt, P.C.; Gladfelter, W.L.; Harley, A.D.; Fox, J.R.; Geoffroy, G.L. *Inorg.Chem.* **1980**, *19*, 332.

63. Nivert, C.L.; Williams, G.H.; Seyferth, D. *Inorg. Synth.* **1980**, *20*, 234.

64. Breck, D.W. *"Zeolite Molecular Sieves"* Wiley-Int. Science, New York **1974**.

65. Taylor, D.F. PhD. dissertation, Virginia Polytechnic Institute and State University Blacksburg VA, **1987**.

66. Rigo, P.; Bressan, M.; Morvillo, A. *J. Organometallic Chem.* **1976**, *105*, 263.

67. Cavit, B.E.; Grundy, K.R.; Roper, W.R. *J. Chem. Soc. Chem. Comm.* **1972**, 60.

68. Cleare, M.J.; Griffith, W.P. *J. Chem. Soc.(A)* **1969**, 372.

69. Johnson, B.F.G.; Lewis, J.; Raithaby, P.R.; Suss, G. *J. Chem Soc. Dalt. Trans.* **1979**, 1356.

70. Lamb, H.H.; Krause, T.R.; Gates, B.C. *J. Chem. Soc. Chem. Comm.* **1986**, 821.

71. Psaro, R.; Dossi, C.; Ugo, R. *J. Mol. Catal.* **1983**, *21*, 331.

72. Venalainen, T.; Pursiainen, J.; Pakkanen, T.A. *J. Chem. Soc. Chem. Comm.* **1985**, 1348.

73. Bruce, M.I.; Humphrey, M.G.; Snow, M.R.; Tiekink, E.R.T.; Wallis, R.C. *J. Organometallic Chem.* **1986**, *314*, 311.

74. Ishida, H.; Tanaka, K.; Morimoto, M.; Tanaka, T. *Organometallics* **1986**, *5*, 724.

75. Sullivan, B.P.; Caspar, J.V.; Johnson,S.R.; Meyer, T.J.; *Organometallics* **1984**, *3*, 1241.

76. Benedetti, E.; Braca, G.; Sbrana, G.; Salvetti, F.; Grassi, B. *J. Organometallic Chem.* **1972**, *37*, 361.

77. Bergmeister, J.J.; Hanson, B.E.; Merola, J.S. Submitted for publication to *Inorg. Chem.*

78. Alyea, E.C.; Ferguson, G.; Muleto, J.; Ruhl, B.C. *Inorg. Chem.* **1985**, 24, 3719.

79. Favas, M.C.; Kepert, D.L.; White, A.H.; Willis, A.C. *J. Chem. Soc. Dalton Trans.* **1977**, 1350.

80. Fischer, V. D.; Krebs, B. Z. *Anorg. Chem.* **1982**, *491*, 73.

81. Giacomelli, A.; Floriani, C.; Duarte, A.O.; Chiesi-Villa, A.; Guastini, C. *Inorg. Chem.* **1982** *21*, 3310.

82. Jones, R.A.; Wilkinson, G.; Galas, A.M.R.; Hursthouse, M.B.; Malik, K.M.A. *J.Chem. Soc. Dalton Trans.* **1980**, 1771.

83. Teulon. P.; Roziere, J. *J. Organometallic Chem.* **1981**, *214*, 391.

84. Lou, X.L.; Schulte, G.K.; Crabtree, R.H. *Inorg. Chem.* **1990**, *29*, 682.

85. Venalainen, T.; Pakkanen, T.A.; Pakkanen, T.T.; Iiskola, E. *J. Organometallic Chem.* **1986**, *314*, C49.

86. Bruce, M.I.; Stone, F.G.A. *Angew Chem. Int. Ed. Engl.* **1968**, *7*, 427.

87. *"Aldrich Library of Infrared Spectra"*, ed. Pouchert, C.J. Aldrich Chem. Co. **1981**.

88. Nagel, C.C.; Shore, S.G. *J. Chem. Soc. Chem. Comm.* **1980**, 530.

89. Churchill, M.R.; Wormald, J. *J. Amer. Chem. Soc.* **1971**, *93*, 5670.

90. Bradley, J.S.; Ansell, G.B.; Hill, E.W. *J. Organometallic Chem.* **1980**, *184*, c33.

91. Pakkanen, T.A. Personal Communication.

92. Wertz, J.E.; Bolton, J.R. *"Electron Spin Resonance, Elementary Theory and Practical Applications"* McGraw-Hill, New York, **1972**.

93. Tyler, D.R.; Levenson, R.A.; Gray, H.B. *J. Amer. Chem. Soc.* **1978**, *100*, 7888.

94. *"The Sadtler Handbook of UV Spectra"* pg. 171 Ed. Simons, W.W., Publ: Hyden and Sons LTD. London **1979**.

95. Folkesson, B. *Acta. Chim. Scand.* **1973**, *27*, 287.

96. Battistoni, C.; Furlani, C.; Mattogno, G; Tom, G. *Inorg. Chim. Acta.* **1977**, *21*, 225.

97. Psaro, R; Ugo, R.; Zanderighi, G.M.; Besson, B.; Smith, A.K.; Basset, J.M. *J. Organometallic Chem.* **1981**, *213*, 215.

98. Verdonck, J.J.; Schoonheydt, R.A.; Jacobs, P.A. *J. Phys. Chem.* **1983**, *87*, 683.

99. Hidai, M.; Orisaku, M.; Ue, M.; Koyasu, Y.; Kodama, T; Uchida, Y. *Organometallics* **1983**, *2*, 292.

100. Schneider, R,; Howe, R.F.; Watters, K.L. *Inorg. Chem.* **1984**, *23*, 4593.

101. Lauher, J.W. *J. Am. Chem. Soc.* **1986**, *108*, 1521.

The vita has been removed from the scanned document